CHARACTERIZATION, IMAGING AND QUANTITATION OF SMALL MOLECULES BY AMBIENT IONIZATION MASS SPECTROMETRY

SHAMINA SAIYARA PROVA

A DISSERTATION SUBMITTED TO
THE FACULTY OF GRADUATE STUDIES
IN PARTIAL FULFILMENT OF THE REQUIREMENTS
FOR THE DEGREE OF
DOCTOR OF PHILOSOPHY

GRADUATE PROGRAM IN CHEMISTRY

YORK UNIVERSITY

TORONTO, ONTARIO

April 2019

ABSTRACT

For more than a century mass spectrometry has been a well-known technique in the field of chemical analytics. Its selectivity and sensitivity has made it popular in various fields. From analysis of pure organics, its use is still being explored in the analysis of biomolecules, either purified or direct from tissue sections. For analyzing these vast arrays of molecules, typically the front end is modulated depending upon the need of the user. For direct analysis of a sample of interest, ionization techniques such as DESI, PS, MALDI, etc are incorporated into the front of the mass spectrometer. In this work, the ambient ionization techniques, DESI-MS and PS-MS was modulated for characterization, imaging and quantification of small molecules. The use of DESI-MS and PS-MS in the field of forensics, microbiology and pharmaceutics is described. With the optimization of the front end modes, better sensitivity, selectively and robustness was ensured.

ACKNOWLEDGEMENT

TABLE OF CONTENTS

LIST OF TABLES

LIST OF FIGURES

LIST OF ABBREVIATIONS

AIMS	Ambient Ionization Mass Spectrometry
AU	Arbitrary Unit (manufacturer's unit)
B. subtilis	*Bacillus subtilis* (Gram positive bacteria)
CH_3CN	Acetonitrile
$CHCl_3$	Chloroform
CH_3OH	Methanol
CID	Collision-Induced Dissociation
CRMS	Centre for Research in Mass Spectrometry
DESI-MS	Desorption Electrospray Ionization Mass Spectrometry
DESI-MSI	Desorption Electrospray Ionization Mass Spectrometry Imaging
E. coli	*Escherichia coli* (Gram negative bactria)
ESI-MS	Electrospray Ionization Mass Spectrometry
HCD	High-energy Collisional Dissociation
HRMS	High Resolution Mass Spectrometry
HMBC	Heteronuclear Multiple Bond Correlation
HMQC	Heteronuclear Multiple-Quantum Correlation
HPLC	High Performance Liquid Chromatography
HPTLC	High Performance Thin Layer Chromatography
H_2O	Water
IPA	Isopropyl Alcohol
ISP2	Yeast Malt Broth
LB	Luria Bertani Media
LC-MS	Liquid Chromatography coupled with Mass Spectrometry
LOD	Limit Of Detection
MassPREP	Standard mix to intact proteins from Waters to assess chromatographic run
MIC	Minimum Inhibitory Concentration
MS	Mass Spectrometry/Mass spectrometer
MSI	Mass Spectrometry Imaging
MS/MS	Mass Spectrometry/Mass Spectrometry (Tandem Mass Spectrometry)
m/z	Mass to Charge ratio
NH_4OH	Ammonium Hydroxide
NMR	Nuclear Magnetic Resonance
OTC	Over the counter medication

PDA	Potato Dextrose Agar
P. roqueforti	*Penicillium roqueforti* (Blue cheese fungus)
PTFE	Polytetrafluoroethylene
PS-MS	Paper Spray Mass Spectrometry
RF	Retention Factor
RSD	Relative Standard Deviation
Recom Std	Recombinant Standard Antigen
SAP	Single Amino acid Polymorphism
SD	Standard Deviation
S/N	Signal to Noise ratio
TIC	Total Ion Count
TLC	Thin Layer Chromatography
TOCSY	Total Correlated Spectroscopy
UV/UV-Vis spec	Ultraviolet and Visible Absorption Spectroscopy
%v/v	percent volume by volume (no. of mL of solute in total 100mL solution)
%w/v	percent weight by volume (no. of grams of solute in 100mL solution)

LIST OF PUBLICATIONS

- Rodrigues, J. P.*, **Prova, S. S.***, Moraes, L. A. B., & Ifa, D. R. (2018). Characterization and mapping of secondary metabolites of Streptomyces sp. from caatinga by desorption electrospray ionization mass spectrometry (DESI–MS). Analytical and Bioanalytical Chemistry, 410(27), 7135-7144. (*equal contributor)
- Perez, C. J., Bagga, A. K., **Prova, S. S.**, Taemeh, M. Y., & Ifa, D. R. (2018). Review and perspectives on the applications of mass spectrometry imaging under ambient conditions. Rapid Communications in Mass Spectrometry.
- Woolman, M., Tata, A., Dara, D., Meens, J., D'Arcangelo, E., Perez, C.J., **Prova, S.S.**, Bluemke, E., Ginsberg, H.J., Ifa, D. and McGuigan, A., (2017). Rapid determination of the tumour stroma ratio in squamous cell carcinomas with desorption electrospray ionization mass spectrometry (DESI-MS): a proof-of-concept demonstration. Analyst, 142(18), 3522-3522.
- Khatami, A., **Prova, S. S.**, Bagga, A. K., Yan Chi Ting, M., Brar, G., & Ifa, D. R. (2017). Detection and imaging of thermochromic ink compounds in erasable pens using desorption electrospray ionization mass spectrometry. Rapid Communications in Mass Spectrometry, 31(12), 983-990.
- Rahman, M. M., Hunter, H. N., **Prova, S.**, Verma, V., Qamar, A., & Golemi-Kotra, D. (2016). The Staphylococcus aureus methicillin resistance factor FmtA is a d-amino esterase that acts on teichoic acids. mBio, 7(1), e02070-15.

CHAPTER ONE

Introduction

1.1 Mass Spectrometry

Mass spectrometry is an indispensable analytical tool that is rapidly gaining a lot of attention due to its scope in qualitative and quantitative assessment of a wide array of compounds, in the fields of Chemistry, Biochemistry, Pharmacy and Medicine. (1) It employs detection of charged analytes after separation by electro and/or magnetic fields.

The basic mass spectrometer setup consists of an ionization source, mass analyzer and a detector (Fig. 1.1). The ionization source converts molecules in the sample into ions by addition or removal of electrons, or through protonation / deprotonation.(2) The charged gas-phase ions make their way into the mass analyzer, where they are separated according to their mass to charge ratio due to the presence of electric and/or magnetic field. Upon separation, the ions are later detected by a detector and the output is displayed on a computer screen. The separation of the analytes requires that the system is kept under vacuum.
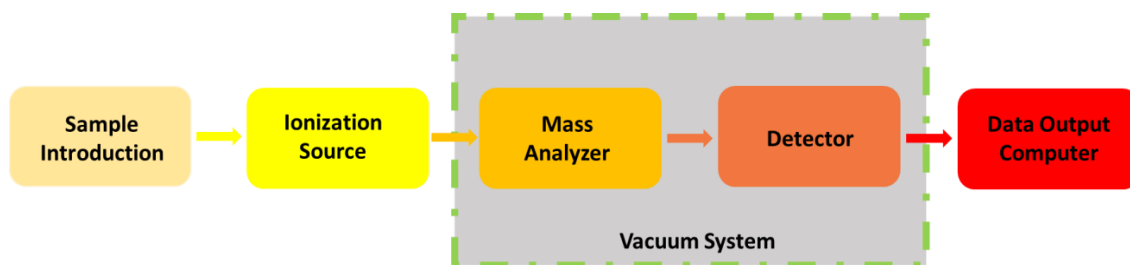
Figure 1.1: Typical mass spectrometer setup

In 1912 the first mass spectrometer was created by J. J. Thomson for detection of stable isotopes of Neon-20 and Neon-22.(3) Since then, its use evolved from small inorganic compounds to detecting biological macromolecules. The detection of this wide array of analytes was made possible by the development of efficient ionization and powerful mass analyzers.(1) Initially detection was made possible from electron ionization in a vacuum chamber with a heated filament.

Filament-released electrons bombarded the analyte of interest, thereby charging it and making it suitable for detection. Later chemical ionization was explored, where a charged gas, typically methane, bombarded the molecules of interest. All these ionization techniques were really harsh on the molecules, which frequently led to their fragmentations.

1.2 Electrospray Ionization (ESI)

For detection of intact ions, the soft ionization technique ESI was developed. Electrospray ionization, involves exposure of a solvent to a high electric voltage that enable their electrolysis due to which protons build up in the system. When a positive voltage is applied to the capillary, positively charged ions start to accumulate at the tip of the spray needle capillary and the negative ions are retained in the capillary. Repulsion between positive ions in solution and positively charged capillary causes the formation of a Taylor cone at the capillary tip (3). Once coulombic repulsion exceeds the surface tension, the cone shatters to spray out individual droplets that are highly positively charged (Figure 1.2). Solvent in the charged droplets evaporates under atmospheric pressure as they make way towards the negatively charged slit. Desolvation gas, nitrogen, helps the process of solvent evaporation. The droplets continue to fission upon reaching Rayleigh limit, reducing in size until they are a few µm in radius, which is when the gas phase ions form as the residual solvent evaporates. Sometimes a slight increase in temperature is introduced to aid this overall process of evaporation.

ESI-MS is widely utilized to study non-covalent interactions because the species are retained in the gas-phase. In addition to mass, multiple reactions as well as the pathways each reaction follows can also be monitored simultaneously using this technique. ESI-MS allows for large non-volatile molecules to be analyzed directly from the liquid phase and is regularly coupled to other separation techniques such as high performance liquid chromatography (HPLC). This

mode of ionization later on paved its way towards ionization under ambient conditions.
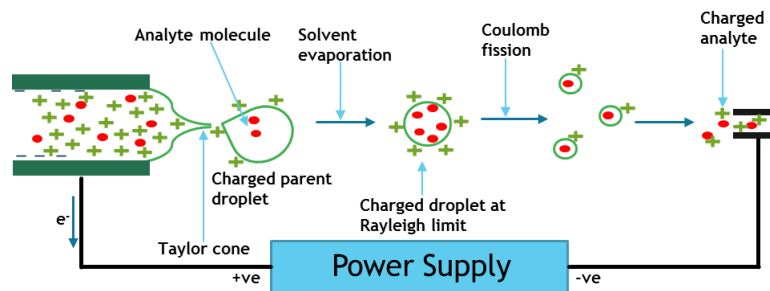
Figure 1.2: Schematics of positive mode ionization by ESI-MS.

1.3 Ambient ionization mass spectrometry

Ambient ionization technique eliminates the need of vacuum and enables the ionization of the analyte outside the mass spectrometer under ambient conditions. This technique was first introduced by Cooks *et al*. in 2004(2) with the introduction of DESI and later, on 2005 Cody *et al* introduced Direct Analysis in Real Time Mass Spectrometry (DART-MS)(4). Both these techniques were used for surface analysis under ambient conditions without the need of any sample preparation prior to analysis. While ambient ionization is very user friendly, it requires solvent optimization to ensure efficient desorption and ionization of the molecules of interest. In other words, analysis by this technique requires solvent optimization and thus suffers from selectivity and sensitivity issues. Nevertheless, this technique is growing in popularity for its ease of use and also since it allows spatial distribution of compounds to be determined by techniques like imaging mass spectrometry. Several ambient ionizations techniques have been explored. They differ in their modes of desorption / ionization. Table 1.1 summarizes them based on their modes of operation.

Table 1.1: Different Ambient Ionization Techniques characterized by their modes of operation.

Mode of operation	Acronym	Name	Ref
Spray and Solid-Liquid extraction based Techniques	DESI	Desorption Electrospray Ionization	(5)
	EASI	Easy Ambient Sonic-Spray ionization	(6)

	PESI	Probe Electrospray Ionization	(7)
	ND-EESI	Neutral Desorption Extractive Electrospray Ionization	(8)
	AP-TD/SI	Atmospheric Pressure thermal desorption-secondary ionization	(9)
	LMJ-SSP	Liquid Microjunction-Surface Sampling Probe	(10)
	LESA	Liquid Extraction Surface Analysis	(11)
	ESA-Py	Electrospray Assisted Pyrolysis Ionization	(12)
	PS	Paper Spray	(13)
	TPD/ESI	Thermal Probe Desorption Electrospray Ionization	(14)
Plasma-Based Techniques	DART	Direct Analysis in Real Time	(15)
	FAPA	Flowing Atmospheric Pressure Afterglow	(16)
	LTP	Low Temperature Plasma Probe	(17)
	DBDI	Dielectric Barrier Discharge Ionization	(18)
	---	Microplasmas	(19)
Chemical Sputtering/Ionization Techniques	DAPCI	Desorption Atmospheric Pressure Chemical Ionization	(20)
	DCBI	Desorption Corona Beam Ionization	(21)
	ASAP	Atmospheric Pressure Solid Analysis Probe	(22)
Multimode Techniques	DEMI	Desorption Electrospray/Metastable-induced Ionization	(23)
Laser Desorption/Ablation techniques	LAESI	Laser Ablation Electrospray Ionization	(24)
	IR-LDESI	Infrared Laser Desorption Electrospray Ionization	(25)
	MALDIESI	Matrix-Assisted Laser Desorption Electrospray Ionization	(26)
	ELDI	Electrospray-assisted Laser Desorption Ionization	(27)
	IR-LAMICI	Infrared Laser Ablation Metastable-Induced Chemical Ionization	(28)
	LS	Laser Spray	(29)
Acoustic Desorption Methods	LIAD-ESI	Laser-Induced Acoustic Desorption-Electrospray Ionization	(30)
	RADIO	Radio-Frequency Acoustic Desorption and Ionization	(31)

Others	DAPPI	Desorption Atmospheric Pressure Photo-Ionization	(32)
	SwiFerr	Switched Ferroelectric Plasma ionizer	(33)
	BADCI	Beta Electron-Assisted Direct Chemical Ionization	(34)
	REIMS	Rapid Evaporative Ionization Mass Spectrometry	(35)

1.3.1 Desorption electrospray ionization (DESI-MS & DESI-MSI)

Desorption electrospray ionization (DESI) is a widely used technique in the field of mass spectrometry. Its ease of direct analysis of any sample at ambient condition, with minimal to almost no sample preparation makes it convenient and user-friendly. DESI-MS uses a high voltage to generate charged solvent droplets under nitrogen gas flow. These droplets hit the sample surface to desorb the analyte into ionized species such as cationized gas phase molecules, deprotonated $[M-H]^-$, or protonated $[M+H]^+$ molecules. Further splash of the charged solvent droplets on the desorbed sample surface directs the ionized analytes into the inlet of the mass spectrometer for their detection.

1.3.1.1 DESI ion source

Figure 1.3 demonstrates a graphical representation of a typical DESI ion source. It consist of a pneumatically assisted solvent spray held at high voltage, typically 5kV. The solvent sprayer is mounted on a vertical rotating stage to modulate the impact angle/incident angle α from 0 to 90°. Usually at an incidence of 55° the maximum 'droplet pickup' by the mass spectrometer inlet, representative by the best signal intensity, occurs at a collection angle (β) of 10°. The sample is held on a 3D moving stage. The movement of the moving stage helps alteration of the collection angle as well as the impact point of the solvent spray on the sample surface (36).

The mechanism of surface solid-liquid extraction and "droplet pickup" has long been

assumed and studied using Phase Doppler Anemometry (PDA). It has been found that the charged solvent spray forms a thin mist film on the surface of the sample as can be viewed on top of a glass slide but not over a porous PTFE surface. Upon subsequent solvent spray, the momentum is transferred to the mist film which results in the production of progeny droplets. High voltage on the sprayer tip and the electric field from the inlet capillary of the mass spectrometer provides electrostatic forces that primarily result in droplet formation and accelerating their velocities in a simulated model. The nebulizer gas in the solvent spray assist in drying the droplets, which by hydrodynamic forces (nebulization pressure and pressure drop at the inlet of MS) can be captured by the mass spectrometer. Figure 1.4 shows the velocity distribution 0.4 μs after impact time when the most number of droplets have the highest speed indicated with red arrows and can reach the inlet of the mass spectrometer successfully (37).

Term	Description
α	Incident angle
β	Collection angle
d_1	Distance from the surface to the sprayer tip
d_2	Distance from the surface to the MS inlet
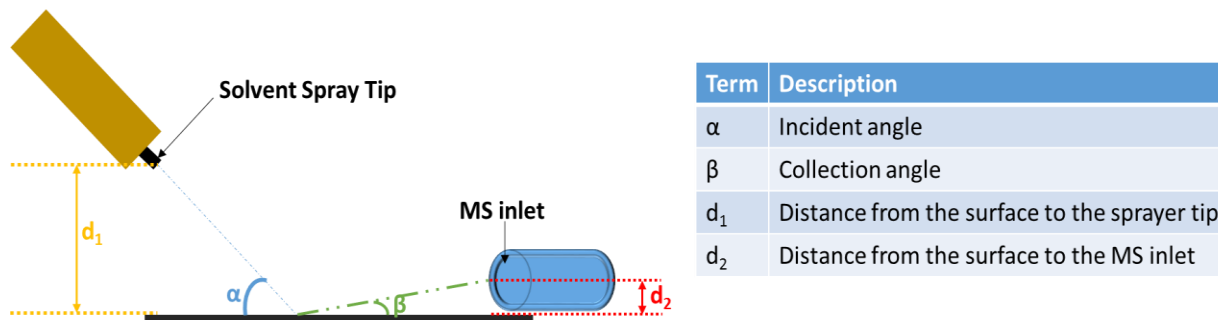
Figure 1.3: Graphical representation of a typical DESI ion source.
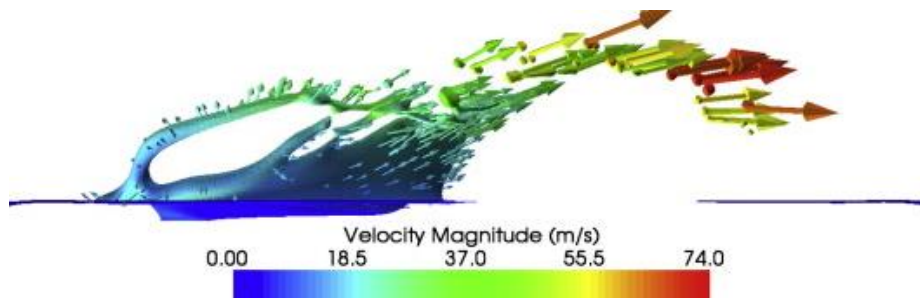
Figure 1.4 Velocity distribution of droplets 0.4μs after impact.

1.3.1.2 DESI imaging

Imaging mass spectrometry is a powerful analytical and bioanalytical technique that not only allows identification of unknown compounds but also allows determination of their spatial distribution. DESI by virtue of its ease of sample preparation and ambient mode of ionization allows acquisition of 2D and 3D chemical ion images effortlessly. Since DESI utilizes solid-liquid phase extraction, choice of solvents and/or their combinations mainly drives the type of analyte molecules being imaged. Droplet pick-up lasts for a few milliseconds and hence is limited to capture of mostly small molecules in DESI-MSI. The resolution of a DESI image is determined by pixel size in the lateral direction and is limited to the diameter of the silica capillary carrying the droplet. Typically DESI produces ion images having 100-200µm in resolution. The requirement of a higher resolution image is a trade off with the acquisition speed. The total imaging acquisition time is dependent on the size of the tissue section under analysis, MS scan rate, raster speed and lateral resolution. For DESI-MSI if the resolution is decreased below 100µm, the spot area under analysis will overlap, which not only maps misleading ion intensity but also hampers the overall quality of the image (38).

DESI-imaging involves cutting the sample of interest into thin sections (20-50µm) and fixing them on to glass slides. The glass slide having the sample under analysis is dried in a vacuum desiccator and mounted on an automatic 3D moving stage. DESI-solvent spray geometry is then adjusted for optimal acquisition of MS spectra. The moving stage then rasters through the surface of the article in horizontal lines at a certain speed determined by the scan rate and resolution selected for performing imaging. The space between two horizontal lines is the pixel size or resolution chosen to perform imaging. All the horizontal line spectra are then compiled with an imaging software such as the freeware BioMap, Image J and other commercially available variants

(i.e. MSI Quickview) to create 2D images of ion intensities over the sample surface coordinates. Likewise for acquisition of a 3D ion-image, a collection of representative 2D ion-images are compiled in 3D space within its topographical feature. It is a compromise between image quality and the cumulative acquisition time of all the 2D sections (39).

1.3.1.3 DESI applications

The ability to desorb an analyte from a surface depends on its interaction with the DESI spray solvent. Solubility is a key factor since the detection of the analyte is dependent on the solid-liquid surface extraction process. DESI has been used for a broad range of compounds including small polar or non-polar molecules or large polar molecules like proteins or peptides. It has been used in metabolomics studies to detect small biomolecule from animal (40–42), plant (43–45) or microbial (46–50) cell culture. In the pharmaceutical field it has been employed to analyse drugs or excipients (51,52). Forensics have also benefited by its detection of chemicals like explosives (20,53–57), inks (58–60), polymers etc (61). Its application has also been successful for analysing peptides / proteins with molecular weights up to 66kDa (62,63). This mode of ionization is limited to the detection levels in the femtomolar range, but its reproducibility and quantitative assessment ability has been reported to be very robust, having inter-day variation below 10%.

1.3.2 Paper Spray Mass Spectrometry (PS-MS)

Paper Spray is also an ambient ionization technique, introduced by Cooks and coworkers in 2010 (13). It utilizes a triangular shaped paper held at high voltage (3-5kV) and kept about 4 mm away from the inlet of the mass spectrometer (Figure 1.5). At the tip of the paper the analyte solution is spotted and upon solvent drizzle the analytes get extracted. The presence of an electrostatic field carries the charged droplets contaning the analyte molecule into the inlet of the mass spectrometer. This technique does not suffer matrix or salt suppression effects as only the

solvent-soluble analyte makes its way into the mass spectrometer (64). This allows a clean-up of sample mixture. Like ESI, the solvent coming in contact with the electrified paper forms Taylor cone at the tip and bursts, releasing charged progeny droplets containing the soluble analytes. The internal energy distribution and the size of the droplets is shown to be similar to nano-electrospray ionization (65). This technique has been employed for direct screening of complex mixtures (13,66,67). Dispensing paper in each run helps eliminate the carryover effect typically observed with LC-MS and GC-MS and thus improves the limit of quantitation (68,69).
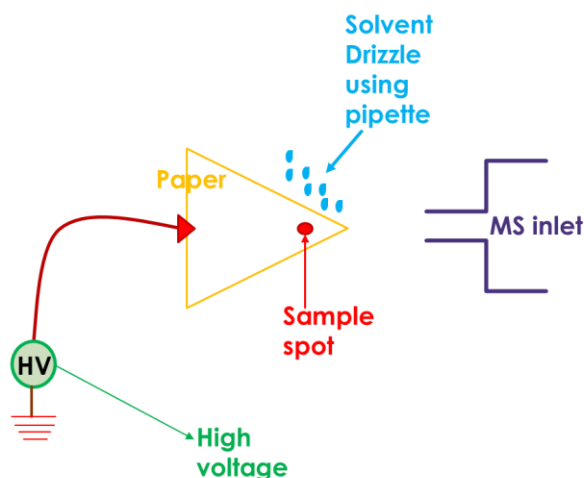
Figure1.5: Schematics of Paper Spray.

1.4 Mass Analyzers

Mass Analyzers are the heart of mass spectrometer. They only selects the ions of interest but also separates them according to their mass to charge ratio and respective intensities. All this typically happens under vacuum in an applied electric field. Several parameters define the performance of a mass analyzer. To list a few are, resolution (ability to separate ions having slight difference in their *m/z* ratios), mass accuracy (error percentage in calculating exact m/z values), scanning range of *m/z*, ability to perform tandem mass spectrometry and precision of isotopic pattern. Some of the most commonly used analyzers are listed below:

1. Quadrupole analyzer

      a. Single

      b. Triple

2. Ion traps

      a. Paul Traps (3D)

      b. Linear Ion traps (2D)

3. Time-of-flight analyzer (TOF)

4. TOF with Reflectron

5. Magnetic Analyzer

6. Ion Cyclotron Resonance (ICR)

7. Orbitrap

1.4.1 Linear Ion Trap

Linear Ion Traps are typically designed like quadrupole with two end confining electrodes (70). Ion are confined radially with the application of a two dimensional (2D) radio frequency (RF) field and axially by stopping potential applied to end electrodes (71). Ramping the AC frequency sequentially ejects ions according to their masses. In case of tandem mass spectrometry (MS/MS), ramping the voltage causes all the stored ions to eject leaving behind only one selected. The selected ion then undergoes oscillation with He collision gas to produce fragment ions. Again, one single fragment ion can be selected, ejecting the other daughter ions and in this way MS^n can be performed for structural elucidation. They offer advantage over Paul (3D) traps due to increased ion storage and ultimately greater total charge capacity space, which allows accurate quantification. Linear Ion trap can be used as a stand-alone analyzer in mass spectrometer or can be coupled with other analyzers like Orbitrap to offer better resolution translating into enhanced mass accuracy for studying ion-molecule chemistry (70,71).

1.4.2 Orbitrap

Orbitraps are the newest mass analyzer, introduced in 2005 by Thermoelectronics (72). It consists of two outer barrel shaped electrode confining a central spindle shaped electrode, which allows it to work both as an analyzer and detector (Figure 1.6). As small packets of ions enter into the equator of the orbitrap, voltage is increased in the central spindle electrode, which forces ions to 'electrodynamically squeeze' in the central electrode (73). Upon cessation of the voltage ramp the ions get trapped inside the orbitrap. The trapped ions oscillate radially around the central electrodes and in between the two outer electrodes. As the ions move closer to the inner surface of the outer electrode, they induces charge on the outer electrode detected as image current by differential amplifier (73). As they go back and forth around the space it generates sinusoidal signals of induced currents varying with time. Different ions have different image current, which translates into distinct frequencies by induced Fourier Transform (FT). These frequencies translate into different *m/z*. Unlike Fourier Transform-Ion Cyclotron Resonance (FT-ICR), Orbitrap does not require huge and expensive super conducting magnets. It also allows high transmission of signal resulting in one to two fold higher sensitivity than any other high accuracy mass analyzer (72–74).
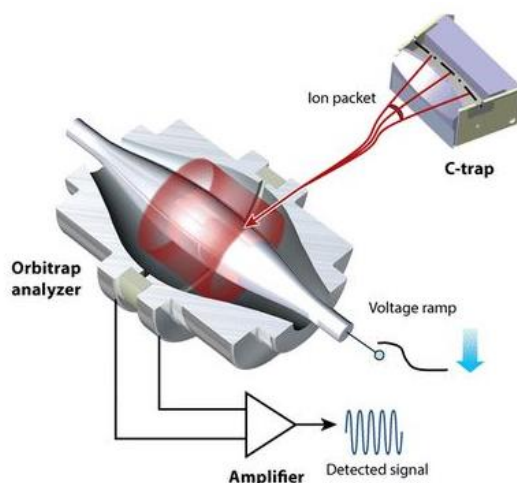
Figure 1.6: Orbitrap mass analyzer. (Figure copied from Thermo Fischer website)

1.5 Aim of my Thesis

The ambient ionization technique, namely DESI-MS, is gaining attention due to its ease of use, requiring no sample preparation and its ability to detect compounds under ambient conditions along with providing information about their spatial distribution though imaging mass spectrometry (MSI). The aim of the research is to depict its potential as a means of qualitative and quantitative assessment of samples in the field of forensics, drug discovery, food and pharmaceutical industry. Chapter two focuses on identifying forgery with the use of Thermochromic ink. DESI- MS and DESI-MSI helped identify different fingerprints representative of the visible and invisible state of the ink without any sample extraction or pretreatment steps. In chapter three, DES-MS and DESI-MSI have been employed to detect and image drug compounds from microbial culture of actinobacteria. The analysis enabled detection of a potential drug candidate which is an analogue of lienomycin along with another drug moiety, Lysoliphin I previously identified to be released by this class of bacterium. With imaging mass spectrometry, this drug compounds were mapped during the bacterial lifecycle, as well as in the zone of inhibition in disc diffusion study carried out with the media extract on *B. subtilis*, *E. coli* and *P. roqueforti*. Chapters four and five discuss the use of DESI-MS as a quantitative tool for analysis of food and pharmaceutical products. TLC was coupled with DESI as a means of separation prior to quantifying. Three quantification methods were performed to quantify caffeine in energy drinks and active principals in eye drop preparations. All modes of quantification showed accuracy and robustness, further affirming DESI-MS use as a quantification tool that can be readily used in the food and pharmaceutical industries.

CHAPTER TWO

Detection and imaging of thermochromic ink compounds in erasable pens using Desorption Electrospray Ionization Mass Spectrometry (DESI-MS)

A version of this chapter published in Rapid Communications in Mass Spectrometry:

• Khatami, A., Prova, S. S., Bagga, A. K., Yan Chi Ting, M., Brar, G., & Ifa, D. R. (2017). Detection and imaging of thermochromic ink compounds in erasable pens using desorption electrospray ionization mass spectrometry. Rapid Communications in Mass Spectrometry, 31(12), 983-990.

2.1 Summary

Thermochromic ink pens are widely accessible worldwide and have gained popularity among the general public. These pens are very useful to undo mistakes while writing important documents or exams. Yet, they are also extensively misused in committing crimes such as counterfeiting checks or wills. Thus, the forensics community is in need of techniques that will allow these forgeries to be detected rapidly, reliably and conveniently. Desorption Electrospray Ionization (DESI) coupled with an LTQ mass spectrometer was used to identify the ink components. Chemicals markers characteristic to the state of ink (visible or invisible) were identified and mapped in ink traces by the use of DESI-MS imaging (DESI-MSI). These markers can generate fingerprints in forged documents by the forensic experts. The markers were also characterized by conducting tandem mass spectrometry using paper spray in an Orbitrap LTQ mass spectrometer.

2.2 Introduction

The introduction of pens featuring erasable ink in the late 1970s was one of the most compelling applications of invisible ink technologies (75–78). Erasable inks are convenient with numerous benefits. However, like any other device; they can be used for illegal purposes in counterfeiting checks or wills (79–81). Thus, forensics applications for detecting the trace ink compounds have been significantly amplified in recent years (81,82). Erasable ink can be classified into three groups based on their mode of erasing off ink traces. The first type are the rubber-erasable pens in which ink from printing paper surfaces can be rubbed off with rubbers provided due to the binding affinity of the ink compounds with the paper fibers, similar to pencils. The second types are the thermochromic pens, where the printed ink changes colour with an alteration in temperature. A colour film dissolving pen is the third type of erasable pen which can transform

14

in its invisible form by the use of another special correction pen (83). The primary focus of this paper is on the thermochromic ink and its analysis in the visible and invisible state. Thermochromic dyes are based on mixtures of leuco dyes with supplementary chemicals, displaying a colour alteration, typically among the colourless and the colored leuco form, with respect to temperature change (84,85).

In 2006 Pilot Pens Inc. introduced Pilot Frixion pens using thermochromic ink to the global market. The erasable ink composition mainly had solvent, colorant and resin film forming agent (85,86). The ink microcapsule consisted of an electron-donating organic dye that reacts with a developer compound which is electron-accepting in nature to give the ink color (85,87–90). The reaction medium along with the dye and developer had a crystalline substance (esters or ketone of long chain fatty acid) which was classified as a decolourant. At temperatures below 65°C the ink maintained its colored state due to reaction between the dye and the developer. During that time the crystalline substance was in the solid state. However, at temperatures above 65°C, heat causes the crystalline substance to melt and both the dye and developer dissolve, which hinders their interaction and renders the thermochromic ink colorless. At temperatures lower than -10°C the ink reverts back to its visible state as the crystalline substance restores its solid state (85,87–90).

Forensics detection and identification of ink currently conducted are predominantly physical methods of a non-destructive nature which includes microscopy, irradiation with UV and infrared radiation, exposing the document to various dichroic filters or employing lycopodium powder to detect eraser remains (91,92). However, these methods are only limited to the detection, differentiation and identification of inks being used to conduct forgery, thus making it essential to resort to chemical analytical methods. Chemical analytical methods include performing TLC, high performance liquid chromatography (HPLC), mass spectrometry (field-desorption ionization

(FDI), laser desorption ionization (LDI), matrix-assisted laser desorption ionization (MALDI), and electrostatic method of detection (capillary electrophoresis and micellar electrokinetic capillary electrophoresis (MECE)) (80,89,93–95). These techniques typically rely on the separation of compounds from the original sample, thereby destroying the original sample (93). Conversely, desorption-electrospray ionization (DESI), as an ambient ionization technique is able to conduct analysis of a sample in its native state; this reduces sample preparation time, as well as eliminating the necessity of a matrix in the process, thereby making DESI-MS a more convenient, cost and time effective method for analysis of a mixture of compounds (59). Combined with Mass Spectrometry Imaging (MSI), DESI helps to attain both chemical and spatial information of multiple compounds in a sample with little or no sample preparation (58,59,96,97). Eberlin *et al*., 2010 have illustrated the use of DESI-MS coupled with imaging as a convenient tool to chemically profile and map ink traces from authentic and counterfeiting bills (58). DESI-MSI being a minimally destructive technique can also provide valuable information of any restored sample even if the researcher lacks its former data. Furthermore, with the recent advancement of field portable miniature mass spectrometers, this mode of analysis will be of immense convenience to the mobile forensics specialists who are dedicated to operate in the field and are in constant need of fast reliable techniques that can perform onsite forensic analysis (98–100).

In this study, desorption electrospray mass spectrometry coupled with imaging was employed to conduct an investigation of a commercially available Pilot FriXon erasable ball pen to detect and image erased writing ink traces. The compounds specific to the erased state of the writing ink were scrutinized by performing TLC and tandem mass spectrometry. Analysis of these compounds can generate useful fingerprints for forensics experts to profile forgery in written documents.

2.3 Result and Discussion

2.3.1 DESI analysis of ink spots

Study of the thermochromic ink resulted in the detection of numerous compounds with m/z 245, 356, 467, 578, 689 and 800 in the visible state of the ink (Figure 2.1a). Upon examination, it was apparent that the difference between the ions detected were of a series of 111 Da. Kao YY and coworkers in their work on ink analysis by electrospray-assisted laser desorption ionization (ELDI) proposed that the ions evident are polymers of polyvinylpyrrolidone (PVP) $[(C_6H_9NO)_n]$ as Δm between the neighboring peaks of polymer ion series demonstrates a difference of 111 Da (86). Thus the polymer ion signals $[245 + (111)_n]$ were tentatively assigned as PVP (86). PVP is a water soluble polymer and is frequently found in several writing ink and jet printers ink composition as a polymeric flocculent to impart viscosity and adhesiveness in the overall formulation (101). In this work only one polymer ion series $[245 + (111)_n]$ was evident. The other series reported by Kao, Y.Y., *et al*. (86) were absent. This could be due to the different techniques used (ESI vs LDI), the ink colors used in the experiments or the different batches of ink formulations using different polymeric flocculent.

Subsequently, the ink spot was exposed to heat (+75°C), where it transformed into the colourless (invisible) state. The alteration of the spectrum from the visible form resulted in the appearance of several new compounds with a mass to charge ratios (m/z) of 400, 405, 511, 615, 786 and 851 (Figure 2.1b). Followed by the analysis of the ink spot in its invisible state, the ink was cooled at (-18°C) where it reverted back to its visible form. The spectrum acquired was nearly identical, displaying the same ion peaks as the original analysis of the ink spot with ions of m/z 245, 356, 467, 578, 689 and 800 along with the presence of trace amount of heated compound markers of m/z 400, 405, 511, 615 which were detected specifically in the invisible state (Figure

2.1c).
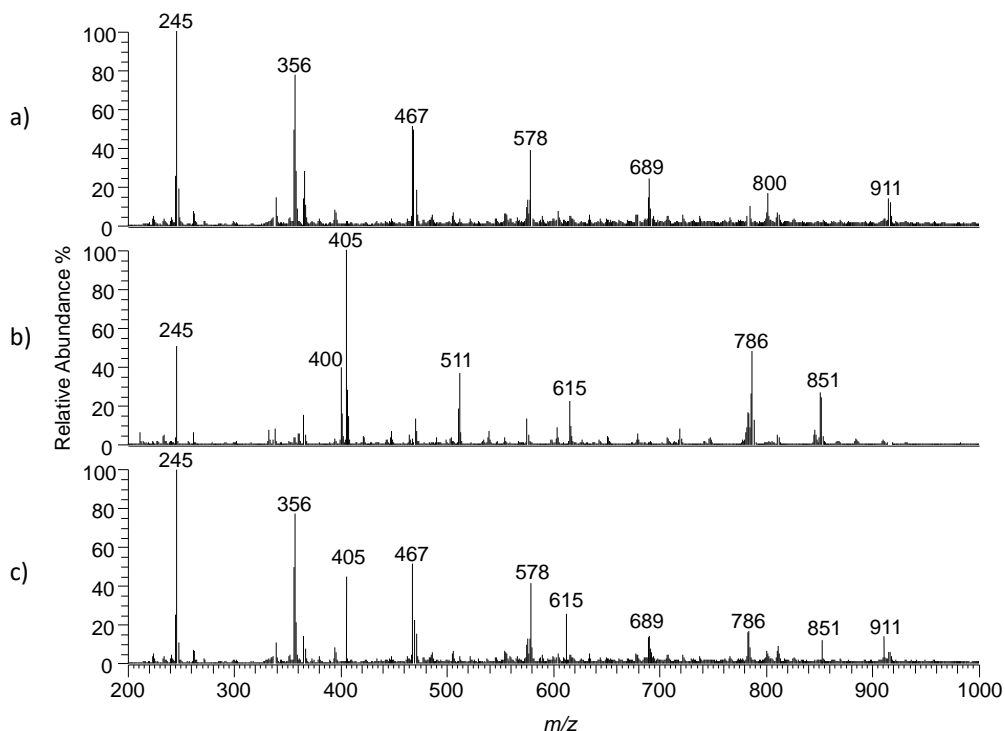
Figure 2.1: DESI-MS full scan spectra using an LTQ mass spectrometer in positive ion mode of the Pilot FriXion ink at a) room temperature (25° C) (original), b) heated (+75° C) (invisible state) and c) cooled (-18° C) reverted back to visible state.

Analysis of the ions of *m/z* 245.1262, 356.1944, 578.3307 and 800.4678 by tandem mass spectrometry (MS/MS) employing an Orbitrap mass spectrometer resulted in fragments of *m/z* 160.0733, 271.1416, 493.2780 and 715.4150 respectively (Figure 2.2). These were due to the loss of mass 85.0529 Da which was identified as C_4H_7NO (the ring structure of PVP). The MS/MS results also assisted in the hypothesis of the main ink compound of *m/z* 245 having a chemical formula of ($C_{11}H_{19}NO_5$) with 0.41 ppm difference and the other polymeric unit of PVP were characterized by Xcalibur software with their probable chemical formulae and parts per million (ppm) difference (Table 2.1). Other MS/MS data upon CID fragmentation in Orbitrap mass spectrometer are also provided in the Appendix, section A (Figure A1 and A2).
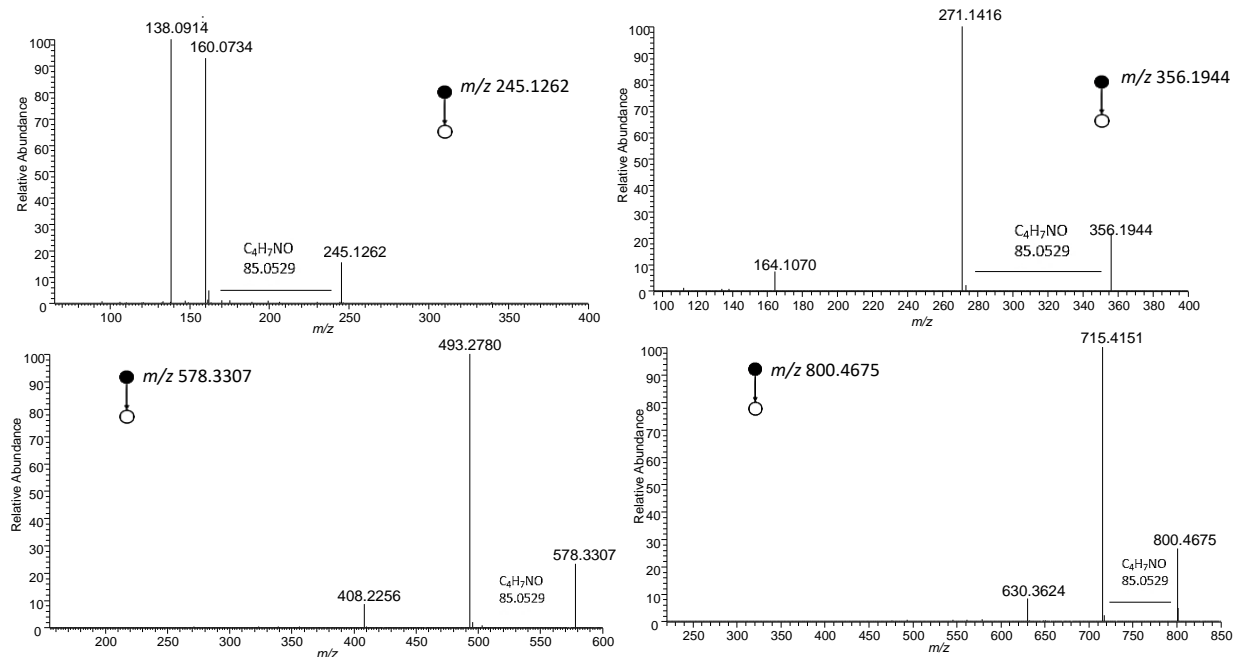
Figure 2.2: Tandem MS (MS/MS) spectra of thermochromic ink compounds acquired on an Orbitrap mass spectrometer; A) *m/z* 245.1262, B) *m/z* 356.1944, C) *m/z* 578.3307 and D) *m/z* 800.4678. Loss of 85.0529 Da was observed which was identified as C_4H_7NO.

Table 2.1: Characterisation of polymeric unit of PVP specific to the visible and recurred state of the ink.

m/z	Exact mass (*m/z*)	Possible chemical formulae	Difference in ppm
245	245.1262	$C_{11}H_{19}O_5N$	0.41
356	356.1944	$C_{17}H_{28}O_6N_2$	0.84
467	467.2625	$C_{23}H_{37}O_7N_3$	2.01
578	578.3307	$C_{29}H_{46}O_8N_4$	1.56
689	689.3991	$C_{35}H_{55}O_9N_5$	1.16
800	800.4675	$C_{41}H_{64}O_{10}N_6$	1.12
911	911.5359	$C_{47}H_{73}O_{11}N_7$	0.99

2.3.2 Paper spray analysis of ink

Paper spray mass spectrometry was a parallel method to confirm the reproducibility of the data acquired using DESI-MS. Paper spray has been proved to be a fast and sensitive technique for characterization of ink formulations and forgery (83,102). However, it requires analysis of cut

paper which cannot be performed on original valuable documents.

The analysis of the thermochromic ink at room temperature by paper spray displayed identical results to that obtained by DESI-MS and ESI (Refer to Appendix, section A, Figure A3 for comparison), depicting compounds of *m/z* 245, 356, 467, 578, 689 and 800 (Figure 2.3a). Similarly, the heated ink (+75°C) revealed an analogous spectrum with the DESI-MS having *m/z* 405, 511, and 786 profiling the characteristic of the ink in its invisible state (Figure 2.3b). The cooled ink back to its visible state also showed an identical mass spectrum compared to DESI-MS. The results obtained from paper spray confirmed the reliability of DESI-MS; however unlike paper spray, DESI does not require the extraction of the sample (ink) or cutting of the document to conduct analysis, thus making it a minimally destructive technique.

The exact masses of the compounds specific to the invisible and reappeared states of the ink were determined using the Orbitrap. These compounds were further characterised with probable chemical formulae having the least ppm difference using Xcalibur software (Table 2.2). The appearance of these compounds specific to the colourless and the recurred state of the thermochromic ink are valuable markers to identify any fabrication carried out with the document under question. Identification and characterization of such fingerprints for different thermochromic inks by DESI-MS could be useful for the forensic experts to detect forgery expediently.
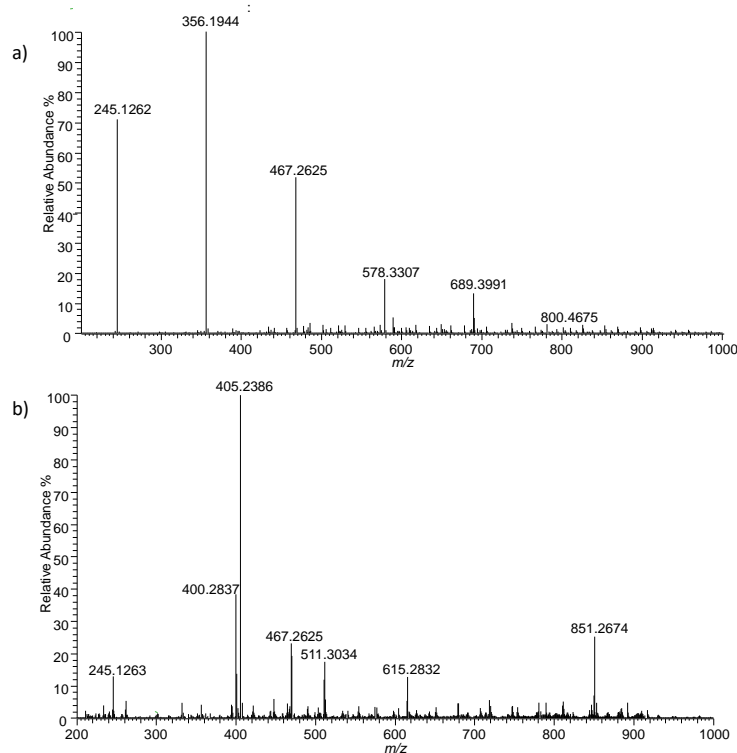
Figure 2.3: Paper spray full scan spectra acquired on an Orbitrap mass spectrometer in positive-ion mode of Pilot Frixion ball pen ink at a) room temperature (25°C) and b) heated Pilot Frixion ink at (+75°C), showing the matching profile characteristic of thermochromic ink analyzed by DESI-MS.

Table 2.2: Characterisation of compounds specific to the invisible state of the ink detected by DESI-MS and paper spray. A fingerprint to detect forgery.

m/z	Exact mass (m/z)	Possible chemical formulae	Difference in ppm
400	400.2837	$C_{25}H_{38}O_3N$	2.40
405	405.2386	$C_{22}H_{33}O_5N_2$	0.69
511	511.3034	$C_{29}H_{41}O_5N_3$	1.30
615	615.2832	$C_{39}H_{39}O_5N_2$	3.49
851	851.2674	$C_{60}H_{37}O_5N$	0.91

2.3.3 Thin Layer Chromatography (TLC)

Examination of the TLC plates using DESI-MS in positive ion mode allowed to observe the difference between heated and non-heated states of the ink. When the non-heated ink was run,

the presence of the heated markers were observed starting from the origin (RF 0) and the polymers separated based on their molecular weights (Table 2.3, Figure A4 and A5). When the heated ink was run, the same heated markers appeared from RF 0.438 to 1.0, along with the separated polymers (Figures A4 and A5). When the TLC plate was heated after the TLC run of the non-heated (visible) ink, the results were the same as from the non-heated ink run. Our hypothesis to explain these results is the presence of microcapsules in the ink formulation. The company's patent US 20120014740 A1 referred to the presence of a dye mixture inside microcapsules (85). For the first experiment the heated markers are inside the microcapsules which hinders their migration through the TLC plate. After heating the ink, the microcapsules break open to release the heated markers allowing them to migrate through the TLC plate from RF 0.69 to 1.0. Optical images of the TLC plates are provided in the Appendix, section A (Figure A8).

Table 2.3: TLC retention factors of ink components in the ink mixture.

m/z	Retention Factor (RF)	
	Original	Heated
400, 405, 615, 786 (Heated Markers)	0.000-0.625	0.438 till 1
245	0.781	0.781
356	0.656	0.656
467	0.500	0.500
578	0.375	0.375
689	0.300	0.300
800	0.219	0.219

In conclusion, the presence of the heated markers (m/z 400, 405, 615, and 786) in both the non-heated and heated spotted ink suggests that these compounds were not products of a reaction due to heat. Instead, these compounds were originally present in the ink composition and their

appearance is dependent on the treatment of the ink with heat. We speculate that the heated markers inside the microcapsules cannot be detected in the presence of the polymers due to ion suppression. On the other hand, if the heated markers are outside of the microcapsules, their signal will supress the polymer ion peaks (Figure 2.1a and 2.1b).

2.3.4 Imaging

DESI-MS imaging was conducted to map the ink components in both visible and invisible form drawn to simulate forgery. A number '7' was printed on a PTFE surface with Pilot FriXion erasable pen; after 15 minutes, the number was erased with the exposure to heat (+75°C) for 10 seconds. DESI-MS was used to characterize and run a two-dimensional image of the chemical compounds in its visible and invisible state (Figure 2.4).
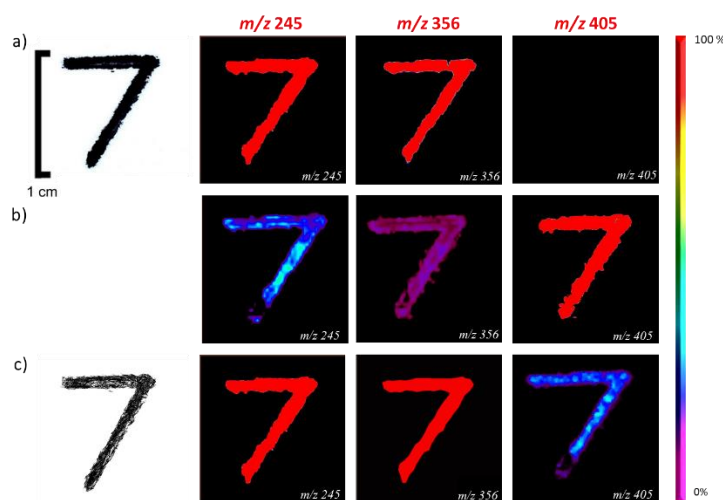
Figure 2.4: DESI images from a number drawn on PTFE paper acquired on a LTQ mass spectrometer. a) two-dimensional ion image of Pilot FriXion pen at room temperature (25°C), *m/z* 245, 356 and 405; b) two-dimensional ion image of Pilot FriXion pen upon exposure to heat (+75°C), *m/z* 245, 356 and 405; c) two-dimensional ion image of Pilot Frixion pen upon cooling (-18°C), *m/z* 245, 356 and 405.

Figure 2.4a shows the optical image (on the left) (original) and the mapped ion images of the ink compounds of number '7' at room temperature (+25°C) (on the right) *m/z* 245, 356 and

405. Figure 2.4b displays the optical image of the erased number '7' (on the left) (invisible state) upon exposure to temperature of (+75℃) and the mapped ion images of the ink compounds upon exposure to heat (on the right) *m/z* 245, 356 and 405. Figure 2.4c depicts the optical image of the cooled (-18℃) number '7' (on the left) (visible state) and the mapped ion images of ink compounds (on the right) *m/z* 245, 356 and 405. Of note, the heated marker *m/z* 405 was only evident in the heated and reappeared state of the ink but absent in the original state (before heating) of the ink.

Simultaneously, imaging was performed on paper written documents to check if the results were consistent with that acquired on a PTFE surface. The result obtained was identical with lower intensities and more background noise (Figure A6). 'CRMS' printed using a Pilot Fixon pen on a paper was mapped for ions; *m/z* 245, 356, and 405 at room temperature (Figure 2.5a), upon heating at +75°C (Figure 2.5b) and followed by cooling at -18°C (Figure 2.5c). All the images revealed similar results to that obtained by PTFE.

Ion images of *m/z* 405 on both PTFE and printing paper illustrates the presence of this compound specifically on the heated and reappeared state of the ink (Figure 2.4b, 2.4c, 2.5b and 2.5c). In the original state (non-heated) of the ink, *m/z* 405 was absent (Figure 2.4a and 2.5a). These results confirm that compounds like *m/z* 405 are useful markers to detect forgery. Whether the ink is in invisible state or restored back fully or in parts, imaging of ink traces will help to detect the presence and precise location of such markers, which will enable easy validation of malpractice while handing the document under investigation. Identifying such fingerprints using DESI-MS for various thermochromic inks could to be particularly beneficial to the forensic experts to profile forgery. Other ion images of the heated markers *m/z* 400, 578, 615 and 786 on both PTFE and printer paper are also provided in the Appendix, section A (Figure A7).
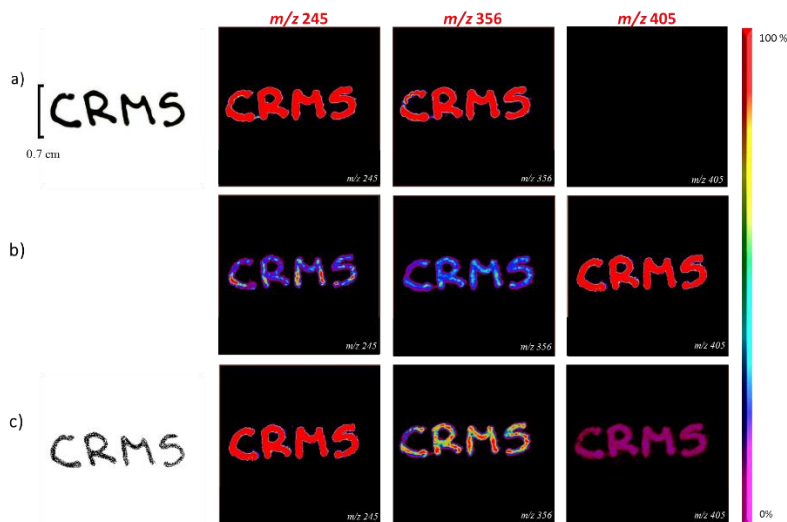
Figure 2.5: DESI images of 'CRMS' writing on letter format printing paper acquired on an LTQ mass spectrometer. a) two-dimensional ion image of Pilot FriXion pen at room temperature (25°C), *m/z* 245, 356 and 405; b) two-dimensional ion image of Pilot FriXion pen upon exposure to heat (+75°C), *m/z* 245, 356 and 405; c) two-dimensional ion image of Pilot FriXion pen upon cooling (-18°C), *m/z* 245, 356 and 405.

2.4 Conclusion

DESI-MS, as an ambient ionization technique, has been demonstrated to be exceedingly valuable in detecting ink chemical components specific to the invisible form and providing two-dimensional ion images of thermochromic ink compounds which otherwise would have been difficult to detect with the naked eye. Detection of a chemical fingerprint (*m/z* 400, 405, 786, and 615) specific to the invisible and recurred state of ink will confirm the act of misconduct with the concerned document. This method can be of practical use in forensic investigations to monitor and characterize visible and invisible ink components in various forged documents. Furthermore, the data collected by paper spray confirmed the accuracy of DESI-MS having similar mass spectra in both visible and invisible state.

Since the forensics community is in search of a more cost effective and prompt method of analysis,

DESI-MS could be an effective tool in providing reliable, stable and reproducible data with good signal-to-noise ratio while requiring little to no sample preparation making DESI-MS less laborious and time-consuming. Correspondingly, DESI displayed an immense improvement compared to formerly reported techniques in ways such that it eliminates the need for original sample to be destroyed or damaged and allows reprocessing for further analysis when needed.

2.5 Experimental

2.5.1 Instruments and Materials

Black Pilot FriXion Ball Erasable gel pen of 0.7 mm tip diameter was purchased from York University bookstore (Toronto, Canada) and was used throughout the analysis. Chemicals and solvents such as methanol and acetic acid were HPLC grade purchased from Sigma (Oakville, Canada). Printing paper (8.5 X 11 inch) was purchased from Staples (Toronto, Canada). Polytetrafluoroethylene (PTFE) and HPTLC platten Nano-Sil 20 (5 X 5cm) were purchased from Sigma (Oakville, Canada) and Macherey-Nagel (Düren, Germany), respectively. Thermo Finnigan LTQ ion trap mass spectrometer (San Jose, CA, USA) and Thermo Scientific Orbitrap Elite mass spectrometer (San Jose, CA, USA) were the two mass spectrometers used to conduct the analyses for this study.

2.5.2 DESI Ion Source Set Up and Parameters

All MS and DESI imaging experiments were conducted using a Thermo Finnigan LTQ ion trap mass spectrometer. Data were acquired in the positive ion mode and processed using Xcalibur 2.0 software (Thermo Fisher Scientific). Negative ion mode was performed initially; however, no relative difference in spectrum was observed between the heated and non-heated state of the ink. The ions intensities in the negative ion mode were also very low. The DESI ion source was custom-built to fit the LTQ mass spectrometer. Furthermore, the capillary of the ion source was adjusted

to position at an incident angle of 52° to the X-Y stage for all experiments. The fused silica capillary voltage was set to 5 kV and the MS inlet capillary was set at 285℃. The outer diameter and the inner diameter of the fused silica capillary carrying the spray solvent were 150 μm and 50 μm respectively. The distance of the silica capillary tip to the sample surface was 2.55 mm and 2 mm approximately to the mass spectrometer inlet. Nitrogen gas (N_2) and methanol were electrosprayed through the silica capillary tip which was positioned 2 mm above the sample plate into the MS inlet. A flow rate of 2.5 μL/min was maintained via a 500 mL syringe pump to prevent any damage to the surface of the paper under analysis (59). The MS injection time was 200 ms and 3 microscans were averaged. The mass range was set to *m/z* 200-1000 in full scan mode in positive ion mode for all of the experiments. The pressure of the nebulizing nitrogen gas was set to 100 psi. For optimization, rhodamine cations generated from a spot of red Sharpie ink was scanned. The spectrum showed highly intense species of rhodamine B at *m/z* 443. Additionally, a detected compound, *m/z* 245 in the thermochromic ink was used to autotune the LTQ mass spectrometer parameters for all further experiments.

2.5.3 DESI Analysis

For investigation of ink components, a circle-filled dot of Pilot Frixion ink was printed on a sheet of PTFE and later analyzed by DESI-MS.

For the characterization of the ink at room temperature (25°C), the Pilot Frixion erasable ball pen was used to draw a filled ink spot of 0.5 cm diameter on PTFE surface. The PTFE was cut into a 3 X 6 cm dimension rectangle and was fixed on a stainless steel sample plate using adhesive tapes. The stainless steel plate was then mounted on the DESI X-Y stage for analysis. A blank spectrum of the PTFE was obtained to observe the impurities on the surface and to normalize the signal before analyzing the erasable ink. For analysis of the heated ink, the same PTFE with

ink spot was heated with a laboratory blow dryer (~75℃) for 10 seconds and then analyzed again by DESI-MS. Furthermore, to analyse the ink upon cooling, the same ink spot was placed inside a freezer (-18℃) for 45 minutes followed by immediately examining it by DESI-MS to prevent additional contamination.

For further identification of the compounds detected by DESI-MS, tandem mass spectrometry (MS/MS) was performed using an Orbitrap mass spectrometer. Ink was extracted from the pen by the use of a Hamilton syringe. The extracted ink was then mixed with methanol, centrifuged at 12000g for 3 minutes and the supernatant was collected. The supernatant was then analysed by Orbitrap. Flow rate was maintained at 3 µL/min and Orbitrap with Fourier transform mass spectrometry (FTMS) ion detector was used for the analysis.

2.5.4 Paper Spray

Paper spray been proven to be beneficial to conduct analysis in real time and relatively easily and rapidly (83,102). Paper spray was performed to confirm the results obtained by DESI-MS as well as to do tandem mass spectrometry of the chemicals specific to the heated ink state (*m/z* 400, 405, 511 and 615). Printing paper was cut in triangular form and was made to stand at the same height of the MS inlet using a clamp stand. The paper was held by a clip which was subjected to 5 kV during analysis. Distance between the inlet and paper tip was always maintained around 4 mm. At the tip of the paper an ink spot was made using Pilot Frixion erasable pen and during the time of analysis methanol was drizzled using a pipette to carry the ink components from the paper into the MS inlet because of the generated electric gradient. All the analyses were done in the positive ion mode and the mass range scanned was *m/z* 200-1000.

2.5.5 TLC

TLC was performed to separate the ink components both in its original and invisible form

to understand if the compound *m/z* 405 and 786 (invisible ink markers) are products of reaction between different compounds in the ink composition upon heating or is it a component of the ink itself. Thermochromic ink was spotted on glass based silica HPTLC plates. Sharpie red ink was simultaneously used as control. The mobile phase used was methanol with 1% acetic acid (acetic acid improved separation of the ink components on silica plate). After running, the plates were air dried and using DESI with methanol as the solvent, the dried plates were analysed from retention factor (RF) 0 to 1. All the analyses were performed in the positive ion mode.

Two modes of heating were performed; heating the spotted ink on silica plate just prior to running it with methanol and acetic acid and heating the air dried developed silica plate before analysis by DESI-MS.

2.5.6 DESI-MS Imaging

DESI-MS imaging was conducted on both PTFE and printing paper surface to check the feasibility of using DESI to detect the heated markers of the ink on both kinds of surfaces.

A number "7" was hand-written on a new piece of PTFE with the Pilot FriXion erasable pen. The sample was then placed on the X-Y moving stage and by the DESI ion source, solvent (methanol) was sprayed across the sample for 40 minutes. The dimension of the sample (number "7") was 0.8 X1.0 cm. The second and the third DESI images were acquired from the heated and frozen ink lines respectively. For DESI-MS imaging, the DESI ion source and the sample stage parameters were set as follow: x-direction; 8000 μm, y-direction; 10000 μm, scan time; 0.94 ms, resolution, 200 microns; number of lines, 50; and total solvent volume; 235 μL.

The word 'CRMS' was hand-written on a new piece of printing paper with the Pilot FriXion erasable pen. The sample was then placed on the X-Y moving stage and analysed for 35 minutes. The dimension of the sample (CRMS) was 2.3 X 0.7 cm. The second and the third DESI

images of 'CRMS' were successively performed on the same written piece of paper upon heating and cooling the remaining ink traces respectively. For DESI-MS imaging, the DESI ion source and the sample stage parameters were set as follow: x-direction; 23000 μm, y-direction; 7000 μm, scan time; 0.52 ms, resolution, 200 microns; number of lines, 35; and total solvent volume; 157 μL.

The software BioMAP was used to create ion images in two-dimensional coordinates, Converter v3.0 was then used to translate Thermo Fisher LTQ '.raw' files into a format compatible with the imaging software BioMAP.

CHAPTER THREE

Characterization and Mapping of secondary metabolites of *Streptomyces sp*. from Caatinga by Desorption Electrospray Ionization Mass Spectrometry (DESI-MS)

3.1 Summary

The discovery of new secondary metabolites is a challenge to biotechnologists due to the emergence of superbugs and drugs resistance. The knowledge of biodiversity and the discovery of new microorganisms have become the major objective; thus, new habitat like extreme ecosystems become places of interest to research. In this context, Caatinga arises as an unexplored biome. The ecosystem of Caatinga is a rich habitat for thermophilic microbes. Its high temperature and dry climate influence selective microbes to flourish and establish. Actinobacteria (Caat 1-54 genus *Streptomyces spp.*) isolated from the soil of Caatinga was investigated to identify and map its secondary metabolites by desorption electrospray ionization mass spectrometry imaging (DESI-MSI). With this technique, the production of bioactive metabolites was detected and associated with the different morphological differentiation stages within a typical *Streptomyces spp.* lifecycle. High-resolution mass spectrometry, tandem mass spectrometry, UV-Vis profiling and NMR analysis were also performed to identify the metabolite ions detected by DESI-MS. A novel compound, which is presumed to be an analogue of the antifungal agent Lienomycin, along with the antimicrobial compound Lysolipin I were identified in this study. The potency of these bioactive compounds was further studied by disc diffusion assays. These bioactive metabolites may prove to be useful leads in the pharmaceutical industry especially when there is an arising concern of increasing resistance to the available drugs options with the emergence of superbugs. Consequently, the unexplored habitat of Caatinga unveils new possibilities for new bioactive compounds that are yet to be discovered.

3.2 Introduction

The understanding of biodiversity and the discovery of new microorganisms have become an inevitable part in the field of biotechnology, due to their potentials in generating a rich and

assorted library of new bioactive compounds. With the emergence of superbugs and the increasing resistance to available drugs in the pharmaceutical field, exploration of new sources of bioactive metabolites became essential(103,104). Unexplored habitats such as marine, mountains and deserts are thus places of interest to many biotechnologists (105). Accordingly, Caatinga has a unique biome that is still unexplored for biological potential and may prove to be an important source for new active compounds (106,107).

Caatinga is in the tropical zone having a hot semi-arid climate. Since the biome is located in semi-arid region, the soil has a lower amount of organic matter, with 50% being sedimentary and rich in groundwater (108). The average precipitation is about 250 to 1000 mm causing scarcity of water almost throughout the year (109). This molds the habitants in the ecosystem with a high resilience power because of their ability to adapt in extreme conditions.(110) The diversity of species is lower in relation to other biomes; however, there lies a high bioprospecting potential. Likewise the conditions are favorable for actinomycetes microorganisms, which mainly establish themselves in different kind of soils (111).

Actinomycetes have high GC (guanine-cytosine) content, Gram-positive bacteria with fungal morphology. Similarly to fungi it grows to form vegetative mycelium and produce spores (111). Although they have different characteristics in different biological backgrounds, their common features are assumed to be due to adaptation in similar ecological niches (112). Briefly, when the spore acquires suitable condition and nutrients, it germinates and grows into one or two germ tubes to become hyphaes. The vegetative hyphae grow perpendicular to form extension and branches also known as vegetative mycelium, which are evident over the surrounding substrate. Due to nutrient depletion and/or other factors, morphological differentiation causes the aerial hyphae to break open in air. The aerial hyphae fragments then start to divide to form chains of

prespore compartments that later mature into spores (113) (Appendix, section B, Figure B1). The spores typically can survive in the dormant state for a long time. Actinomycetes are a rich source of secondary metabolites having diverse biological activities. Overall, they contribute about 70% of the available antibiotics and various other non-antibiotic bioactive metabolites such as enzymes, enzyme inhibitors, immunological regulators, antioxidants which are of high commercial value and numerous practical uses. Among actinomycetes, the largest group studied is *Streptomyces sp*, accounting for up to 95% of the actinomycetes found in soil.(114,115) The actinobacterium was isolated from the rhizosphere of Caatinga, the part of the soil that is in direct contact with roots of the plants. It is a niche with great microbial diversity and likewise aids actinomycetes to reside and offer advantages to plants through the production of various bioactive compounds (116,117).

Currently, identification and investigation of any active metabolite from a microbe involves its isolation by performing the conventional chromatographic techniques with spectrometric mode of detection eg. HPLC, GC, UV-Vis, NMR and MS. All of these techniques require multiple sets of analysis to be performed prior to their detection and identification, thereby making the overall process time consuming and laborious. Matrix-assisted laser desorption ionization mass spectrometry (MALDI-MS) offers to solve this problem, since it can be used directly on the colony for instantaneous detection of metabolites. However, the use of matrix to ionize analytes for detection purposes also requires time for sample preparation (118,119). Desorption electrospray ionization mass spectrometry (DESI-MS) on the other hand being an ambient ionization technique, allows direct analysis of sample surfaces with almost no sample preparation and consequently is gaining popularity in various fields as a fast mode of analysis (40,120). Few studies involving DESI-MS have also been reported in the field of microbiology (121). The requirement of high spray and gas pressure to perform DESI hinders its use directly on

the agar plate or on soft uneven surfaces like fungi. Fungi, unlike bacteria, have soft and irregular morphology, due to the formation of spores and hyphae (46,49,122). In this work, actinobacteria were mapped for metabolites using DESI-MS imaging (DESI-MSI). Since actinobacteria have similar morphology to fungi, imprint DESI-MSI was performed for detection and mapping of metabolites (46,47). Along with imprint DESI-MSI, direct analysis and imaging of the bacteria was performed with the use of a glass slide inside an agar plate, as reported by Angolini *et al*, 2015 (123).

In this study, DESI-MS and DESI-MSI were used to detect, characterize and map secondary metabolites from actinobacteria Caat 1-54 colony (Streptomyces mashuensis, ATCC 2934) isolated from Caatinga. Production of these metabolites was monitored by performing analysis with different culture duration lengths (4 and 14 days) to better understand the environmental impact on their release. High resolution mass spectrometry (HRMS), tandem mass spectrometry, NMR and UV profiling were also performed to probe the structural features of the major metabolites (Figure 3.1) detected by DESI-MS. Inhibition bioassays with fungi, Gram positive and Gram negative bacteria were also conducted to check the potency of crude growth media of the bacterium.
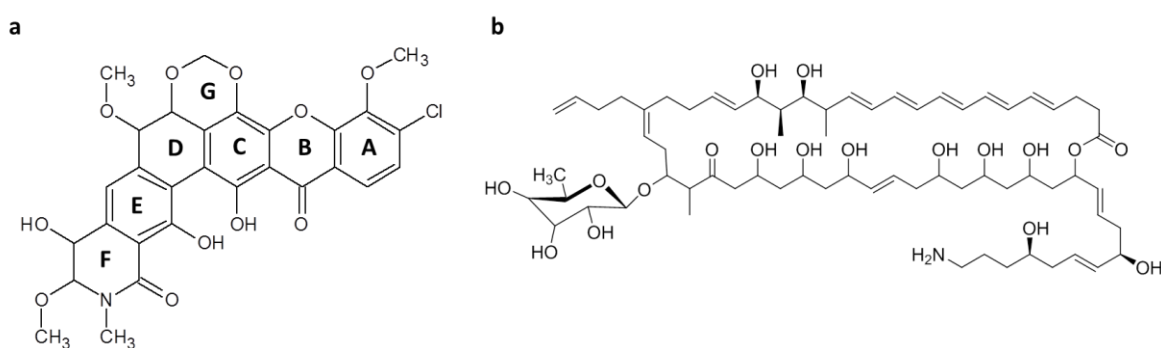
Figure 3.1: Structures of compounds identified a) Lysolipin I and b) Lienomycin.

3.3 Results and Discussion

3.3.1 DESI Analysis and Imaging

DESI analysis of the bacteria directly from a glass slide after 4 days and 14 days of incubation, the ions of *m/z* 1229, 626, 634, 606 and 598 were observed (Figure 3.2). To check if there were other detectable secondary metabolites produced by the bacteria, an imprint of the top surface of colony was made on double sided tapes. DESI analysis of the imprint showed relatively high abundance of the metabolite *m/z* 598 from both 4 days and 14 days incubation colony (Appendix, section B, Figure B3). Interestingly *m/z* 606, 626, 634 and 1229 were absent on the spectrum obtained from the imprint. Hard imprinting (hard press on the tape for long duration) on the double sided tape, showed the presence of both *m/z* 598 and 1229 but at a relatively low signal intensity compared to direct analysis from a glass slide or soft imprint on tape. These observations led to the conclusion that the cream colored cells were the new dividing cells near to the media surface. As further cells divided the old ones were pushed to the top. Due to nutrition depletion the top layer dries up, and under stress, the bacteria (aged cells) produce the compound at *m/z* 598; upon pressing it hard to get an imprint, the aged cells cover the top of the tape along with some young cells from underneath, where ion of *m/z* 1229 becomes apparent. Since the dry aged bacterial cells residue resided at the top of the tape imprint, the signal to noise ratio of both the ions, *m/z* 598 and 1229, appeared low (Appendix, section B, Figure B3c). All the scans were performed several times (more than three times) and the profile obtained was reproducible.

Our hypothesis was further supported by the results obtained by DESI imaging. Spatio-temporal distribution of the compounds was checked by performing DESI-MSI. It was observed that the compound at *m/z* 1229 was only apparent both at the center and edges after 4 days of incubation (Figure 3.3) but only on the edges after 14 days of incubation. Optical images (Figure

3.3a and 3.3b) depict the presence of *m/z* 1229 ion was only evident at the cream colored region of the bacteria. This supports that the secondary metabolite at *m/z* 1229 was synthesized by the healthy young cells of the bacterial colony. When these young cells (cream colored) were covered by old cells (white colored) the signal for *m/z* 1229 declined, which is the reason while mapping the ion of *m/z* 1229 in the ion images the compound did not appear as a full solid circle.
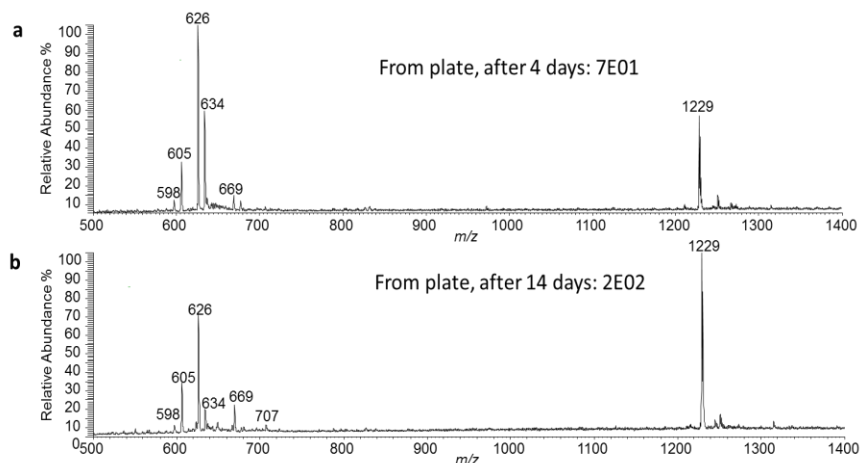
Figure 3.2: DESI-MS scan directly from a glass slide. a) DESI-MS scan of a colony after 4 days of incubation at 37°C on a potato agar plate. 7E01 represents the intensity of the most abundant ion. b) DESI-MS scan of a colony after 14 days of incubation at 37°C on a potato agar plate. 2E02 represents the intensity of the most abundant ion.
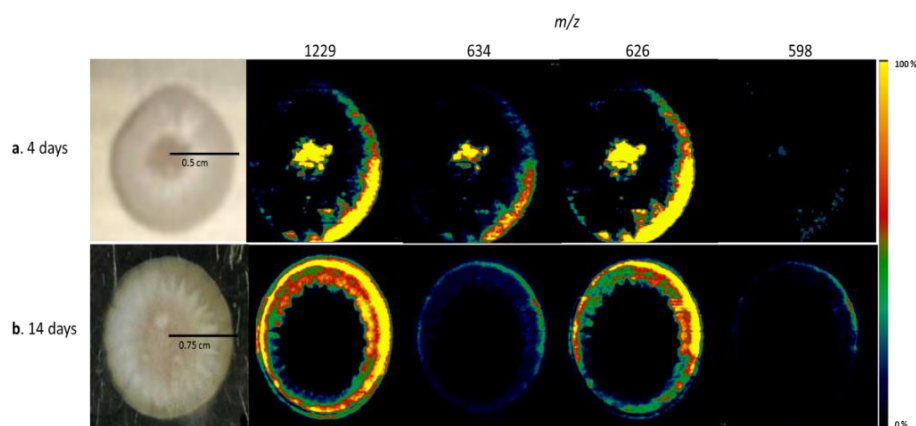
Figure 3.3: DESI-MS imaging (DESI-MSI) of a colony directly from a glass slide. a) DESI-MSI of a colony after 4 days of incubation at 37°C on a potato agar plate. b) DESI-MSI of a colony after 14 days of incubation at 37°C on a potato agar plate.

In contrast, the ion of *m/z* 598 appears at the top surface of the dried bacterial residue. Imprinting from the top surface by a tape helps to trap the dried surface on the sticky tape film and thus can be imaged adequately by DESI-MSI (Figure 3.4). The high gas pressure blows away most of the dried material while rastering through the colony surface for data acquisition during imaging directly from the glass slide. Furthermore, spectra from the imprints showed the ion of *m/z* 583, which is a characteristic peak from the tape (Appendix, section B, Figure B3). The abundance of this ion assists in understanding the production pattern of the compound at *m/z* 598. Several scan analyses of tape imprints for both 4 and 14 days led to the conclusion that after 4 days of incubation the compound at *m/z* 598 is relatively less produced compared to the amount produced after 14 days of incubation (Figure B3a, B3b, 4a and 4b) with respect to the ion at *m/z* 583.
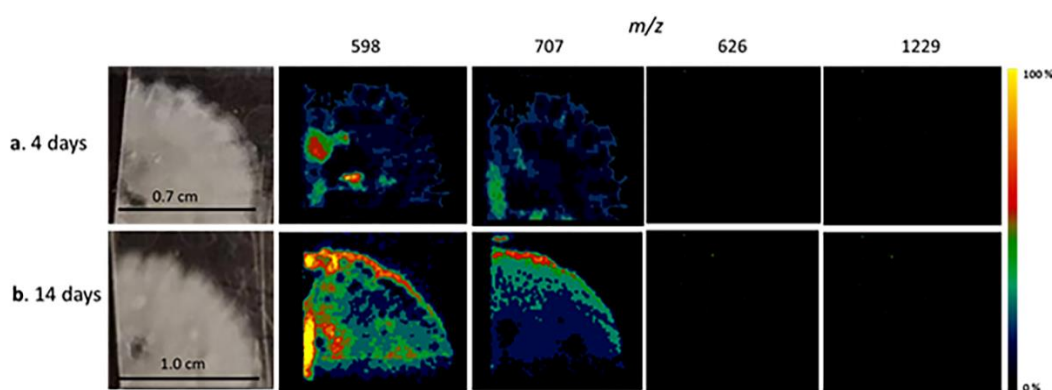
Figure 3.4: DESI-MS imaging (DESI-MSI) of an imprint of a colony on double-sided tape. a) DESI-MSI of an imprint of a colony after 4 days of incubation at 37°C on a potato agar plate. b) DESI-MSI of an imprint of a colony after 14 days of incubation at 37°C on a potato agar plate.

Based on conventional analytical techniques associated with databases search such as the Dictionary of Natural Products and high resolution mass spectrometry and tandem mass spectrometry (described later in detail), the ion at *m/z* 1229 was identified as an analogue of Lienomycin and the ion at *m/z* 598 as Lysolipin I. Therefore, we hypothesize that the production of the Lienomycin analogue occurs during the formation of germ tube and vegetative mycelium.

On the other hand, Lysolipin I is associated with the sporulation stage (113). DESI-MS not only helps to identify and localize the metabolites, but also aids in understanding their roles in the bacterial life cycle under different environmental conditions. In conclusion, all these observations suggest that the bacteria under stress condition produce the compound *m/z* 598 whereas healthy viable bacterial cells produce mostly the metabolite *m/z* 1229. This is also supported by the colony images obtained upon imaging them directly from glass slides, as after 4 days it is seen that the cream colored cells (optical image) and the spatiotemporal distribution of the compound at *m/z* 1229 is relatively higher than that observed in the optical image and chemical images of colony after 14 days of incubation.

Along with *m/z* 598, 605, 626, 634, and 1229, DESI-MS spectrum depicts that Caat 1-54 also produces many other secondary metabolites at *m/z* 669, 707 and others, which have relatively low abundance or ionization efficiency in the current extraction solvent and thus needs other solvents or conventional means of characterization through separation by HPLC prior to their identification.

3.3.2 High Resolution and Tandem Mass Spectrometry

The dried potato dextrose agar plates with the bacteria colony was soaked in DESI spray solvent, vortexed and centrifuged to obtain an extract which was further diluted 500 folds with the same solvent prior to direct infusion into the mass spectrometer to perform high resolution and tandem mass spectrometry. Initially, the crude extract was analysed by high resolution mass spectrometry (HRMS) to identify the compounds apparent while performing DESI-MS and DESI-MSI. Remarkable amount of ions at *m/z* 598.1114, *m/z* 605.3605, *m/z* 625.8626, *m/z* 633.8497 and *m/z* 1228.7489 were observed in the DESI-MS scan. The HRMS spectrum (Appendix, section B, Figure B4) upon direct infusion showed presence of these ions that enabled their structural

identification through tandem mass spectrometry (MS/MS). Table 3.1 summarizes the mass discrepancies calculated between the proposed theoretical masses and the experimental parent and fragment ions observed. For all ions the difference observed was below 3.5 ppm. Among the tentatively identified ions, one of the secondary metabolites released by actinobacteria Caat 1-54 have been previously isolated and identified using conventional analytical techniques, such as high performance liquid chromatography-mass spectrometry (HPLC-MS) and nuclear magnetic resonance (NMR)(124) was Lysolipin I (Figure 3.1a), and other most abundant, readily ionized secondary metabolite detected and identified in this work is a new compound, an analogue of Lienomycin, the macrolide polyene pentaene (Figure 3.1b) (125).

Table 3.1: Discrepancy between the observed and theoretical exact masses as observed with HRMS from the Orbitrap mass spectrometer.

Parent Ion	Fragments Measured mass	Calculated Exact Mass	Formulae	ppm Difference
1228.7389		1228.7359	$C_{67}H_{106}NO_{19}$	2.44
	1210.7254	1210.7253	$C_{67}H_{104}NO_{18}$	0.08
	1192.7154	1192.7148	$C_{67}H_{102}NO_{17}$	0.50
	1174.7042	1174.7042	$C_{67}H_{100}NO_{16}$	0
	1156.6936	1156.6936	$C_{67}H_{98}NO_{15}$	0
	1064.6695	1064.6673	$C_{61}H_{94}NO_{14}$	2.07
	1046.6554	1046.6569	$C_{61}H_{92}NO_{13}$	1.43
605.3615		605.3627	$[C_{67}H_{104}NO_{18}]^{+2}$	1.98
625.8626		625.8628	$[C_{67}H_{106}NO_{19}Na]^{+2}$	0.32
633.8497		633.8498	$[C_{67}H_{106}NO_{19}K]^{+2}$	0.16
598.1114		598.1116	$C_{29}H_{25}ClNO_{11}$	0.33
	568.1019	568.1011	$C_{28}H_{23}ClNO_{10}$	1.41
	537.0578	537.0589	$C_{27}H_{18}ClO_{10}$	2.05

Lysolipin I was isolated for the first time in 1975 (126) from *Streptomyces violaceoniger Tü* 9629 and later from *Streptomyces tandae Tü* 4042 (127). It is an important antimicrobial polyketide, which has activity against a high range of Gram - positive bacteria and thus can be used as a lead compound for the development of drugs. Lysolipin I has a cyclic amide, which is

rarely found in aromatic polyketide (ring F in Figure 3.1a). The compound is presumed to interact with a lipid carrier namely C_{55}-bactoprenol, which is involved in the cell wall synthesis of Gram positive bacteria (128). Collision-induced dissociation (CID) of the precursor ion of *m/z* 598 (Lysolipin I) having ^{35}Cl isotope, showed fragment ions at *m/z* 568 and *m/z* 537, attributed due to the loss of CH_2O (30 Da) from ring G and the sequence loss of CH_3NH_2 (61 Da) from ring F, respectively (Appendix, section B, Figure B5a).

Polyene antibiotic belongs to an enormous set of antifungal agents, produced mainly by *Streptomyces*. These compounds are amphipathic in nature and have been proposed to interact with sterols from membrane with their hydrophobic portion to form complexes; thus altering the permeability in fungi and yeast, but not in bacteria (129–135). For the assignment of the ion at *m/z* 1229, along with UV-Vis profiling (Appendix, section B, Figure B4) and tandem mass spectrometry (Appendix, section B, Figure B5b), NMR experiments were also performed.

Most polyene macrolides have a sugar moiety attached with macrocyclic ring by glycosidic bond. They usually have aminosugar, mycosamine, but in case of Lienomycin, there is a rhamnose (136). The loss of this neutral sugar was observed in the CID spectrum of *m/z* 1229, with the formation of a product ion of *m/z* 1064.6695 upon a neutral loss of 164 Da, Figure 3.5b. The other product ions were characterised as sequential losses of water, while the lactone ring remained intact. Amphotericin and nistatin are polyene macrolides and their fragmentation patterns reported by Ulrych *et al*.(137) were similar to that observed here for the *m/z* 1229 ion using the orbitrap mass spectrometry. For amphotericin and nystatin, a loss of 163 Da was attributed to the loss of the mycosamine moiety (Appendix, section B, Figure B7). While the fragmentation pattern of *m/z* 1229 depicts a neutral loss of 164 Da relating to the loss of a neutral rhamnose moeity, reinforcing the hypothesis of its similarity with Lienomycin structure (Figure 3.1b).

The structural details of the macrolide compound as to the position of hydroxylation followed by double bonding are not determined due to the complexity of overall bulky molecule. The fragmentation profile and ultraviolet absorption spectrum suggest that the ion of m/z 1229 is a polyene pentane analogue of Lienomycin (Figure 3.1b). To support this hypothesis, NMR experiments were conducted in order to identify a few key aspects of the molecule. Due to the complexity and the instability of the isolated compound, the exact structure of the compound was not completely determined.

Likewise, it is suggested that the antibiotic is an analogue of Lienomycin, a novel compound ($C_{67}H_{105}NO_{19}$) not yet described in previous literatures, with the structural modification of a further hydroxylation and an additional C=C double bonding. In proposing this hypothesis, the difference between the theoretical mass and the observed mass obtained by HRMS was 2.44 ppm. (Table 3.1)

The other ions at m/z 605, 626 and 634 are doubly charged ions, observed by the profile shown in Figure B8 (Appendix, section B). The ions at m/z 626 and m/z 634 corresponds to the adducts $[M+H+Na]^{+2}$ and $[M+H+K]^{+2}$ respectively, and m/z 605 corresponds to the doubly charged ion of the major fragment ion of m/z 1210, formed from the parent ion m/z 1229. All the observed masses showed below 3 ppm difference with their theoretical exact masses as presented in Table 3.1.

3.3.3 UV-Visible Profiling

A relatively large number of polyenes were recently reported as metabolites from actinomycetes (133). These molecules were characterised by the presence of a hydroxylated macrocyclic lactone ring, usually attached with a sugar moiety; typically they are recognised based on of the characteristic chromophoric property observed due to the presence of three to seven

conjugated double bonds in the macrolactone ring. These structures are commonly very large, bearing a lactone ring of 26-44 carbons atoms and are named as trienes, tetraenes, pentaenes, hexaenes and heptaenes, based on the number of conjugated double bonds. They also display unique physicochemical properties, which includes strong UV-visible light absorption and poor water solubility (138).

The UV-Visible light absorption spectra of this set of compounds show characteristic multipeak pattern which is associated with the number of conjugated double bonds in the structure (130,138). Polyenes with five conjugated double bonds, (pentaenes), show UV bands around 317, 331 and 349 nm (139). The absorption profile observed with the compound at m/z 1229 was similar having bands at 318, 333 and 349 nm (Appendix, section B, Figure B6). Thus the presence of three coincident peaks in the absorption profile assisted in characterising the ion at m/z 1229 as likely being a pentene (140), analogous of Lienomycin. Usually, purification of these compounds requires multiple chromatographic separations, but since concomitant degradation was also evident, rather than improving the purity level, impurities from degradation built up. However, in the region of 300 nm there was relatively low interference due to degradation products in the UV profile.

3.3.4 NMR Analysis

Upon isolation of the compound, the ^{1}H and ^{13}C spectra (Appendix, section B, Figures B9 and B10 respectively) were acquired. The ^{1}H NMR spectrum displayed signals in the vinylic region between δ5-7.5 along with alcohol related aliphatic hydrogen from δ3.5 to 4.5. Despite the low sensitivity, the ^{13}C spectrum shows a peak at 169.4 ppm consistent with the presence of an ester carbon (C_1). Several other signals between δ125.5 - δ137.0, δ60 - δ80 ppm and δ18.3 - δ46.5 are representative of olefinic, carbinolic and aliphatic carbons respectively. The low sensitivity of

the ^{13}C spectrum led to the indirect study of J (^1H-^{13}C) couplings using the HSQC-DEPT experiment as shown in Appendix, section B, Figure B11.

Figure B11 distinctly shows four regions of vinylic hidrogens and ^{13}C nuclei between $\delta 7.5$ and $\delta 5.3$ in the hydrogen domain and $\delta 140$-120 in the ^{13}C domain. There are also numerous peaks consistent with carbohydrate components between $\delta 4.3$ to 3 and $\delta 85$ to 60 in the hydrogen and ^{13}C domains respectively. Methylene correlations can be seen from $\delta 3.3$ to 1.2 and $\delta 50$ to in the hydrogen and ^{13}C domains respectively. In the upper right corner of the spectrum are correlations (blue) consistent with CH/CH$_3$ groups.

Additional longer range J (^1H-^{13}C) couplings can be viewed in the 2D HMBC spectrum as shown in Appendix, section B, Figure B12. This spectrum shows long range coupling between vinylic hydrogens (H$_{23}$) and methylene (C$_{24}$) at around $\delta 40$ as well as between vinylic hydrogens (H$_{23}$) and carbinolic carbons (C$_{25}$) near $\delta 65$. There is also unique long range correlation between hydrogen at $\delta 0.93$ and the carbonyl (C$_{27}$) at $\delta 210$. This correlation is consistent with a carbonyl ketone carbon resonance.

Finally, an experiment was performed to detect the presence of the nitrogen atom. Figure B13 (Appendix, section B) depicts the resultant spectrum obtained upon combining HMQC and ^{15}N NMR spectra; and it was possible to verify the existence of long distance nitrogen with correlation signals at $\delta 120$ with hydrogens at $\delta 1.78$. Due to the equidistant equivalence of the neighboring peaks, the central peaks represents a nitrogen atom in the molecule apparent as an NH$_2$.

3.3.5 Disc Diffusion Study

A Disc diffusion study was performed to further verify the production of the antibacterial and antifungal agent identified as Lysolipin and Lienomycin analogues respectively by mass

spectrometry. Figure B14 depicts that the crude extract is active against fungus (*P. roqueforti*) and Gram- positive bacteria (*B. subtilis*) but inactive against Gram negative bacteria (*E. coli*). The plate from 14 days of Caat 1-54 incubation, produced a larger zone of inhibition than the media extracted after 4 days of incubation of Caat 1-54 and this can be attributed to the increased accumulation of the active metabolites in the culture media due to a prolonged time of incubation. Higher concentration of Lysolipin and Lienomycin analogue in the culture media resulted in an increased activity against bacteria and fungus. Again, the crude media proved to have a more potent antifungal effect than an antibacterial as comprehended from the size of the diameter of the zone of inhibition (Figure B14). An average diameter of 4 mm inhibition zone was measured from the *P. roqueforti* plate having discs with media obtained after 14 days of incubation for Caat 1-54. In case of *B. subtilis* the zone was measured to be around 2 mm in diameter from the same 14 days media extract.

The zone of inhibition was imaged by DESI-MS using the moving stage to map the distribution of active components (Figure 3.5). It was found that compounds from the growth media uniformly diffused into the zone of inhibition, and at the point where the microbe (fungus or bacteria) starts re-establishing, their intensity was the least. All these observations reinforce that the compounds *m/z* 598 and 1229 are actually responsible for inhibition of growth of the bacteria and fungus, forming the clear zone of inhibition. Their radial diffusion from the disc onto the agar plate restricted the growth of the microbe around the disc, at the zone of inhibition (clear region); once the concentration reduces below the minimum inhibitory concentration, the microbe starts to re-establish. Figure 3.5i maps ions at *m/z* 699 from the fungal surface whereas figure 3.5j and 3.5k map two ions at *m/z* 745 and 793 from agar plate to show that they have uniform intensity throughout the region mapped. The region where the disc was placed appeared dark when mapped

45

for the compounds from the growth media (Figure 3.5d-h). This led to the assumption that after the required incubation time the disc went dry and so imprinting from it did not result in sufficient amounts of compounds getting transferred to the PTFE surface. Again the radial diffusion from the disc itself reduced its actual concentration and thus appeared to be devoid of those compounds at that specific region.
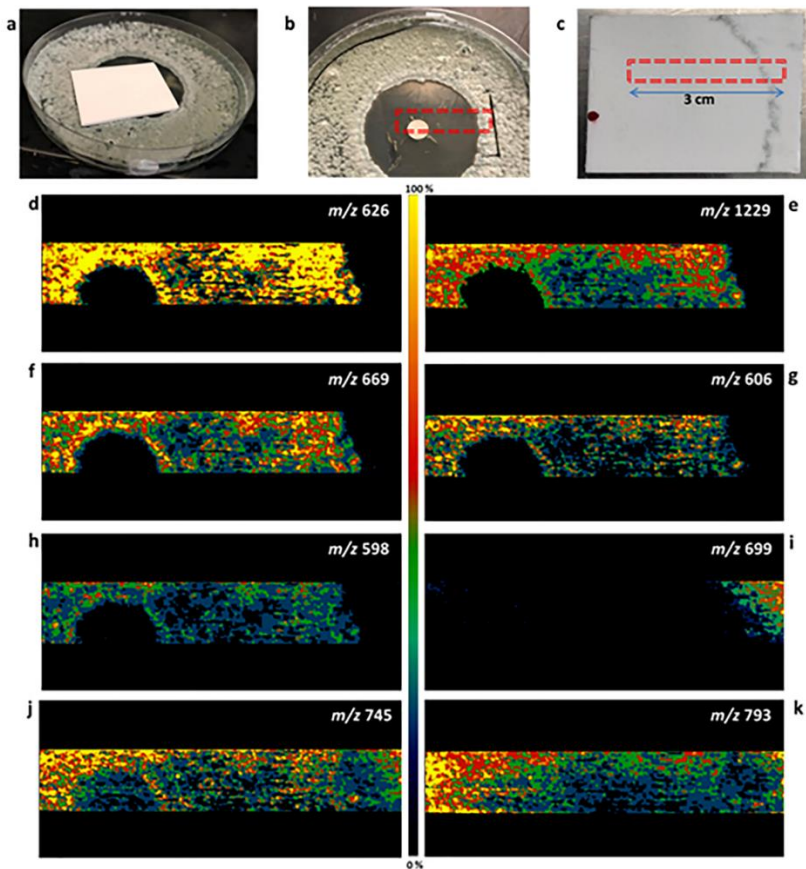
Figure 3.5:DESI-MS imaging of the zone of inhibition by imprinting on a PTFE surface. a) Optical image of the PTFE on the agar plate. b) Optical image of the agar plate with the red border enclosed area representing the region imaged. c) Optical image of the imprint on PTFE surface with the red border enclosed area representing the region imaged. d) Ion image showing the distribution of the m/z 626 ion in the region image. e) Ion image showing the distribution of the m/z 1229 ion in the region image. f) Ion image showing the distribution of the m/z 669 ion in the region image. g) Ion image showing the distribution of the m/z 606 ion in the region image. h) Ion image showing the distribution of the m/z 598 ion in the region image. i) Ion image showing the distribution of the

m/z 699 ion in the region image from the fungus. j) Ion image showing the distribution of the *m/z* 745 ion in the region image from the agar plate. k) Ion image showing the distribution of the *m/z* 793 ion in the region image from the agar plate.

3.4 Conclusion

Based on the morphological differentiation of Streptomyces, compounds identified in this work can be correlated with the life cycle of the bacterium. We hypothesize that the analogue of Lienomycin is produced during the initial step in the formation of the germ tube and vegetative mycelium. On the contrary, Lysolipin I may be a product of the sporulation stage. It is evident from this study that Caat 1-54 is an excellent source of useful secondary metabolites. The crude growth media do not require any sample preparation like isolation and/or concentration of the active compound to exhibit their activity and this demonstrates the efficacy of the compounds as an antifungal and anti-Gram-positive agent. Direct and imprint DESI-MSI show different distribution profiles of metabolites which reinforces the need for three dimensional mapping of the bacterial colony to enable detection and characterization of all the metabolites released by the bacterium at different stages of its lifespan. Ambient techniques such as DESI-MS and DESI-MSI proved to be very useful to monitor, characterize and map metabolites directly from the bacteria. In conclusion, Caatinga is a rich habitat that needs more attention to explore the prevalent wide range of thermophilic microbes. The region will be of high interest to biotechnologist as it will serve as a potential source of new lead compounds.

3.5 Experimental

3.5.1 Materials

Yeast malt broth (ISP 2), Luria-Bertani (LB) medium, Potato dextrose agar (PDA), and Agar were purchased from Sigma-Aldrich (Oakville, ON, Canada). Chemicals (Formic acid,

Thiazolyl blue tetrazolium bromide/MTT, Resazurin sodium salt) and solvents (acetonitrile, methanol and water) were HLPC grade purchased from Sigma-Aldrich (Oakville, ON, Canada). Glass slides were purchased from Sigma-Aldrich (Oakville, ON, Canada) and Polytetrafluroethylene (PTFE) was imported from Bergohf (Germany). 12.7 mm x 33 m Scotch double sided tape, 3M, 665 was purchased from York University book store (Toronto, ON, Canada). 100 X 15 mm Petri dishes and filter paper of medium porosity were purchased from Fisher Scientific (Pittsburg, PA, USA). *Streptomyces* sp. designated as Caat 1-54 characteristic of the Caatinga soil was obtained from Prof Dr Itamar Soares de Melo from EMBRAPA-Environment, Brazil. *Penicillium* sp. (*P. roqueforti*) was selectively grown from blue cheese sold in Shoppers Superstore (North York, ON, CA). York University (ON, Canada) Biology Department was generous to provide us with *Escherichia coli* (DH5-Alpha) and *Bacillus subtilis* 168 stains used in the teaching labs. A Thermo Fischer Scientific LTQ mass spectrometer (San Jose, C.A., USA), a Thermo Scientific Orbitrap Elite mass spectrometer (San Jose, CA, USA) and Xevo TQ-S™ Waters equipped mass spectrometer (Milford, Massachusetts, USA) were used to conduct this study. Compounds were purified by LC-MS using, liquid chromatography Shimadzu (Sao Paulo, Brazil) with CBM-20ª, two pumps of LC-6DA and UV-Vis SPD-20A detector. Liquid Chromatograph Acquity-UPLC™ (Milford, Massachusetts, USA) coupled to a tandem mass spectrometer Xevo TQ-S™ Waters was used for UV-Visible profiling of the purified compound. A Bruker Advance III HD 600 (14,IT) spectrometer with a Triple Inverse TCI Cryo-probehead (Rheinstetten, Germany) was used for acquiring NMR data.

3.5.2 Bacterial and Fungal Culture Conditions

Autoclaved ISP-2 media were used to inoculate with Caat 1-54 glycerol stock. The culture was grown overnight (16-18 hours) at 37°C, 200 rpm. Next day single spore was collected from

the flask using a 1000 µL pipette tip and was placed on top of a previously made PDA plate having glass slide underneath. The PDA plate with the bacteria was incubated at 37 °C for 4 to 14 days. After the required incubation time, the plates were stored at 4°C until further use to perform DESI-MS and DESI-MSI experiments to map secondary metabolites.

For performing disc diffusion assay, crude bacterial growth medium was used. The media extracts were obtained upon incubating Caat 1-54 in ISP-2 media at 37°C, 200 rpm for 4 and 14 days. After the required incubation times, the medium was centrifuged to get rid of the bacterial residues followed by impregnating them on a disc made from filter papers.

Penicillium sp. (*P. roqueforti*) was selectively grown from blue cheese. Briefly, using a pipette tip the blue fungi was scraped off from the cheese and was used to inoculate previously autoclaved distilled water. The resulting solution was incubated at 28°C without shaking for 48 hours. After two days, 600 µL of the solution was spread on a previously made PDA plate using a glass rod and the plate was later incubated at 28°C for a further two days.

For both *E. coli* and *B. subtilis* 168, the respective bacterial glycerol stock was used to inoculate autoclaved LB media. The seed culture was grown for 16-18 hours at 37°C for *E. coli* and 30°C for *B. subtilis* at 200 rpm. Next day 600 µL of the culture solution was poured on to LB agar plates to perform the disc diffusion study. The respective plates of *E. coli* and *B. subtilis* were incubated at their respective temperatures (30°C for *B. subtilis*, 37°C for *E. coli*) for another 16 hours.

3.5.3 DESI-MS and DESI-MSI Experiments

After four and fourteen days of incubation of the Caat 1-54 strain on the PDA plate at 37°C, the solid media dried into a thin film. Prior to running DESI-MS and DESI-MSI experiments a glass slide having a single colony was separated from the dried plate (123) (Appendix, section B,

Figure B2) and was fixed on a custom built 2D moving stage by the use of adhesive tapes, or using a double-sided tape imprint from the colony adhered on a glass slide. Typical instrument parameter such as capillary voltage was set at 5 kV and the capillary temperature at 285°C. The mobile phase used was a mixture of methanol, water and formic acid in the ratio 9/0.9/0.1 respectively. The flow rate of the solvent was maintained at 5 µL/min with simultaneous nebulization by N_2 gas set at 100 psi. The sprayer was kept at an incident angle of 52-54°, 1-2 mm above the slide surface and 2-4 mm away from the inlet of the mass spectrometer to maintain an overall collection angle of 10-12° into the inlet of the mass spectrometer. All the analysis was performed in positive ion mode scanning the mass range of *m/z* 500-1400. The MS injection time was set to 200 ms and three scans were averaged to obtain a spectrum. Data acquisition and management was performed using X-calibur 2.0 software from Thermofischer Scientific (San Jose, C.A., USA).

For DESI imaging, the sprayer was rastered over the sample surface in the horizontal direction at a constant speed of 179 µm/s until 90 to 130 vertical rows were scanned to obtain a full image. DESI-MSI spatial resolution was achieved by setting the coordinate or pixel size to 150 µm. Prideaux *et al*, 2014 reported that the resolution of DESI-MSI is restricted to the inner diameter of the capillary carrying the charged solvent and the distance it is placed away from the surface under analysis (38). In the study the inner capillary used to carry the charged solvent had a diameter of 50µm, so a pixel size set to 150 µm ensured greater area for solvent contact and thereby higher signal intensity and also minimal region of overlap between spots. No further reference was used to assess the resolution accuracy. BioMap imaging software compatible with the X-calibur spectral data was used to obtain ion images in two dimensional coordinates.

3.5.4 High Resolution Mass Spectrometry

To identify the secondary metabolites tandem mass spectrometry was performed using an

Orbitrap Elite mass spectrometer. An extract of the bacterial culture was made prior to performing high resolution analysis. Briefly, dried potato dextrose agar plates with the bacteria colony were soaked in 1 mL of methanol, water and formic acid (DESI spray solvent) solvent for 10 minutes. The mixture was vortexed for complete extraction of the metabolites from the plate. Further, it was centrifuged at 12000g for 2 minutes to separate the immiscible component from the miscible part. The resultant solution was diluted 500 folds with the same solvent prior to direct injection into the mass spectrometer to perform tandem mass spectrometry. The low rate was maintained at 5 µL/min and mass resolution was set at 120,000. The collison energy used was between 25-30% (manufacturer's unit). The Orbitrap mass analyzer was used to discriminate between ion masses.

3.5.5 Disc Diffusion Assay

Caat 1-54 strain was grown in ISP-2 medium for 4 to 14 days at 37°C and 200 rpm. At the end of either 4 or 14 days the resultant media was separated from the bacteria by centrifugation at 3000g for 3 minutes. Discs were made using filter paper of medium porosity and by a paper punch. 100 µL of the centrifuged media was used to soak each disc to be used for conducting the inhibition study. Using a glass rod *B. subtilis*, *E. coli*, and *P. roqueforti* were evenly spread on their respective agar plates from overnight seed culture. Upon spreading, the culture solution was allowed to dry for some time (3-5 min) inside the bio safety cabinet. Using tweezers the soaked disk was placed at the center of the plate and pushed a little deeper for enhanced diffusion of the media components into the agar. Later the plate was incubated at 28°C for *P. roqueforti* for 48 hours and 16 hours for *B. subtilis* and *E.coli* at 30 and 37 °C respectively. Using a ruler the diameter of the zone of inhibition was measured. The imprint of the inhibition zone was also taken on the PTFE surface for further analysis about the distribution of the chemical determinants from the impregnated disc on the agar surface by DESI-MS.

As negative control, discs were soaked in autoclaved ISP-2 media prior to introduction in the respective culture plates of *B. subtilis*, *E. coli*, and *P. roqueforti* and were incubated for the same duration of time as the test plates.

3.5.6 Isolation and Purification of Compounds

The actinobacterium Caat 1-54 was fermented in large scale (6L). To isolate Lysolipin I, the crude extract was separated by preparative HPLC, using column Shim-Pack C18 (19 X 250mm, 5µm). In the case of the Lienomycin analogue, the crude extract was pre-purified using size exclusion chromatography utilizing Sephadex (LH-20) as the stationary phase and methanol as the elution solvent. The fractions were analyzed by mass spectrometry to check their constituents. Fractions containing the ion at *m/z* 1229 were combined and separated by semi-preparative HPLC, using C18 column Zorbax Eclipse XDB (Agilent 250 x 9.4 mmm, 5µm).

For Lysolipin, the chromatographic conditions had a linear gradient with the mobile phase A (ultrapute water with 0.1% formic acid) and B (methanol with 0.1% formic acid) starting at 30 %B and increasing to 98% within 10 minutes and keeping this percentage within the next 50 minutes and finally returning to the initial condition at the flow of 16 mL/min. The λ (nm) scanned was 280 nm and 310 nm.

For Lienomycin analogue, the chromatographic conditions were the linear gradient with the same mobile phase as for Lysolipin, starting at 30 % B and increasing to 50% within 5 min, followed by a further increase to 72% within 10 min and then to 80% B within the next 40 min and finally returning to its initial condition at the flow rate of 15 mL/min. The λ (nm) scanned was 320 nm and 332 nm.

Liquid Chromatography Shimadzu was used with CBM-20ª, two pumps of LC-6DA and UV-Vis SPD-20A detector. Data was acquired by Labsolution software.

3.5.7 UV-Vis Profiling

The UV analyses were characterized on a Liquid Chromatograph Acquity-UPLC™ coupled to a tandem mass spectrometer Xevo TQ-S™ Waters equipped with an electrospray ion source TQ-S mass spectrometer, quaternary pump and an automatic injector coupled to a PDA UPLC Acquity™ (Waters®). The chromatographic conditions were Ascentis Express HPLC Column F5 (10 cm x 2.1 mm, 2.7 μm), eluents A (acetonitrile with 0.1% formic acid) and B (ultrapure water with 0.1% formic acid) starting with 90% A and decreasing this percentage to 10% A within 12 min, followed by returning to the initial condition within 15 min at a flow rate of 0.5 mL/min; scanning the region between 200 nm to 800 nm wavelength. Data was acquired with MassLynxV4.1 software (Waters Corp., Milford, MA, USA).

3.5.8 NMR Analysis

NMR experiments were conducted using Bruker Avance III HD 600 (14,IT) spectrometer with a Triple Inverse TCI Cryo-probehead. Experiments performed were ^{1}H, proton decoupled ^{13}C, HMBC, HMQC, ^{15}N HMBC and TOCSY to characterize the ion at *m/z* 1229.

CHAPTER FOUR

Quantitative Assessment of 5-Hour Energy drink using Thin Layer Chromatography-Desorption Electrospray Ionization Mass Spectrometry (TLC-DESI-MS)

- Prova, S. S., Paraparasingam, E., Ifa, D. R.

The manuscript of this study is in process.

4.1 Summary

In this study a simple analytical technique, thin Layer Chromatography coupled with desorption electrospray ionization mass spectrometry (TLC-DESI-MS), was used to establish the presence of trace amounts of illicit drugs in commercial energy drinks. Amphetamine, one of the most abused drug, was spiked in 5 Hour Energy Drink to develop a detection method using TLC-DESI-MS. The detection limit (LOD) by this technique was determined to be 100pg.

Caffeine is the energy-deriving ingredient in most energy drinks. Quantitative assessments were demonstrated by three DESI-MS modes of quantitation: (1) standard calibration utilizing TLC-DESI-MS analysis; (2) a calibration curve using the ratio between deuterated caffeine (d_9) and standard caffeine through TLC-DESI-MS analysis; and (3) direct spot analysis by DESI-MS. Additionally, paper spray quantitation was also performed to check the reliability of the aforementioned quantitation methods by TLC-DESI-MS. The results retrieved from all methods showed reliability and reproducibility with less than 5% relative standard deviation.

4.2 Introduction

According to a 2013 survey, globally on an average about 30% of drivers abuse with amphetamine and 3% with cocaine (141). People mostly consume energy drinks to keep themselves awake and alert. Researchers at the University of Maryland's School of Public Health concluded that consumption of sugars and energy drinks increases the likelihood that young adults will abuse with illicit drugs in later years (142).

Determining the presence of illicit drugs in drinks is essential as it not only concerns the health of an individual taking it, but also the safety of others in a society. Truck drivers were found to mix amphetamine or other stimulants for non-medical use in their drinks (energy drinks or coffee) to keep them awake during long trips (141). Thus accurate determination of these

compounds is critical for prevention of illicit drug abuse. Energy drinks usually have caffeine as an active ingredient, but caffeine is not the only factor responsible for boosting energy. The drink also constains some vitamins such as B3, B6, B9 and B12 and an energy blend which comprises of malic acids, taurine, glucuronolactone, citicoline and amino acids (phenylalanine and tyrosine) (143). The focus of this study was to develop a simple analytical approach which will determine the presence of both caffeine and illicit drugs, if any, in an energy drink sample. Determination of the limit of detection (LOD) of illegal drugs is necessary to understand the extent to which the method can be applied to detect the drugs.

Among most analytical techniques, mass spectrometry is one of the fastest growing technologies with various applications in the field of proteomics, environmental studies, food analysis and forensics (14,144). Desorption Electrospray Ionization (DESI) is a mode of ionization which allows surface analysis under ambient conditions (14,144,145). The method was introduced by Cooks and co-workers in 2004 (145) and the analysis of surfaces with an automated imaging system was demonstrated by Ifa *et al* in 2007.(146) DESI-MS is well known for its potential in detecting a broad range of compounds including small non-polar molecules or large polar molecules; applications include analysis of tanned porcine leather, sections of stems or seed from vegetables and more (145,147–152).

The studies of beverages have been previously reported using high-performance liquid chromatography or gas chromatography coupled to mass spectrometery (LC-MS or GC-MS).(153,154) However, the use of solvent, sample and standard preparations along with the analysis period makes the overall process time-consuming (30,151,154). TLC-GC-MS and Paper Spray Mass Spectrometry (PS-MS) have been also used for the analysis of caffeine in beverages.(153,155) Coupling DESI-MS with TLC was reported previously as a relatively fast

and simple analytical approach for analysis of food, medical diagnostics, pharmaceutical mixtures, plant extracts, etc. (14,144,145,149,154,156–158) This technique helps to overcome the effect of ion suppression, thereby facilitating the detection of target compounds for quantitation purpose (30,144,149,154,157), especially detection of minute amounts (14,151,156,159–161).

In this study, TLC-DESI-MS was coupled to a linear ion trap mass spectrometer for analysis of the 5-Hour Energy Drink. A well-known illicit drug, amphetamine was spiked in the drink to illustrate the separation of amphetamine and caffeine from other substances in the drink preparation by TLC. The developed TLC plate was later analyzed by DESI-MS. Two types of 5-Hour Energy drinks were analyzed namely, Original Berry flavored and Extra Strength Berry flavored. The caffeine content mentioned in their label was 190mg in 57 mL for the Original strength, and 200mg in 57 mL for Extra Strength drink. Quantitative analysis with the use of a calibration curve was performed in two ways: (1) The ion intensity of caffeine was plotted against the respective concentration of caffeine standards, (2) ion intensity ratio of standard caffeine to deuterated (d_9) caffeine was plotted against their respective standard caffeine concentration. As a rapid mode of analysis, caffeine content was also quantified by direct analysis of spots having energy drinks spiked with deuterated (d_9) caffeine standard by DESI-MS. Additionally, Paper Spray Mass Spectrometry (PS-MS) using caffeine d_9 spiked in energy drink samples was also used to validate the results obtained by TLC-DESI-MS.

LOD of amphetamine was determined upon spiking energy drinks with standard amphetamine solution. The technique was designed to be fast, reliable and reproducible, so that it can be promptly used by forensic experts to detect even minimal levels of illicit drugs.

4.3 Results and Discussion

4.3.1 High resolution and tandem mass spectrometry

High resolution mass spectrometry and tandem mass spectrometry was performed using an Orbitrap mass spectrometer (Appendix, section B, Figure C1) to characterize the compounds present in the energy drink and standard amphetamine. The HRMS confirms the identity of the components in the 5-Hour Energy drink as reported by *M. Sneha and co-workers* using paper-spray mass spectrometry analysis (155).

Table 4.1: Exact mass measurements for components of 5-Hour Energy drink by ESI using the Orbitrap mass spectrometer.

Parent compound	Parent ion formulae	Fragment ion formulae	Experimental (*m/z*)	Theoretical (*m/z*)	Error (Δppm)
Amphetamine	$C_9H_{13}N$		136.1120	136.1126	4.41
		C_9H_{11}	119.0869	119.0861	6.72
		C_7H_7	91.0542	91.0547	5.49
Caffeine	$C_8H_{10}N_4O_2$		195.0871	195.0882	5.63
		$C_6N_3H_8O$	138.0661	138.0667	4.35
Niacinamide	$C_6H_6N_2O$		123.0550	123.0558	6.50
		C_6H_4NO	106.0286	106.0293	6.60
		C_5H_6N	80.0495	80.0500	6.25
Phenylalanine	$C_9H_{11}NO_2$		166.0858	166.0868	6.02
		$C_8H_{10}N$	120.0808	120.0813	4.16
Pyridoxine	$C_8H_{11}NO_3$		170.0806	170.0817	6.46
		$C_8H_{10}NO_2$	152.0705	152.0712	4.60

Table 4.1 describes the accurate mass deviation of the parent and fragment ions from the exact mass value in terms of ppm difference. All mass differences calculated were within 7 ppm. Figure C2a and C2b show the MS/MS spectra of amphetamine and caffeine respectively, with their fragment ions produced upon introduction of collision energy. Under collision-induced dissociation, amphetamine loses its amine and methylamine to form fragment ions at *m/z* 119 and *m/z* 91, respectively (162). In the case of caffeine, methylamine and the carbonyl loss produces the fragment at *m/z* 138 (163). Niacinamide shows fragment ions at *m/z* 106 and *m/z* 80 due to the loss

of primary amine and amide, respectively (164,165). With phenylalanine, the loss of the carbonyl moiety along with a water molecule results in the formation of the fragment ion at m/z 120 (166); whereas for pyridoxine, the loss of a water moiety generates the fragment ion at m/z 152 (165,167).

4.3.2 Optimization of DESI spray solvent and mobile phase for TLC

The selection of a suitable solvent as the TLC mobile phase and DESI solvent spray is essential for effective separation and detection (14,149,151). For optimizing DESI spray solvent, several solvents and their combinations were tested using CH_3OH, CH_3CN, CH_3CN / CH_3OH and CH_3CN / H_2O (Appendix, section C, Table C1). Figure 4.1 shows a bar graph that depicts the desorption efficiency of ions at m/z 136, 195, 123, 166 and 170 for amphetamine, caffeine, niacinamide, phenylalanine and pyridoxine in each DESI solvent sprays while the TLC plate development and instrumental conditions were kept constant. It was found that the combination of CH_3CN / H_2O in the ratio 7:3 (v/v) enabled desorption of most components present in the energy drinks and also showed highest ion intensity for caffeine and amphetamine (Figure 4.1). Hence, it was chosen as the optimum DESI-MS spray solvent.

The mobile phase plays a crucial role for efficient separation of all the compounds in the drink formulation. The separation helps eliminate ion suppression by specific components, and thereby aids in efficient detection and quantification of any specific component (14,161). Characterized components from the energy drink spiked with standard amphetamine were amphetamine, caffeine, niacinaminde, phenylalanine, and pyridoxine. Methanol and ethyl acetate composition were analyzed with and without 1.5% NH_4OH as the mobile phase. Ammonium hydroxide was added as an additive as suggested by Brien *et al* in 1982 for analysis of amphetamine by TLC (168). For caffeine separation, non-polar solvents such as, ethyl acetate, benzene, acetone and chloroform were investigated (169).
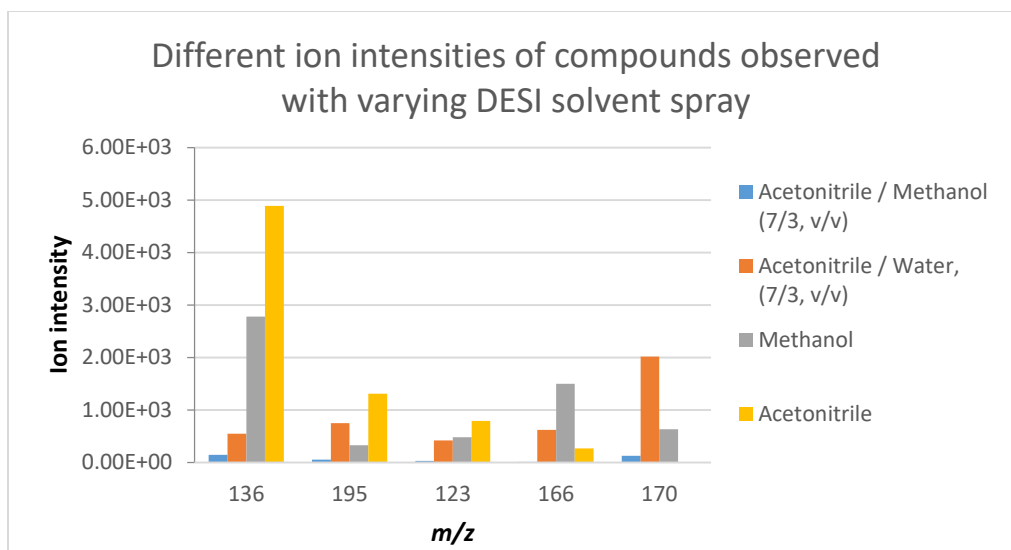
Figure 4.1: Bar chart illustrates optimization of DESI spray solvent for efficient desorption and ionization of amphetamine (*m/z* 136) and energy drink components, namely caffeine (*m/z* 195), niacinamide (*m/z* 123), phenylalanine (*m/z* 166) and pyridoxine (*m/z* 170).

With the inclusion of 1.5% NH_4OH in the mobile phase, the retention factor (RF) for amphetamine and caffeine were calculated to be 0.13 and 0.71 respectively. Without 1.5% NH_4OH, the amphetamine spot was at the initial point of spotting and the RF value for caffeine was 0.79. Even though the separation between caffeine and amphetamine improved, the caffeine (*m/z* 195) spot had niacinamide (*m/z* 123) and pyridoxine (*m/z* 170) at the same position, while amphetamine (*m/z* 136) had phenylalanine (*m/z* 166) apparent at the same spot. (Appendix, section C, Table C2).

The polarity indices of ethyl acetate and methanol are 4.4 and 5.1 respectively (169). To reduce the overall polarity of the mobile phase, the ethyl acetate amount was increased to check whether the less polar mobile phase enhances separation of most of the compounds in the energy drink; unfortunately the separation did not improve much. Based on RF value, the substances separated in the order of *m/z* 136, 166, 170, 123 and 195, starting from the origin of spotting to the solvent font (Appendix, section C, Table C2). The order indicated that caffeine travelled along the

solvent font. Consequently, caffeine was deduced to be the least polar in the mixture. Therefore, chloroform (a more nonpolar solvent) (169), was used instead of ethyl acetate and the ratio examined initially was 1:1 (v/v) combination of chloroform and methanol. The separation improved remarkably, but amphetamine appeared to split into two spots (Appendix, section C, Figure C3). It was found that upon spiking amphetamine with energy drink the pH of the solution drops, which causes amphetamine to coexist in two forms with different retention times. To overcome this problem, the energy drink mixture with amphetamine was further treated with ammonium hydroxide solution (10% final concentration). The resultant mixture was spotted prior to plate development with $CHCl_3 / CH_3OH$ (1:1, v/v) as the mobile phase. Upon analysis by DESI-MS the plate showed amphetamine to be concentrated on a single spot (Appendix, section C, Figure C4).

4.3.3 Lowest limit of detection of amphetamine

In case of drug abuse with amphetamine taken in conjunction with energy drinks, TLC showed good separation of amphetamine from the energy drink components with the use of $CHCl_3/CH_3OH$ (1:1, v/v) mobile phase, that enhanced its selectively and sensitivity by DESI-MS mode of detection. To identify the detection limit of amphetamine by this mode of analysis its lower limit of detection (LOD) was determined. It was found that 100 pg for 0.1 µL spot from 1.0 µg/mL amphetamine had a signal to noise ratio (S/N) of 3.33. In the case of 0.5 µg/mL amphetamine (50 pg), the S/N ratio appeared as 2.27 with an ion intensity of 1.17E2. It can thus be concluded that small amounts, as low as 50pg can be readily detected by TLC-DESI-MS, as depicted in Figure 4.2. Hence, any trace of illicit drugs can be readily spotted.
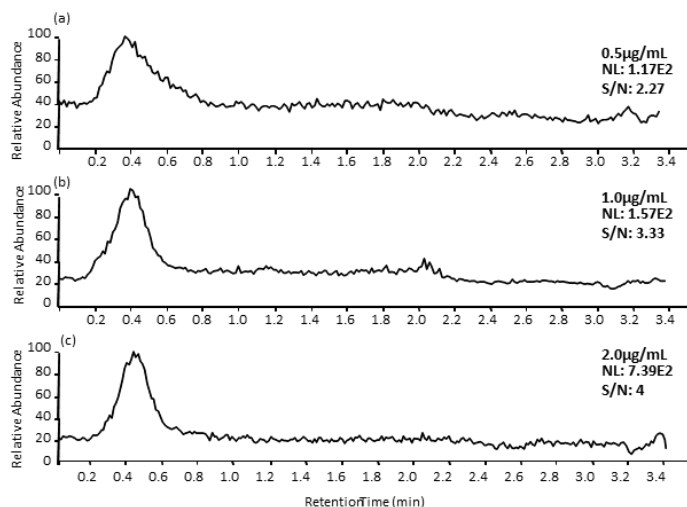
Figure 4.2: Lower limit of detection for amphetamine content. 0.1µL of different concentration of amphetamine (a) 0.5µg/mL, (b) 1.0µg/mL and (c) 2.0µg/mL was spotted with 0.1 µL of berry energy drink on TLC plate and analyzed using $CHCl_3/CH_3OH$ (1:1, v/v) as the mobile phase and CH_3CN/H_2O (7:3, v/v) as the DESI spray solvent. DESI spray solvent started just below the initial point.

4.3.4 Quantitative Analysis of Caffeine in Energy Drinks

4.3.4.1 Calibration curve using standard caffeine

Quantitation was based on a calibration curve where the concentration of the analyte was directly proportional to its signal intensity or peak area. Based on the sample label, caffeine content in Berry Flavored and Extra-Strength 5-hour energy drinks were 3.33 mg/mL (190 mg in 57 mL) and 3.51 mg/mL (200 mg in 57 mL) respectively.

Three independent runs were performed with the caffeine standards (Appendix, section C, Table C3). Figure 4.3 depicts the calibration curve generated upon plotting the average ion intensity of standard caffeine of the three runs against their respective concentration. From the derived equation of line, the concentration (x) of caffeine in the Berry flavored and Extra Strength drinks were calculated to be 4.28 ± 0.06 mg/mL and 4.83 ± 0.15 mg/mL respectively (Table 4.2). The derived concentration values reflect that berry flavored energy drink was about 29% and extra-

62

strength energy drink had 38% more caffeine than the indicated label amount.
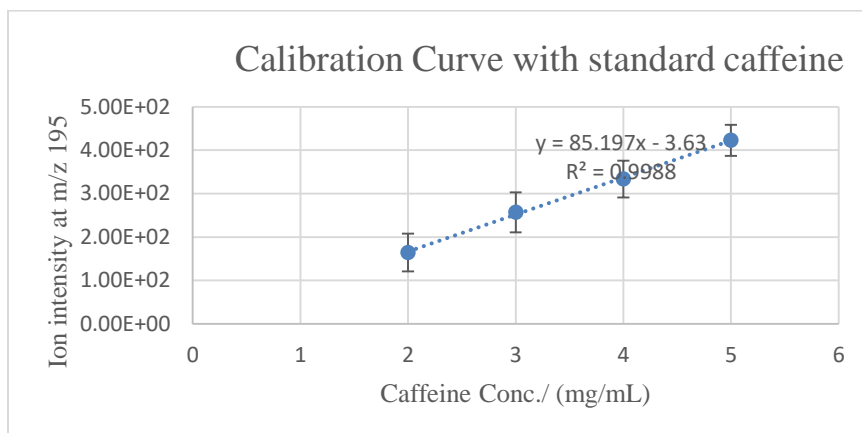
Figure 4.3: Calibration curve of caffeine developed using ion intensity ratio of caffeine against caffeine standard concentration. All standards were prepared by serial dilution from a caffeine stock solution of concentration 12 mg/mL. 0.1µL of extra strength sample was spotted. $CHCl_3/CH_3OH$ (1:1, v/v) and CH_3CN/H_2O (7:3, v/v) were used as the TLC mobile phase and DESI spray solvent respectively.

Table 4.2: Analysis of energy drinks using a calibration curve for standard caffeine solution. Using the equation from the calibration curve and the ion intensities of caffeine *(m/z* 195) from energy drink samples, the concentration of caffeine in energy drinks was calculated.

Berry flavored drink	Ion intensity	Concentration derived (mg/mL)		Extra strength drink	Ion Intensity	Concentration derived (mg/mL)
Run 1	504	4.33		**Run 1**	572	4.93
Run 2	368	4.27		**Run 2**	411	4.86
Run 3	210	4.22		**Run 3**	239	4.65
Average	360.67	4.28		**Average**	407.33	4.82
RSD (%)	40.80	1.30		**RSD (%)**	40.88	3.00

4.3.4.2 Calibration curve using ratio of deuterated and standard caffeine

The ratio of the signal intensity of deuterated caffeine and standard caffeine was used to plot a calibration curve. Three independent runs allowed to calculate average ratio (Appendix, section C, Table C4), which were plotted against their respective standard caffeine concentration with error bars (Figure 4.4). From the ion intensity ratio calibration curve, the concentration of

caffeine in Berry Flavored and Extra Strength drink were found to be 4.28 ± 0.012 mg/mL and 4.87 ± 0.019 mg/mL respectively (Table 4.3). Subsequently, the percentage difference from the labeled amount observed was 29% and 39% respectively.
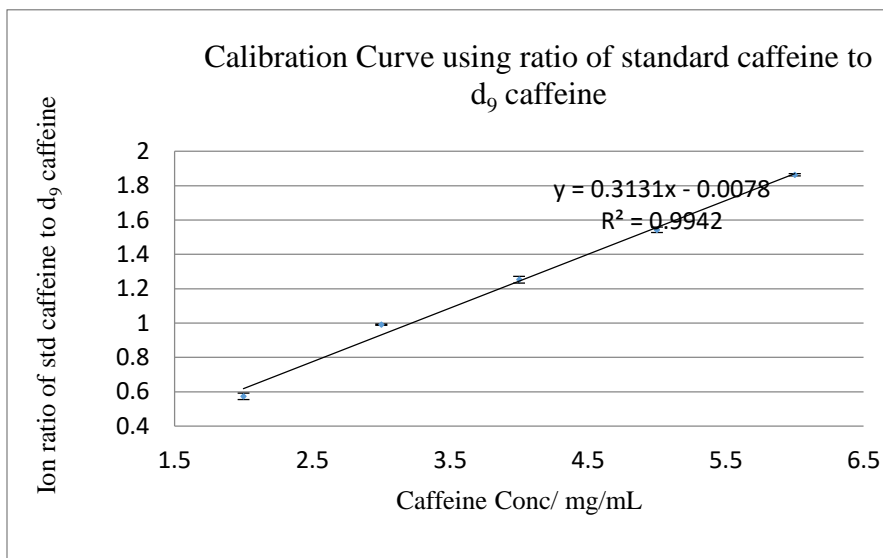
Figure 4.4: Calibration curve of caffeine plotted using the ion intensity ratio of standard caffeine to deuterated caffeine-d_9 against the respective standard caffeine concentration present in that mixture. All ion intensities are reported in Table C1 of the Appendix along with the calculation of ratios. $CHCl_3/CH_3OH$ (v/v, 1:1) and CH_3CN/H_2O (v/v, 7:3) were used as the TLC mobile phase and DESI spray solvent respectively.

Table 4.3: Analysis of energy drinks using a calibration curve of the ratio between standard caffeine and d$_9$-caffeine. Using the equation from the calibration curve and the ion intensity ratio of caffeine *(m/z* 195) from energy drink sample and standard deuterated caffeine (*m/z* 204), the concentration of caffeine in energy drinks was calculated.

Berry Flavored	Ion Intensity *m/z* 195	*m/z* 204	Ratio between intensities	Conc. derived/ mg/mL	Extra Strength	Ion Intensity *m/z* 195	*m/z* 204	Ratio between intensities	Conc. derived/ mg/mL
Trial 1	5.34E+01	1.01E+02	5.29E-01	4.28	**Trial 1**	1.86E+01	3.09E+01	6.02E-01	4.87
Trial 2	3.90E+01	7.36E+01	5.30E-01	4.29	**Trial 2**	1.83E+01	3.03E+01	6.04E-01	4.88
Trial 3	4.71E+01	8.94E+01	5.27E-01	4.27	**Trial 3**	1.69E+01	2.82E+01	5.99E-01	4.85
Average			5.28E-01	4.28	**Average**			6.02E-01	4.87
RSD (%)			0.29	0.286	**RSD (%)**			0.39	0.384

4.3.4.3 Direct spot analysis of a mixture of deuterated caffeine standard and energy drink

A spot test was performed using 3 mg/mL concentration of caffeine-d_9 as a rapid, easy mode of analysis to assess the concentration in the energy drinks independent of instrumental or concentration variability. This method is based on a comparative assessment of a known concentration of deuterated caffeine with an unknown caffeine concentration in the energy drinks with respect to their relative ion counts/abundance as measured by DESI-MS. Figure C5 (Appendix, section C) depicts the relative ion counts and abundance as observed from a spot having a 2.5X diluted berry flavored energy drink with 3 mg/mL deuterated caffeine standard. Based on the ion intensity ratio between m/z 195 and 204, actual concentration derived for Berry flavored and Extra Strength drink was 4.33 mg/mL and 4.81 mg/mL respectively (Table 4.4).

By this mode of quantitation too, the percentage difference of caffeine was higher than 20% of labeled caffeine content. To check batch variability of the energy drinks, new bottles of both types of 5 hour energy drinks were assessed for caffeine concentration by direct spot analysis. Both the energy drinks were found to have the same concentration ~4.50 mg/mL (Appendix, section C, Table C5).

Table 4.4*: Analysis of energy drinks by the direct spot analysis method. Ion intensity ratio of caffeine (m/z 195) from the energy drink sample and standard deuterated caffeine (m/z 204) were used to calculate the caffeine concentration in energy drinks.

Berry flavored drink	m/z 204	m/z 195	Conc. derived mg/mL	Extra strength drink	m/z 204	m/z 195	Conc. derived mg/mL
Spot 1	6.85E+02	3.93E+02	4.30	Spot 1	5.93E+02	3.78E+02	4.78
Spot 2	7.04E+02	4.26E+02	4.54	Spot 2	4.90E+02	3.13E+02	4.79
Spot 3	6.39E+02	3.73E+02	4.38	Spot 3	5.84E+02	3.85E+02	4.94
Spot 4	6.53E+02	3.56E+02	4.09	Spot 4	5.53E+02	3.47E+02	4.71
Mean			4.33	**Mean**			4.81
St Dev.			0.19	**St Dev.**			0.10
RSD (%)			4.31	**RSD (%)**			2.08

4.3.4.4 Paper Spray

Paper spray mass spectrometry (PS-MS) is a well-known analytical technique for rapid qualitative and quantitative assessment of complex mixtures. The same mixture of energy drinks used in direct spot method of quantitation was analyzed by PS-MS (Appendix, section C, Figure C6). Table 4.5 summarizes the ion intensity obtained in each scan for both types of 5-Hour Energy Drinks and the derived resultant concentration of caffeine, along with their mean, standard deviation and relative standard deviation (RSD) values. The concentration derived from paper spray mode of quantitation was similar to that of TLC-DESI-MS, reporting caffeine value for berry and extra strength energy drink to be 4.33 mg/mL and 4.50 mg/mL respectively. Sneha *et al*, 2016 reported that the concentration of 5- Hour Energy Drink to be 2.8 mg/mL by paper spray method. The difference in value can be attributed to their reported correlation coefficient, 0.86 (155). Of note, the literature did not report the coefficient of determination, R^2 value of the calibration curve they generated. The time elapsed between performing the analysis after opening the energy drink bottles was not indicated. It was observed during our analysis that the caffeine degrades to its fragment ion at *m/z* 138 immensely in a span of 1 week upon coming in contact with air.

Table 4.5: Analysis of 5-Hour Energy Drinks by paper spray mass spectrometry (PS-MS). Ion intensity ratio of the caffeine (*m/z* 195) from the energy drink sample and standard deuterated caffeine (*m/z* 204) were used to calculate the caffeine concentration in energy drinks.

5-Hour Energy Drink samples	*m/z* 195	*m/z* 204	Conc. Derived (mg/mL)	Mean (mg/mL)	Std dev.	RSD
Berry Flavor	7.48E+01	1.33E+02	4.22	4.33	0.16	3.80
	8.56E+01	1.51E+02	4.25			
	7.53E+01	1.25E+02	4.52			
Extra-Strength	6.29E+01	1.09E+02	4.33	4.43	0.09	2.01
	7.32E+01	1.23E+02	4.46			
	6.96E+01	1.16E+02	4.50			

Table 4.6: Caffeine concentration obtained by the three modes of quantitation.

Method	Berry Flavor (mg/mL)	Extra Strength (mg/mL)
Standard calibration	4.28	4.83
Internal standard calibration	4.30	4.82
Direct Spot Analysis	4.33	4.81
Paper Spray	4.33	4.50

4.4 Conclusion

Based on the four models of quantitative assessment, the caffeine content in both Berry and Extra Strength 5-Hour Energy drinks was always found to be higher than the caffeine content labeled on these bottles. All these modes of assessment generated almost similar concentration values of caffeine within the same batch of energy drinks (Table 4.6). According to the label, the amount of energy blend is 1871 mg for Berry flavor and 1980 mg for Extra Strength per serving. Though the manufacturer mentioned that the caffeine content is 190 mg and 200 mg per serving for Berry flavor and Extra Strength 5-Hour Energy Drink respectively. Several other sources (170,171) claim that the label is misleading and often report the concentration to be higher than the labeled amount. Thus, the caffeine content is an unknown factor for consumers and it is stated to be equal to a premium cup of coffee or a 12 ounce cup of coffee, in the range of 100-330 mg for an original 5-Hour Energy shot and Extra Strength Energy shot respectively (143,172). Based on the quantitative analysis, the caffeine content in the Berry flavored and Extra Strength were also found to be 245 mg and 274 mg respectively in each serving and it is within the reported range of 200-300 mg on which there is no legal limit imposed by FDA for energy drinks (171). It was mentioned that lethal dose of caffeine surpasses 10 g for daily consumption for healthy individuals and so it is still not strictly controlled in the market (171,172). However, there are several reports that claim death of individuals due to combined consumption with alcohol or other pharmaceutical supplements and also upon continuous consumption of more than two bottles without any time

lapse between them (171,172).

Among the quantitation methods described here by TLC-DESI-MS, the calibration curve using ratios of standard caffeine and deuterated caffeine is the most reliable. The ratio calculation eliminates the instrumental and environmental variations on ion intensity signals and also allows one to minimize the matrix effect by the use of the derived line equation. The calibration curve equation with intensity values are prone to changes with instrumental or surrounding variations that lead to signal intensity fluctuations. Again, direct spotting and paper spray are fast techniques, but have the limitation of taking into account the background noise signal too. The specificity can be enhanced with the implementation of tandem mass spectrometry in the above described process. Consideration of the signal intensity of the fragment ion peak specific to caffeine will enhance the precision of the quantitation mode.

Simple analytical techniques such as TLC-DESI-MS, paper spray and spot analysis thus prove to be a reliable, robust method for qualitative and quantitative assessment of the energy drinks. It is also demonstrated to be equally effective in detecting trace amounts of amphetamine (as low as 50pg). Thus, this method illustrates the capability of DESI-MS to trace any illicit drug(s) which could be spiked in food, drinks, medicine etc. This analytical method could be implemented in the field of forensic science, drug analysis, environmental testing and biological testing due to its reliability, precision and reproducibility.

4.5 Experimental

4.5.1 Chemicals

HPLC grade acetonitrile (CH_3CN), HPLC grade methanol (CH_3OH), Water (LC-MS CHROMASOLV®), caffeine standard and ammonium hydroxide (28% NH_3 in H_2O) were purchased from Sigma-Aldrich Co (Oakville, ON, Canada). HPLC grade ethyl acetate was

purchased from Caledon Laboratory Chemicals. Standard amphetamine (1 mg/mL) and isotopically labeled caffeine-d$_9$ were from Cerilliant Corporation (Texas, USA) and Toronto Research Chemicals (Toronto, Canada) respectively. As samples, 5-Hour Energy Drinks from Living Essentials, LLC Farm, was purchased from a superstore (Scarborough, Canada).

4.5.2 High Resolution (HRMS) and Tandem Mass Spectrometry (MS^n)

To confirm the identity of the compounds present in energy drink preparation and standard amphetamine solution, high resolution mass spectrometry (HRMS) and tandem mass spectrometry (MS/MS) were performed using a hybrid Thermo Fisher Orbitrap Elite Mass Spectrometer (San Jose, CA, USA). The energy drinks were diluted 50 folds and the amphetamine standard was spiked at a final concentration of 2 µg/mL. The resultant solutions were directly infused at a flow rate of 5 µL/min. The full scan spectrum of the resultant mixture was obtained in the mass range *m/z* 150-1000 and MS/MS of different components were conducted using collision energy between 25-35% (manufacturer's unit).

4.5.3 TLC Analysis

Silica TLC glass based plate with thickness 250 µm was purchased from Sili Cycle Inc (Québec, Canada). The dimension of the plate was 5 x 5 cm. A sharpie pen with rhodamine red ink (control), amphetamine standard (0.1µL of 1mg/mL) and energy drink samples (0.1µL of ~3.5mg/mL) were spotted on the same plate surface, air dried and developed with the use of a suitable mobile phase. Several different solvent combinations were assessed as mobile phase for optimum compound separation (Appendix, section C, Table C2). Developed plates were air dried for 20 minutes prior to analysis by DESI-MS.

4.5.4 Desorption Electrospray Ionization

DESI-MS was operated in full scan mode to scan a mass range from *m/z* 150 - 1000, in the

positive ion mode. The ion source was on a custom-built moving stage, operated by Galil motion control (WSDK) software, moving at a speed of 179 µm/s. Data was acquired using x-calibur software supported on a Thermo Finnigan LTQ Linear Ion-trap Mass Spectrometer (San Jose, CA, USA) at a set resolution of 150 µm. The emitter was set at +5kV, 2 mm above the sample surface, at an incident angle of 54° and a collection angle of 10°. The solvent spray had a flow rate of 5 µL/min. As a nebulizer gas, 100 psi nitrogen was used to support the spraying process.

4.5.5 Lowest limit of detection of amphetamine

Amphetamine standards (0.5 µg/mL, 1.0 µg/mL and 2.0 µg/mL) were prepared by serial dilution of a 1 mg/mL stock solution. Aliquots of 0.1µL of all the concentrations were spotted on the TLC plate along with 0.1 µL of the energy drink samples, followed by development with $CHCl_3$ / CH_3OH (1:1) mobile phase. The developed plate was later analyzed by DESI-MS using CH_3CN / H_2O (7:3) spray solvent to check for the lowest concentration of the amphetamine that gives a signal to noise ratio of ≥3.

4.5.6 Quantitative Analysis of Caffeine in Energy Drinks

4.5.6.1 Calibration curve using standard caffeine

Several different concentrations of caffeine standard (2, 3, 4, 5 and 6 mg/mL) were prepared from a 12 mg/mL stock by serial dilution. An aliquot of 0.1 µL of the prepared standards and 5-Hour Energy Drink (Berry Flavor and Extra Strength) were spotted on the TLC plate, developed and analyzed by DESI-MS. A calibration curve was plotted using the ion intensity of caffeine standards obtained by DESI-MS against their respective concentrations. The concentration of caffeine in both 5-Hour Energy Drinks was calculated using the equation of the line derived and the intensity obtained from the energy drink spots.

4.5.6.2 Calibration curve using ratio of deuterated and standard caffeine

71

Caffeine standards were made of concentration 2 mg/mL, 3 mg/mL, 4 mg/mL and 5 mg/mL from a 16 mg/mL stock solution. Each standard solution was spiked with deuterated caffeine (caffeine-d_9) standard at a final concentration of 3 mg/mL. LC-MS grade water was used to adjust the volume. Similarly, 3 mg/mL caffeine-d_9 was also used to spike energy drink (Berry and Extra Strength) samples, resulting in a mixture having 3 mg/mL caffeine-d_9 and 2.5X diluted Energy Drink sample.

0.1 µL of the spiked standards and energy drinks were spotted on the TLC plate, developed and analyzed by DESI-MS. Calibration curve generation was based on the intensity ratio of caffeine (*m/z* 195) and caffeine-d_9 (*m/z* 204) against the respective concentration of the caffeine standard. Likewise, the actual caffeine concentration in both energy drinks was calculated using the derived line equation from the calibration curve and the dilution factor.

4.5.6.3 Direct spot analysis of the mixture of deuterated caffeine standard and the energy drink

Spot analysis of a mixture having energy drink sample with spiked deuterated caffeine standard was analyzed directly by DESI-MS. 3 mg/mL deuterated caffeine standard was spiked with the energy drink samples; 1µL of the resultant solution was spotted on a TLC plate and directly analyzed by DESI-MS. Three scans were averaged and the resultant spectrum was collected for 1 minute. Three replicates were prepared and analyzed for each energy drink sample. The concentration of caffeine in the samples was determined using the equation, $\frac{I_{caffeine}}{I_{deutrated\ caffeine}} = \frac{C_{caffeine}}{C_{deutrated\ caffeine}}$, where 'I' is the extracted Ion Intensity from the MS scan and 'C' is the corresponding concentration producing that intensity. Utilizing the dilution factor, the actual concentration of caffeine in the energy drink sample was calculated. Similarly, a new batch of both Berry Flavored and Extra Strength Energy Drink was further evaluated by this mode of

quantitation to evaluate the concentration consistency among batches.

4.5.6.4 Paper Spray

A mixture having 3mg/mL deuterated caffeine with 2.5X diluted energy drink sample was spotted on a triangular cut piece of printing paper, held at +5kV voltage in front of the inlet of an LTQ mass spectrometer. A combination of CH_3CN / H_2O mixture in the ratio 7:3 (v/v) respectively was sprayed on the paper piece and spectra were collected for 1 minute having 10 ms injection time. Three scans were averaged and three replicates were analyzed for each energy drink sample.

CHAPTER FIVE

Quantitative method development of imidazole derivatives, Tetrahydrozoline and Naphazoline, by desorption electrospray ionization and paper spray mass spectrometry

- Prova, S. S., Baialardo, E., Ifa, D. R.

The manuscript of this study is in process.

5.1 Summary

Pharmaceuticals play a crucial role in the treatment and cure of ailments. Ensuring its accurate dosage is thus very essential; as it not only influence its efficacy but also the safety of the patient taking it. Hence it necessitates a robust, reliable quantitative method which would ensure both. There have been numerous attempts at method development for specific ingredients (active or additive) in a pharmaceutical preparation. This encompasses both sample preparation and optimization of their mode of detection. In recent years mass spectrometry is of interest as it enables quantitation along with detection of impurities and thereby assesses the quality of the drug product. In this study, desorption electrospray ionization mass spectroscopy coupled with thin-layer chromatography (TLC-DESI-MS) was employed to quantitate the active ingredients in ophthalmic preparations of Visine for Red Eye Original and Clear Eye Allergy. Three different approaches that focused on the ion intensities generated by specific concentrations of the standard, deuterated standard, and sample analysed were used to quantitate the active principal ingredient. All three methods showed high accuracy with low ranges of error compared to the label stated concentration. Furthermore quantitation by paper spray was also performed as a mode to verify the results obtained by TLC-DESI-MS. This new mode of quantitation (TLC-DESI-MS) can be explored further to make it applicable for use in other fields like environmental, biochemical, and biomedical sciences.

5.2 Introduction

The viability of a medication relies on rigorous qualitative and quantitative analysis prior to its launch in the market (173,174). Determination of the exact concentration of a bioactive compound is crucial for the desired effects as well as to avoid side effects. Two currently available over the counter (OTC) redness relief eye drops (Visine for Red Eye Original and Clear Eyes

Allergy) were investigated in this study to develop a relatively fast, reliable mode of quantitation of the active principal in the formulation. Visine for Red Eye Original contains tetrahydrozoline as the active ingredient whereas naphazoline is the active component in Clear Eyes Allergy formulation with distinct concentrations of 0.05 and 0.012 % w/v respectively, as stated in their labels. Benzalkonium chloride is used as a preservative agent due to its antimicrobial activity and is present in both ophthalmic preparations (175). Minor ocular irritants cause eye redness. These imidazoline derivatives, tetrahydrozoline and naphazoline, are α-agonists whose main mechanism of action is by constricting conjunctival blood vessels thereby serving as redness relief compounds (176).

A variety of techniques have been employed to quantify these active compounds including high-performance liquid chromatography (HPLC) using UV, and gas chromatography / mass spectrometry (177). However, desorption electrospray ionization mass spectrometry (DESI-MS) for quantitative measurements of tetrahydrozoline and naphazoline in ophthalmic solutions have not been previously reported.

In this study, a simple analytical method for the quantification of tetrahydrozoline and naphazoline in OTC eye drops has been developed by the use of thin-layer chromatography coupled to DESI-MS. TLC was employed as a mode to separate the components of the eye drop preparation prior to their quantification by DESI-MS (146,147,178,179). It was previously reported that quantification utilizing TLC requires removal or scraping off the spot of interest for extraction prior to analysis. This results in the loss of material (177,180) and also the overall process is time-consuming. In contrast, coupling TLC with DESI-MS, the sample preparation step of extraction can be eliminated since DESI-MS is a surface analysis technique. In addition, TLC

allows separation of the active compounds, thereby minimizing ion-suppression that could affect the accuracy of the quantitative analysis (36,181–183).

Three different approaches were used to quantify the active components of the two ophthalmic solutions. Calibration curves were generated using ion intensity obtained from specific concentrations of the standard, deuterated standard, and drug samples by DESI-MS. Since the concentration in the ophthalmic solutions is specified, the results obtained from the quantitative analysis were compared with label values.

Quantitation by paper spray was also performed to verify the results obtained by TLC-DESI-MS. Paper spray is a relatively fast, convenient, economical mode of analysis, requiring almost no sample preparation and quick assessment of ophthalmic preparations (83,155) .

5.3 Results and Discussion

5.3.1 Identification of Eye drop Components

High resolution mass spectrometry and tandem mass spectrometry were performed using an LTQ Orbitrap Elite mass spectrometer (Thermo Scientific). Ophthalmic preparations being analysed had compounds at m/z 201 (tetrahydrozoline, active component of Visine for Red Eye Original sample), m/z 211 (naphazoline, active component of Clear Eye Allergy sample), m/z 304 and m/z 332 were preservative compounds, benzalkonium chlorides differing in alkyl chain lengths, C_{12} and C_{14} respectively (Figure 5.1).

Accurate mass obtained by the Orbitrap mass spectrometer was compared with the exact monoisotopic mass of each compound to calculate the ppm difference. The ppm difference obtained for tetrahydrozoline and naphazoline (m/z 201, and 211) were 4.972 and 3.316 respectively. For the preservative ions at m/z 304, and 332 the difference was calculated to be 4.929 and 3.911 respectively. All four compounds demonstrated less than 5.0 ppm difference with

their exact monoisotopic mass, thereby confirming their identity (Table 5.1) (183,184).
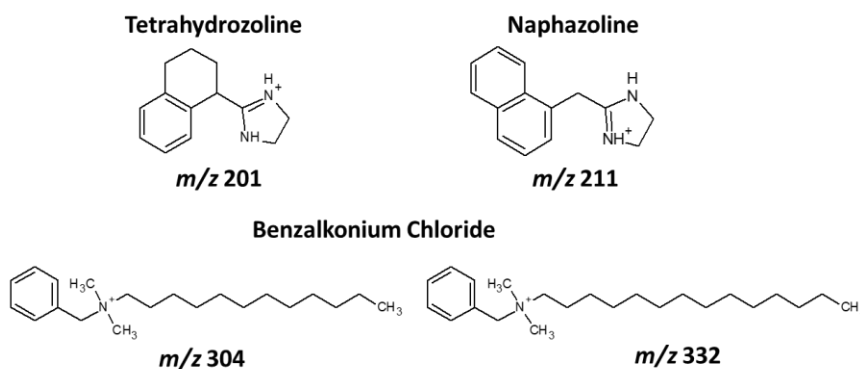
Figure 5.1: Structures of the active and preservative compounds present in Visine for red eye Original and Clear Eyes Allergy eye drops.

Table 5.1: Identification of active components (tetrahydrozoline and naphazoline) and preservative using the LTQ Orbitrap Elite Mass Spectrometer.

Compound	m/z	Molecular formula	Theoretical MW (g/mol)	Experimental MW (g/mol)*	Δ ppm
Tetrahydrozoline	201	$C_{13}H_{17}N_2$	201.1392	201.1382	4.972
Naphazoline	211	$C_{14}H_{15}N_2$	211.1235	211.1228	3.316
Benzalkonium chloride	304	$C_{21}H_{39}N$	304.3004	304.2989	4.929
Benzalkonium chloride	332	$C_{23}H_{43}N$	332.3317	332.3304	3.911

Furthermore, tandem MS (MS/MS) was performed to elucidate their structural features based on their fragmentation profile. Figure D1 (Appendix, section D) illustrates the fragmentation profile of ions m/z 201, 211, 304, and 332. Tetrahydrozoline produces a base peak at m/z 131 which corresponds to the loss of the imidazoline group; whereas for naphazoline, m/z 141 was observed upon dissociation of the imidazoline group. Both C_{12} and C_{14} benzalkonium chloride lose toluene to produce fragment ions at m/z 212 and 240 respectively (175).

5.3.2 DESI Spray Solvent Optimization

The spray solvent influences the dissolution and desorption of an analyte from the surface

along with its ionization (36). The imidazoline group in both tetrahydrozoline and naphazoline is mainly responsible for ionizing the molecule and so they are expected to behave similarly. Both components were soluble in water and methanol (181). Methanol was chosen as the solvent spray for analysis as it is more volatile than water and this aid in better mist formation and ultimately faster drying of the droplets. All four compounds of interest were detected; however, their ion intensities were low. When composition of the solvent was changed to $CH_3OH:H_2O$ (1:1, v/v), however, the ion counts decreased for both the active and preservative molecules. (Figure 5.2)
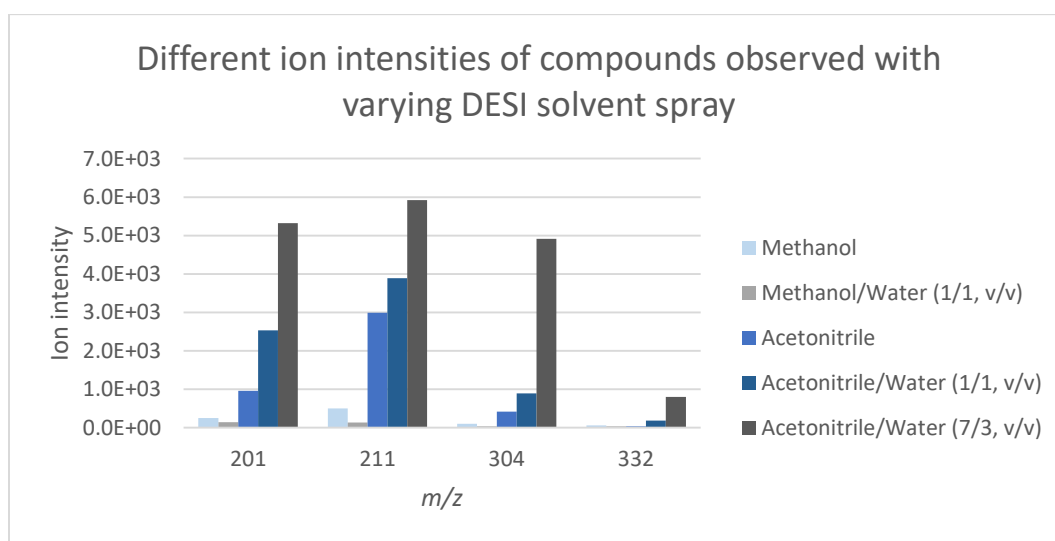
Figure 5.2: Intensity observed of active (*m/z* 201, 211) and additive compounds (*m/z* 304, and 332) ions while using different DESI spray solvent combinations. Refer to Appendix, section D.

The solubility of a compound is dependent on its polarity (182). Since the compounds studied were soluble in CH_3OH, CH_3CN being more polar was anticipated to enhance their dissolution from the silica stationary plate (181). Ion intensities for *m/z* 201, 211 and 304 increased with pure CH_3CN. In combination with water, in the ratio 1:1 (v/v), the intensities further improved. Finally upon fine-tuning the ratio to 7:3 (v/v), in an attempt to enhance droplet formation of the spray solvent, it was found that desorption and ionization for all compounds was maximized. Hence this combination was used in the later part of the study (Figure 5.2).

5.3.3 TLC Mobile Phase Optimization

To achieve optimum separation of the active ingredient from other compounds present in the ophthalmic preparations, different combinations of TLC solvents were tested. The active ingredients in the ophthalmic preparations were polar molecules whereas the preservative molecules had alkyl chains which made them less polar in nature. The hypothesis was to use a nonpolar solvent that would enable separation of both components since they have different polarities (181). Likewise, chloroform was used in combination with methanol in 2:3 (v/v) ratio, respectively. Certain degree of overlap was evident between the active components (*m/z* 201 and 211) and the preservative molecules (*m/z* 304 and 332); which led to further modification of the solvent ratio to 1:1 that resulted in complete separation.

Figure D2 and D3 illustrate the separation of tetrahydrozoline and naphazoline from benzalkonium chloride using the chloroform/methanol (1:1, v/v) combination. The retention factors (RF) calculated were 0.30 for tetrahydrozoline (*m/z* 201) and 0.34 for naphazoline (*m/z* 211). Both, tetrahydrozoline and naphazoline, have an imidazoline group which made their interactions with the silica plate similar. Since *m/z* 304 and 332 were benzalkonium chlorides differing by two carbon atoms in the alkyl side chain, they were anticipated to appear at approximately the same RF; these were calculated to be 0.59 and 0.64 respectively for Visine for Red Eye Original and 0.55 for Clear Eye Allergy. The retention factor was determined by dividing the distance at which they appeared on the plate over the total distance travelled by the solvent front on the TLC plate.

5.3.4 Limit of Detection (LOD) of Tetrahydrozoline and Naphazoline

LOD for both tetrahydrozoline and naphazoline was determined to be 50 pg; with a signal to noise (S/N) ratio of 3.33 (Figure D4 and D5). 100 pg and 25 pg were also spotted on the TLC

plate to observe the S/N variation upon overall amount changed on the spot. 2-fold increase in load, increased the S/N slightly less than 2 fold (4 and 5.88 for 100pg, Figure D4 and D5). For quantitation purposes, it is ideal to have a signal 10 times higher than LOD, so that the variation in signal can be solely attributed to the changes in amount rather than external factors like matrix, temperature, etc. Also, in order to use a calibration curve, a specific range of concentration that depicts linearity is considered to be ideal. Furthermore, for efficient TLC separation, the spot needed to be concentrated at a small region. All these limitations led to spotting, 0.1 µL of 5 µg/mL - 100 µg/mL concentration range on TLC plates for quantitation purposes.

5.3.5 Quantitative Analysis of Active Components

5.3.5.1 Calibration Curve using Tetrahydrozoline and Naphazoline Standards

Ion intensity or the area under the peak of the extracted ion chromatogram of DESI was plotted against the concentrations of tetrahydrozoline and naphazoline standard solutions spotted on the TLC plate to obtain calibration curves.
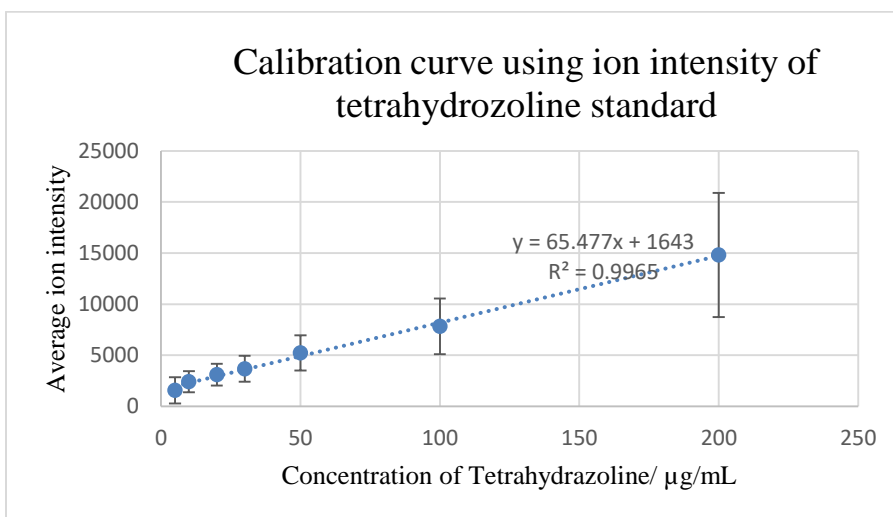
Figure 5.3: Tetrahydrozoline calibration curve plotted using standard solutions of tetrahydrozoline at concentrations 5, 10, 20, 30, 50, 100 and 200 µg/mL with their respective ion intensities obtained by DESI-MS. Equation of the line derived was $y = 65.477x + 1643$ with a correlation factor of (R^2): 0.9965. Raw data tabulated in Appendix, sections D1.

Figure 5.3 shows the resultant calibration curve with tetrahydrozoline standard; the equation of the line derived was y = 65.477x+1643, where *y* represents the ion count and *x* the corresponding concentration of the standard solution spotted.

Table 5.2: Determination of tetrahydrozoline concentration in Visine Red Eye Original preparation from a calibration curve.

Visine Original	Dil. Factor	Intensity	Conc. in spot (µg/mL)	Actual conc. in preparation (µg/mL)	Area under peak	Conc. in spot (µg/mL)	Actual conc. in preparation (µg/mL)
Run 1	12.5X	5370	40.05	500.59	72343	41.29	516.11
	30X	3010	16.82	504.64	33517	16.92	507.58
Run 2	12.5X	2800	41.01	512.69	52629	42.40	529.96
	30X	1510	18.12	543.59	27740	17.80	534.15
Run 3	12.5X	4710	40.88	511.06	51926	41.70	521.31
	30X	3790	17.27	518.17	26152	16.96	508.87
Mean				515.12			519.66
SD				15.25			10.90
% RSD				2.96			2.10

Table 5.2 summarizes the tetrahydrozoline concentration (*x*) calculated for the two dilutions (12.5X and 30X) from the derived line equation. The average concentration calculated was 515.12 ± 15.25 µg/mL indicating a RSD of 2.96 % among the different inter-day runs conducted. This validates the robustness of this method in determining the unknown concentrations of tetrahydrozoline samples. Data corresponding to ion counts and their respective area under peak for three independent runs are tabulated in table D1 and D2 of the appendix, section D.

Calibration curve using area under the resolved
peak of Naphazoline standard

$y = 343.16x + 254.91$
$R^2 = 0.996$

Figure 5.4: Naphazoline calibration curve plotted using standard solutions of naphazoline standard solutions at concentrations 5, 10, 20, 30, 50, 80 and 100 µg/mL with their respective peak area obtained by DESI-MS. Equation of the line derived was $y = 343.16x + 254.91$ with a correlation factor (R^2) of 0.9960. Raw data tabulated in Appendix, sections D4.

Table 5.3: Determination of Naphazoline concentration in Clear Eye drop preparation from a calibration curve.

Clear eye drop	Dil. Factor	Intensity	Conc. in spot (µg/mL)	Actual conc. in preparation (µg/mL)	Area under peak	Conc. in spot (µg/mL)	Actual conc. in preparation (µg/mL)
Run 1	3X	1160	40.56	121.68	14017	41.39	124.17
	10X	423	12.44	124.43	4338	12.76	127.56
Run 2	3X	1470	40.85	122.56	19334	40.78	122.33
	10X	482	12.80	128.03	5940	12.34	123.40
Run 3	3X	786	41.30	123.91	9863	41.97	125.91
	10X	265	13.23	132.27	3745	14.22	142.17
Mean				125.48			127.59
SD				3.98			7.38
% RSD				3.17			5.78

The area under the resolved peak for the compound under investigation was also used to plot calibration curve for quantitative purposes. Figure 5.4 depicts the area under the peak of standard naphazoline plotted against their respective concentrations (5, 10, 20, 30, 50, 80 and 100

µg/mL). The average concentration in the Clear Eye Drop sample was determined to be 127.59 ± 7.38 µg/mL; having a RSD of 5.8 % among runs (Table 5.3). These results also indicate the reliability of the quantitation method. Data corresponding to ion counts and their respective area under peak for three independent runs are tabulated in table D3 and D4 of the appendix, section D.
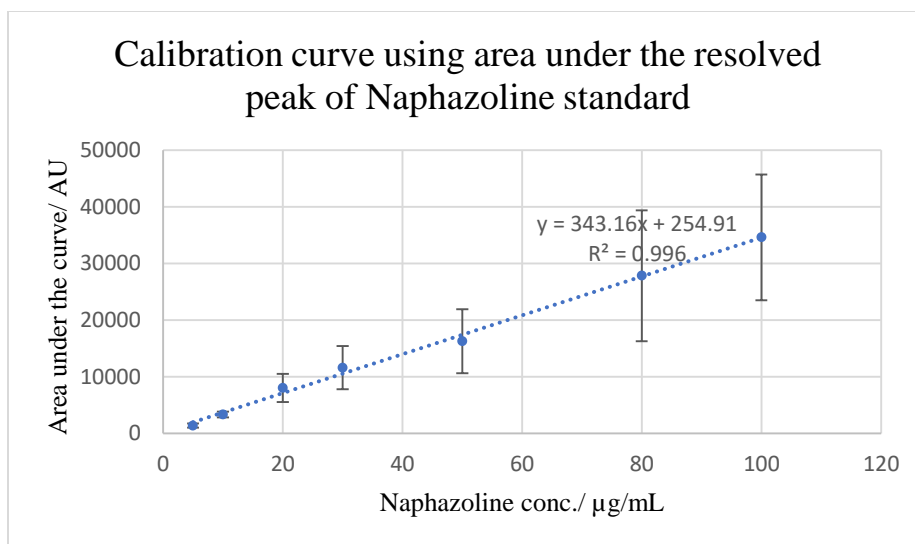
5.3.5.2 Direct spot analysis of a mixture of deuterated standard and Visine from Red Eye Original sample

Concentration is directly proportional to the ion intensity (C_{sample} α I_{sample}) observed in DESI-MS scan. Consequently, the deuterated tetrahydrozoline standard was spiked with the diluted samples of Visine red eye original preparation to calculate the concentration of tetrahydrozoline in the mixture using ion intensity ratios. Using the equation $\frac{I_{205}}{I_{201}} = \frac{C_{205}}{C_{201}}$, the original concentration of tetrahydrozoline present at the spot (C_{201}) was determined.

Three spots were analysed to calculate an average concentration (Table 5.4). Average concentration was determined to be 514.01± 18.90 µg/mL. Comparing it with 500.00µg/mL, as stated on the label, a percentage difference of 2.80 % was found.

Table 5.4: Determination of Tetrahydrozoline concentration in Visine Original preparation by direct spot analysis.

Visine Original	*m/z* 201 Tetrahydrozoline	*m/z* 205 Deuterated Tetrahydrozoline	Conc. in spot (µg/mL)	Actual conc. in preparation (µg/mL)
Spot 1	2.39E+03	1.16E+03	41.21	515.09
Spot 2	3.62E+03	1.70E+03	42.58824	532.35
Spot 3	2.75E+03	1.39E+03	39.56835	494.60
Mean			41.12	514.01
SD			1.51	18.90
RSD			3.68	3.68

Since the ionizing group for both tetrahydrozoline and naphazoline is the same, equimolar concentration (20µg/mL) of both standard tetrahydrozoline and naphazoline were mixed and analysed by DESI-MS to check their ionizability by the DESI solvent spray. Figure D6 depicts the resultant spectrum obtained, which supports that they have almost the same ionization efficiency giving very similar ion abundance and intensity. Due to the commercial unavailability of deuterated naphazoline standard, standard tetrahydrozoline solution was used as an internal standard to quantify naphazoline in ophthalmic preparations, a practice also known as 'internal addition'(185,186).

Table 5.5: Determination of Naphazoline concentration in Clear eye drop preparation by direct spot analysis.

Clear Eye drop	*m/z* 201	*m/z* 211	Conc. in spot (µg/mL)	Actual conc. in preparation (µg/mL)
Spot 1	2.41E+03	4.98E+03	41.33	123.98
Spot 2	2.52E+03	5.34E+03	42.38	127.14
Spot 3	2.68E+03	5.59E+03	41.72	125.15
Mean			41.81	125.43
SD			0.53	1.60
RSD			1.27	1.27

Likewise, the average naphazoline concentration of three spots containing 3X diluted Clear Eye Drop was calculated to be 125.43 ± 1.60 µg/mL (Table 5.5). Comparing it to the label amount of the eye preparation, 120.00 µg/mL, percentage difference was determined to be 4.52 %. Figure 5.5 depicts spectra obtained upon analysis of spot having Visine and Clear ophthalmic preparation spiked with deuterated tetrahydrozoline and standard tetrahydrozoline, respectively.

Relative standard deviation from mean for both preparations were found below 5% which signifies that this method is can be used to determine the unknown concentration of the active component with high precision in a relatively short period of time.
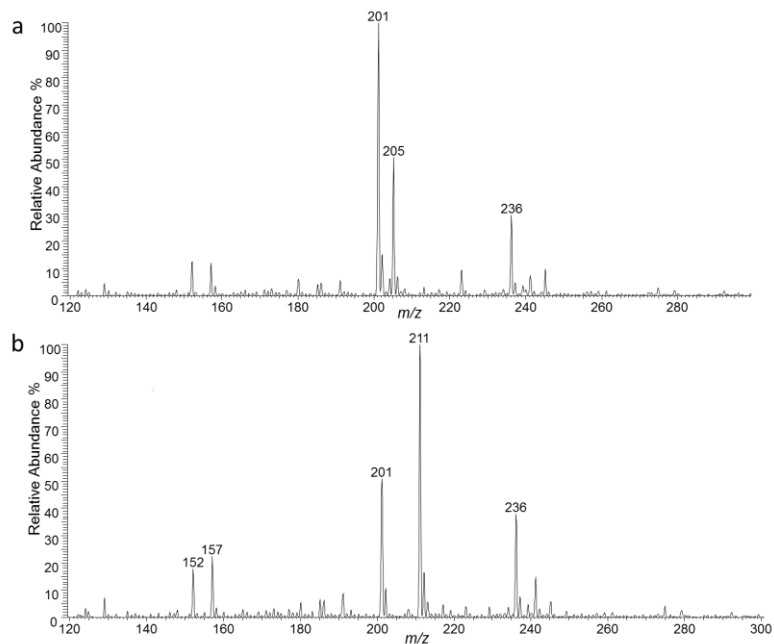
Figure 5.5: Spot analysis by DESI-MS. a) MS spectrum showing the relative abundance observed upon simultaneous spotting 1µL of 20 µg/mL of the deuterated standard at m/z 205 (1.16 x10^3 ion count) with 12.5X diluted drug sample at *m/z* 201 (2.39x10^3 ion count) b) MS spectrum showing the relative abundance observed upon simultaneous spotting 1µL of 20 µg/mL of the tetrahydrazoline standard at *m/z* 201 (2.41 x10^3 ion count) with 3X diluted clear eye drop sample at *m/z* 211 (4.98x10^3 ion count).

Analytical accuracy is limited by instrumental variation including systematic and random errors. The temperature of the room where the instrument is kept, the pressure of nitrogen gas when the cylinder is replaced, or the temperature of the inlet are factors that affect ion intensity (187–189). Therefore, to minimize the effect of all these variations in signal intensity as well as the background matrix effect, it is recommended to acquire the data of samples and standards concurrently followed by generation of calibration curve.

5.3.5.3 Calibration Curve using Deuterated Internal Standard Solution and Standard Solution of Active Component

Figure 5.6 shows the calibration curve obtained upon plotting the ion intensity ratio over the concentration of standard tetrahydrozoline in the mixture. Average intensity ratio from three

replicates of 12.5X diluted tetrahydrazoline sample was found to be 2.043, having a standard deviation of 0.01 (Table D5). The concentration in the Original Red Eye sample calculated using the average ratio and the derived line equation was 501.50 µg/mL, showing only a deviation of 0.3% from the true value (500µg/mL).
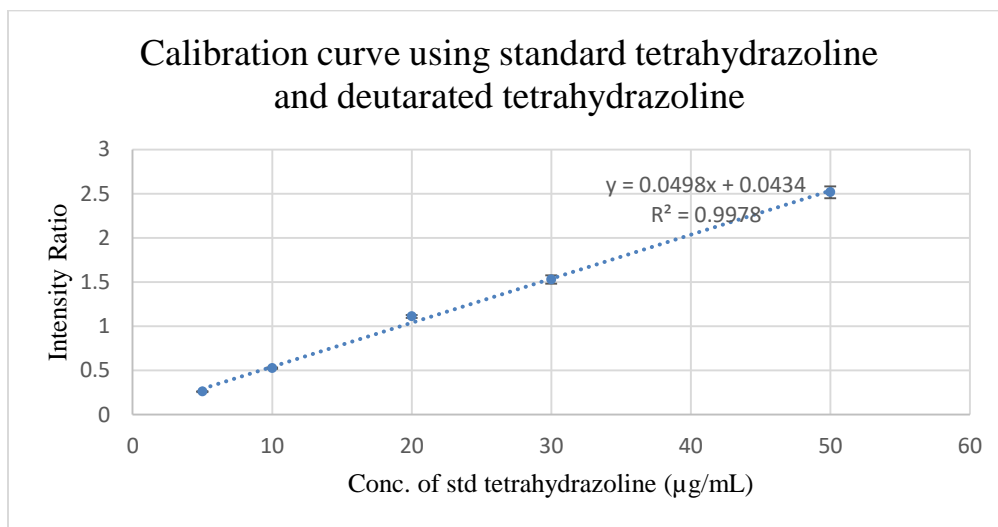
Figure 5.6: Calibration curve plotted using the ratio of standard, tetrahydrozoline, at concentrations 5, 10, 20, 30, and 50 µg/mL with simultaneous spiking with 20 µg/mL deuterated standard, tetrahydrozoline-d4. The equation of the line derived was y = 0.0498x + 0.0434 with a correlation factor (R^2) of 0.9978.

5.3.5.4 Calibration Curve using Tetrahydrozoline Standard Solution and Naphazoline Standard Solution

Calibration curve using standard tetrahydrozoline and standard naphazoline solution resulted in a trend line having a R^2 value of 0.9977 (Figure 5.7). From the equation of line, the concentration of the 3X diluted sample was calculated to be 39.57µg/mL, which deviates only by 1.08% from the true value (40µg/mL). This suggests high reliability of the method (Table D6). Furthermore, this approach eliminates the background matrix effect which limits analytical precision (147,188).
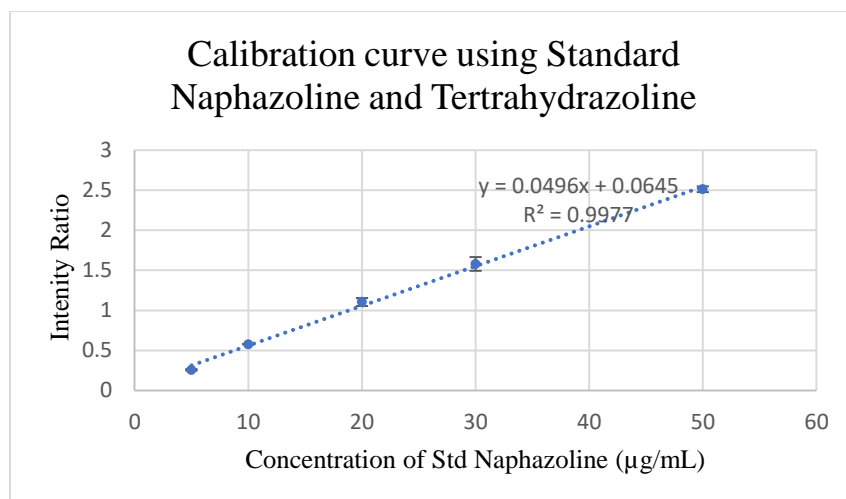
Figure 5.7: Calibration curve plotted using the ratio of standard, naphazoline, at concentrations 5, 10, 20, 30, and 50 µg/mL with simultaneous spiking with 20 µg/mL deuterated standard, tetrahydrozoline-d_4. The equation of the line derived was $y = 0.0496x + 0.0645$ with a correlation factor (R^2) of 0.9977.

5.3.5.5 Quantitation by Paper Spray

Table 5.6: Calculations performed using relative ion intensities obtained by paper spray of a solution having ophthalmic preparation with a deuterated standard.

	m/z 201	*m/z* 205	Spot Conc. µg/mL	Actual Conc. µg/mL	Average Conc./ µg/mL	SD	RSD
Visine							
	6.35E+03	3.05E+03	41.64	520.49			
	6.36E+03	3.15E+03	40.38	504.76	522.97	19.57	3.74
	4.98E+03	2.29E+03	43.49	543.67			
	m/z 211	*m/z* 201	Spot Conc. µg/mL	Actual Conc. µg/mL			
Clear					125.97	5.31	4.21
	2.02E+03	1.01E+03	40.00	120.00			
	2.95E+03	1.36E+03	43.38	130.15			
	4.28E+03	2.01E+03	42.59	127.76			

Quantitation by paper spray of the active components for both ophthalmic preparations showed consistent results similar to those obtained upon performing TLC-DESI-MS (Figure 5.8 and Table 5.6). The relative standard deviation among replicates was below 5.0 %, which further

supports that these modes of quantitation are relatively fast, convenient, and reliable requiring almost no sample preparation.
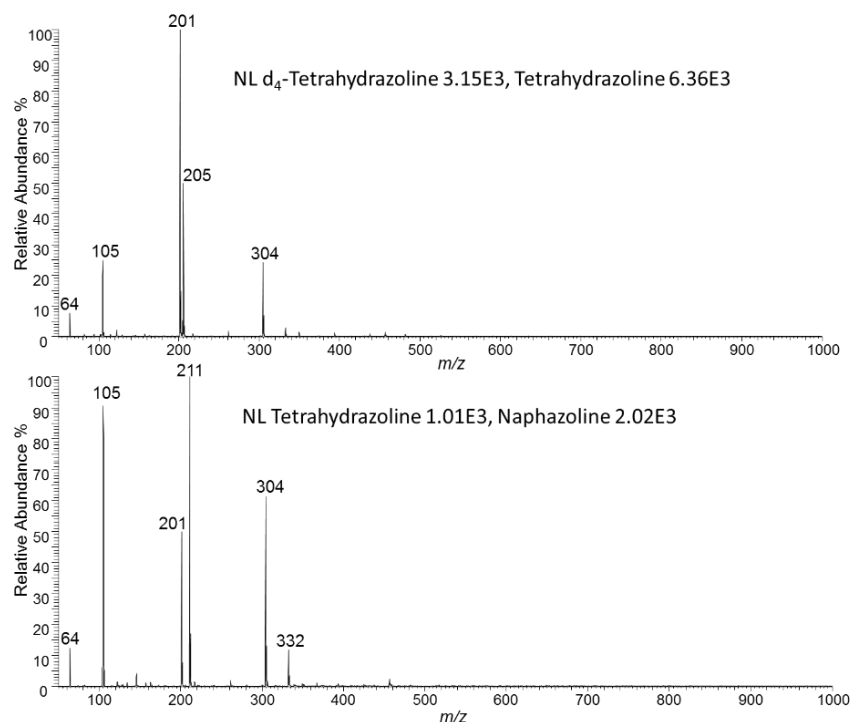
Figure 5.8: Spectra obtained after paper spray of mixtures having ophthalmic solution (Visine original and Clear Eye) and deuterated standard.

5.4 Conclusion

Desorption electrospray ionization mass spectroscopy (DESI-MS) is a versatile technique due to its rapid and reproducible mode of analysis under ambient condition with minimal sample preparation.(36,154,158,190–192) Thin-layer chromatography is also an effective, fast, and inexpensive approach. With appropriate mobile phase for the analyte under investigation, this method can provide good separation of any mixture of compounds (30,147,150,156,180). Coupling TLC with DESI MS facilitate accurate chemical identification and analysis of desired analytes. This work shows that TLC/DESI-MS and PS-MS are promising approach for the quantification of active components present in minute concentration (145,151,157,159,193). It

served to differentiate them from contaminants and product of degradation in any formulation. It can thus be used effortlessly in quantity and quality control of pharmaceuticals (149,160).

Quantification of tetrahydrozoline and naphazoline from Visine for red eye original and Clear eyes ophthalmic solutions were achieved by different approaches that focused on the ion intensities generated from specific concentrations of the standard, deuterated standard, and sample analysed. All the methods show high accuracy with low percentage of discrepancy from the label stated concentrations of the eye drop preparations. The limitation of the first two methods depends on instrumental variations and background effect hence it is recommended to acquire the data corresponding to the ion intensity of the sample and standards concurrently (149,187–189).

5.5 Experimental

5.5.1 Chemicals

HPLC grade acetonitrile, methanol, chloroform, water, ammonium hydroxide solution (28% NH_3 in H_2O, $\geq$ 99.99%) and acetic acid ($\geq$ 99.99%) were purchased from Sigma Aldrich Corp., (Oakville, Canada). Ethyl acetate reagent ($\geq$ 99.5% purity) was obtained from Caledon Laboratory Ltd (Georgetown, Canada). Tetrahydrozoline-d_4, CAS registry no. [1246814-66-3], $\geq$ 96 % chemical purity, was purchased from Toronto Research Chemicals, Inc. (Toronto, ON, Canada). Tetrahydrozoline, and naphazoline, CAS registry no. [522-48-5], $\geq$ 98 % and CAS registry no. [550-99-2], $\geq$ 97.5 %, were purchased from Sigma Aldrich Corp., (Oakville, Canada). Visine for red eye original containing tetrahydrozoline 0.05% w/v and Clear Eyes Allergy with 0.012% w/v of naphazoline were purchased from Shoppers Drug Mart (Toronto, Canada).

5.5.2 High Resolution Mass Spectrometry (HRMS) and Tandem Mass Spectrometry (MS/MS)

To ensure the molecular identity of the ions, HRMS and MS/MS were performed using the

LTQ Orbitrap Mass Spectrometer (Thermo Scientific, San Jose, CA, USA). Visine Original Red Eye containing 0.05% w/v tetrahydrozoline was diluted 200 fold using CH_3CN / H_2O in 7:3 (v/v) combination. The resultant solution was directly injected at a flow rate of 5µL/min. The collision energy was varied from 21 to 42% (manufacturer unit) depending on the ion being analyzed. The same procedure was followed for Clear Eyes Allergy sample which contained 0.012% w/v naphazoline.

5.5.3 Thin-Layer Chromatography (TLC)

TLC was performed on silica plates 5 x 5 cm (250 µm thickness, glass backed, 60Å stationary phase); Silicycle Inc., (Quebec, Canada). Mobile phase checked were combinations of $CHCl_3$ / CH_3OH in ratios of 2:3 (v/v) and 1:1 (v/v). $CHCl_3$ / CH_3OH in ratio 1:1 (v/v) was found the optimum solvent and was continued over the rest of the experiments. Silica plates were washed with methanol and air dried prior to spotting. On the TLC surface, 0.1 µL of standards and samples were spotted.

5.5.4 Desorption Electrospray Ionization Mass Spectrometry (DESI-MS)

A DESI ion source coupled to a Finnigan LTQ Linear Ion Trap Mass Spectrometer with a custom built moving stage was used to conduct the experiments. X-calibur 2.0 software was used to acquire the data (Thermo Scientific, San Jose, CA USA). The LTQ parameters were as follow: spray voltage, 5 kV; MS injection time, 150 ms. The DESI source conditions were as follow: nitrogen sheath gas pressure, 100 psi; incident angle, 52-54°; tip-to-surface distance, 1.5-2 mm; tip-to-inlet distance, 3−4 mm. CH_3CN / H_2O (7:3, v/v) was used as the spray solvent and was delivered at a flow rate of 5.0 µL/min. All mass spectra were obtained in positive ion mode. Scanning was performed towards the solvent font constantly at a speed of 179µm/s. Three scans were averaged. Red ink (rhodamine 6G, *m/z* 443) was used as a control prior to run, to optimize

the geometry of the DESI solvent spray.

5.5.5 DESI-MS Spray Solvent Selection

CH₃OH 100%, CH₃OH / H₂O in ratio 1:1 (v/v), CH₃CN 100 %, and CH₃CN / H₂O in combination 1:1 (v/v) and 7:3 (v/v) were tested as DESI spray solvents. Based on the observed ion count, the solvent or combination was varied until the highest and most reproducible ion signal was obtained for all the active principles.

5.5.6 Determination of limit of detection (LOD) of the Tetrahydrozoline and Naphazoline

Standard solution of tetrahydrozoline and naphazoline were prepared having concentration 1 µg/mL. The solution was then serially diluted to obtain concentration, 100 ng/mL. 0.25 µL, 0.5 µL and 1 µL of the solution were spotted on a TLC plate, prior to its analysis by DESI-MS.

5.5.7 Quantitative Analysis of Active Components

5.5.7.1 Calibration Curve using Tetrahydrozoline and Naphazoline Standards

For the quantification of the active components, standards containing 5, 10, 20, 30, 50, 100, and 200 µg/mL of tetrahydrozoline were prepared by serial dilution using a 500 µg/mL stock solution. Similarly, naphazoline standards of 5, 10, 20, 30, 50, 80 and 100 µg/mL were prepared by serial dilution from a stock of 120 µg/mL.

0.1 µL of the solutions were spotted and analyzed by TLC-DESI-MS. The ion intensity obtained was used to plot calibration curves which were used to determine the tetrahydrozoline and naphazoline concentration in the diluted Visine Red Eye (12.5X and 30X) and Clear Eye Allergy (3X and 10X) ophthalmic preparations.

5.5.7.2 Direct spot analysis of mixture having Deuterated Standard and Ophthalmic solution

Deuterated tetrahydrozoline standard (*m/z* 205) was spiked in 0.05 % w/v Visine Red Eyes preparation to make a mixture having 20 µg/mL deuterated tetrahydrozoline and 12.5X diluted

Visine Red Eyes ophthalmic preparation. The resultant solution was spotted on a TLC plate and the ion intensities were acquired for 1 minute by DESI-MS.

The procedure was repeated with Clear Eye Allergy solution, making a resultant mixture having 20µg/mL standard tetrahydrozoline and 3X diluted clear eye drop ophthalmic preparation.

5.5.7.3 Calibration Curve using Deuterated Internal Standard Solution and Tetrahydrozoline Standard Solution

A fixed amount of the deuterated tetrahydrozoline, 20 µg/mL (final concentration), was spiked in aliquots containing different concentrations of the tetrahydrozoline standard (5, 10, 20, 30, 50 µg/mL). The resultant solutions were spotted on the TLC plate and were developed using the $CHCl_3$ / CH_3OH (1:1, v/v) prior to the DESI-MS analysis. To obtain a calibration curve, the ion intensity ratio of the standard (*m/z* 201) to the deuterated standard (*m/z* 205) was plotted against the concentration of the standard (*m/z* 201). Three plates were analysed and their average ratio with standard deviation was plotted to obtain the calibration curve.

The same procedure was repeated with naphazoline standards having final concentration of 5, 10, 20, 30, and 50 µg/mL, spiked with 20 µg/mL(final conc.) tetrahydrozoline standard.

5.5.7.4 Paper Spray

A printing paper was cut in triangular shapes and was held with a voltage clip infront of the MS inlet. The clip was subjected to 5kV. A solution of 20 µg/mL deuterated tetrahydrozoline standard (*m/z* 205) was spiked in 12.5X diluted sample of 0.05 % w/v Visine Red Eye prepartion. The resultant solution was spotted at the tip of the paper and CH_3CN / H_2O (7:3, v/v) was drizzled on the paper. MS scans were acquired averaging 3 micro scans having 10 ms injection time. Spotting was repeated three times and concentration values were calculated along with the relative standard deviation.

The same procedure was repeated with a 3X diluted sample of 0.012% w/v Clear Eye

Allergy solution and 20 µg/mL of tetrahydrozoline standard (*m/z* 205) as the internal standard.

CHAPTER SIX

Conclusion and Future Work

6.1 Conclusion

The work summarized in this thesis elaborates the usefulness of DESI-MS as a powerful ambient ionization technique for characterization, quantitation and imaging. The fact that it allows direct analysis of sample under ambient condition without any sample destruction, makes it a very suitable analytical tool for field operations. With the advent of potable mass spectrometers, this technique will gain popularity in the field of forensics, microbiology, pharmaceutics, food and drug industry, drug discovery, histology and many others that requires direct sampling. Incorporating a simple mode of separation technique like TLC, eliminated of ion suppression and enabled achievement of great linearity in quantitative assessment of pharmaceutics. Even at minute drug concentration this technique proves to be robust and sensitive enough to pick up slight variation in drug concentration. The identification of antibiotics like Lysolipin I and analogue of Lienomycin by direct sampling of microbial colony depicts its potential in field of microbiology and drug discovery.

This works also illustrates the use of paper spray mass spectrometry for characterization and quantitation of pharmaceutics. Paper spray has high potential in the field of analytical sciences. Even though it suffers from signal fluctuation, it is a reliable, inexpensive and quick method for easy assessment of the article of interest. Its ease of use will make it a valuable method in the field of illicit drug analysis.

6.2 Future Work

As future work different ink colors and different brands pen can be analyzed for identification of more invisible state markers in order to generate library that will be useful to detect forgery. 3D imaging of actinobacteria will enable comprehensive study about its secondary metabolites and will

also allow to determine their role in different stages of its lifecycle. The growth media of actinobacteria can also be tested against a resistant strain to further confirm the compounds identity. Again, analogue of lienomycin characterized in this work can be chemically hydrolyzed with acids to elaborately understand its fragmentation profile upon performing tandem mass spectrometry and also to locate the position of hydroxylation and double bonding.

It will beneficial to use 3-D printing to make a device for holding paper while performing paper spray. This will ensure signal stability and reproducibility in paper spray data. Acquisition of sample signal along with an internal standard also limits signal fluctuation. Calibration curve with caffeine, tetrahydrazoline and naphazoline can also be acquired using PS-MS.

REFERENCES

1. El-Aneed A, Cohen A, Banoub J. Mass spectrometry, review of the basics: Electrospray, MALDI, and commonly used mass analyzers. Vol. 44, Applied Spectroscopy Reviews. 2009. p. 210–30.

2. Konermann L, Ahadi E, Rodriguez AD, Vahidi S. Unraveling the mechanism of electrospray ionization. Anal Chem. 2013;85(1):2–9.

3. Münzenberg G. Development of mass spectrometers from Thomson and Aston to present. Int J Mass Spectrom. 2013;349–350(1):9–18.

4. Cody RB, Laramée JA, Durst HD. Versatile new ion source for the analysis of materials in open air under ambient conditions. Anal Chem. 2005;77(8):2297–302.

5. Takats Z. Mass Spectrometry Sampling Under Ambient Conditions with Desorption Electrospray Ionization. Science (80-) [Internet]. 2004;306(5695):471–3. Available from: http://www.sciencemag.org/cgi/doi/10.1126/science.1104404

6. Haddad R, Sparrapan R, Eberlin MN. Desorption sonic spray ionization for (high) voltage-free ambient mass spectrometry. Rapid Commun Mass Spectrom. 2006;20(19):2901–5.

7. Hiraoka K, Nishidate K, Mori K, Asakawa D, Suzuki S. Development of probe electrospray using a solid needle. Rapid Commun Mass Spectrom. 2007;21(18):3139–44.

8. Chen H, Wortmann A, Zenobi R. Neutral desorption sampling coupled to extractive electrospray ionization mass spectrometry for rapid differentiation of biosamples by metabolomic fingerprinting. J Mass Spectrom. 2007;42(9):1123–35.

9. Basile F, Zhang S, Shin Y-S, Drolet B. Atmospheric pressure-thermal desorption (AP-TD)/electrospray ionization-mass spectrometry for the rapid analysis of Bacillus spores. Analyst [Internet]. 2010;135(4):797. Available from: http://xlink.rsc.org/?DOI=c0an00071j

10. Wachs T, Henion J. Electrospray device for coupling microscale separations and other miniaturized devices with electrospray mass spectrometry. Anal Chem. 2001;73(3):632–8.

11. Kertesz V, Van Berkel GJ. Fully automated liquid extraction-based surface sampling and ionization using a chip-based robotic nanoelectrospray platform. J Mass Spectrom. 2010;45(3):252–60.

12. Hsu HJ, Kuo TL, Wu SH, Oung JN, Shiea J. Characterization of synthetic polymers by

electrospray-assisted pyrolysis ionization-mass spectrometry. Anal Chem. 2005;77(23):7744–9.

13. Liu J, Wang H, Manicke NE, Lin JM, Cooks RG, Ouyang Z. Development, characterization, and application of paper spray ionization. Anal Chem. 2010;82(6):2463–71.

14. Ovchinnikova OS, van Berkel GJ. Thin-layer chromatography and mass spectrometry coupled using proximal probe thermal desorption with electrospray or atmospheric pressure chemical ionization. Rapid Commun Mass Spectrom. 2010;24(12):1721–9.

15. Cody RB, Laramée J a, Nilles JM, Durst HD. Direct Analysis in Real Time (DART tm) Mass Spectrometry. JEOL News. 2005;40(1):8–12.

16. Andrade FJ, Shelley JT, Wetzel WC, Webb MR, Gamez G, Ray SJ, et al. Atmospheric pressure chemical ionization source. 1. Ionization of compounds in the gas phase. Anal Chem [Internet]. 2008;80(8):2646–53. Available from: http://www.ncbi.nlm.nih.gov/pubmed/18345693

17. Harper JD, Charipar NA, Mulligan CC, Zhang X, Cooks RG, Ouyang Z. Low-temperature plasma probe for ambient desorption ionization. Anal Chem. 2008;80(23):9097–104.

18. Na N, Zhao M, Zhang S, Yang C, Zhang X. Development of a Dielectric Barrier Discharge Ion Source for Ambient Mass Spectrometry. J Am Soc Mass Spectrom. 2007;18(10):1859–62.

19. Symond JM, Galhena AS, Fernández FM, Orlando TM. Microplasma discharge ionization source for ambient mass spectrometry. Anal Chem. 2010;82(2):621–7.

20. Takáts Z, Cotte-Rodriguez I, Talaty N, Chen H, Cooks RG. Direct, trace level detection of explosives on ambient surfaces by desorption electrospray ionization mass spectrometry. Chem Commun (Camb) [Internet]. 2005;(15):1950–2. Available from: http://www.ncbi.nlm.nih.gov/pubmed/15834468

21. Wang H, Sun W, Zhang J, Yang X, Lin T, Ding L. Desorption corona beam ionization source for mass spectrometry. Analyst. 2010;135(4):688–95.

22. Mcewen CN, Mckay RG, Larsen BS. Analysis of Solids , Liquids , and Biological Tissues Using Solids Probe Introduction at Atmospheric Pressure on Commercial LC / MS Instruments. Anal Chem. 2005;77(23):7826–31.

23. Nyadong L, Galhena AS, Fernández FM. Desorption Electrospray/Metastable-Induced

Ionization: A Flexible Multimode Ambient Ion Generation Technique. Anal Chem [Internet]. 2009 Sep 15;81(18):7788–94. Available from: https://doi.org/10.1021/ac9014098

24.   Nemes P, Vertes A. Laser ablation electrospray ionization for atmospheric pressure, in vivo, and imaging mass spectrometry. Anal Chem. 2007;79(21):8098–106.

25.   Sampson JS, Muddiman DC. Atmospheric pressure infrared (10.6 µm) laser desorption electrospray ionization (IR-LDESI) coupled to a LTQ Fourier transform ion cyclotron resonance mass spectrometer. Rapid Commun Mass Spectrom [Internet]. 2009;23(13):1989–92. Available from: http://www3.interscience.wiley.com/journal/122440257/abstract

26.   Sampson JS, Hawkridge AM, Muddiman DC. Generation and Detection of Multiply-Charged Peptides and Proteins by Matrix-Assisted Laser Desorption Electrospray Ionization (MALDESI) Fourier Transform Ion Cyclotron Resonance Mass Spectrometry. J Am Soc Mass Spectrom. 2006;17(12):1712–6.

27.   Shiea J, Huang M, HSu H, Lee C, Yuan C, Beech I, et al. Electrospray-assisted laser desorption/ionization mass spectrometry for direct ambient analysis of solids. Rapid Commun Mass Spectrom. 2005;19(24):3701–4.

28.   Galhena AS, Harris GA, Nyadong L, Murray KK, Fernández FM. Small molecule ambient mass spectrometry imaging by infrared laser ablation metastable-induced chemical ionization. Anal Chem. 2010;82(6):2178–81.

29.   Trimpin S, Inutan ED, Herath TN, McEwen CN. Laserspray Ionization, a New Atmospheric Pressure MALDI Method for Producing Highly Charged Gas-phase Ions of Peptides and Proteins Directly from Solid Solutions. Mol Cell Proteomics [Internet]. 2010;9(2):362–7. Available from: http://www.mcponline.org/lookup/doi/10.1074/mcp.M900527-MCP200

30.   Cheng S-C, Huang M-Z, Shiea J. Thin-layer chromatography/laser-induced acoustic desorption/electrospray ionization mass spectrometry. Anal Chem. 2009;81(22):9274–81.

31.   Dixon RB, Sampson JS, Muddiman DC. Generation of Multiply Charged Peptides and Proteins by Radio Frequency Acoustic Desorption and Ionization for Mass Spectrometric Detection. J Am Soc Mass Spectrom. 2009;20(4):597–600.

32.   Haapala M, Pól J, Saarela V, Arvola V, Kotiaho T, Ketola RA, et al. Desorption

atmospheric pressure photoionization. Anal Chem. 2007;79(20):7867–72.

33. Neidholdt EL, Beauchamp JL. Switched ferroelectric plasma ionizer (SwiFerr) for ambient mass spectrometry. Anal Chem. 2011;83(1):38–43.

34. Steeb J, Galhena AS, Nyadong L, Janata J, Fernández FM. Beta electron-assisted direct chemical ionization (BADCI) probe for ambient mass spectrometry. Chem Commun [Internet]. 2009;(31):4699. Available from: http://xlink.rsc.org/?DOI=b909072j

35. Schäfer K-C, Dénes J, Albrecht K, Szaniszló T, Balogh J, Skoumal R, et al. In vivo, in situ tissue analysis using rapid evaporative ionization mass spectrometry. Angew Chemie - Int Ed [Internet]. 2009;48(44):8240–2. Available from: http://www.scopus.com/inward/record.url?eid=2-s2.0-70350002151&partnerID=40

36. Takats Z, Wiseman JM, Cooks RG. Ambient mass spectrometry using desorption electrospray ionization (DESI): instrumentation, mechanisms and applications in forensics, chemistry, and biology. J Mass Spectrom. 2005;40(10):1261–75.

37. Costa AB, Cooks RG. Simulated splashes: Elucidating the mechanism of desorption electrospray ionization mass spectrometry. Chem Phys Lett. 2008;464(1–3):1–8.

38. Howard GC, Brown WE, Auer M. Imaging Life: Biological Systems from Atoms to Tissues. Oxford University Press, USA; 2014.

39. Eberlin LS, Ifa DR, Wu C, Cooks RG. Three-Dimensional Vizualization of Mouse Brain by Lipid Analysis Using Ambient Ionization Mass Spectrometry. Angew Chemie. 2010 Jan;122(5):885–8.

40. Chen H, Venter A, Cooks RG. Extractive electrospray ionization for direct analysis of undiluted urine, milk and other complex mixtures without sample preparation. Chem Commun. 2006;(19):2042–4.

41. Kauppila TJ, Wiseman JM, Ketola RA, Kotiaho T, Cooks RG, Kostiainen R. Desorption electrospray ionization mass spectrometry for the analysis of pharmaceuticals and metabolites. Rapid Commun Mass Spectrom. 2006;20(3):387–92.

42. Pan Z, Gu H, Talaty N, Chen H, Shanaiah N, Hainline BE, et al. Principal component analysis of urine metabolites detected by NMR and DESI–MS in patients with inborn errors of metabolism. Anal Bioanal Chem. 2007;387(2):539–49.

43. Hemalatha RG, Pradeep T. Understanding the molecular signatures in leaves and flowers by desorption electrospray ionization mass spectrometry (DESI MS) imaging. J Agric

Food Chem. 2013;61(31):7477–87.

44. Lane AL, Nyadong L, Galhena AS, Shearer TL, Stout EP, Parry RM, et al. Desorption electrospray ionization mass spectrometry reveals surface-mediated antifungal chemical defense of a tropical seaweed. Proc Natl Acad Sci. 2009;106(18):7314–9.

45. Li B, Knudsen C, Hansen NK, Jørgensen K, Kannangara R, Bak S, et al. Visualizing metabolite distribution and enzymatic conversion in plant tissues by desorption electrospray ionization mass spectrometry imaging. Plant J. 2013;74(6):1059–71.

46. Tata A, Perez CJ, Ore MO, Lostun D, Passas A, Morin S, et al. Evaluation of imprint DESI-MS substrates for the analysis of fungal metabolites. RSC Adv. 2015;5(92):75458–64.

47. Tata A, Perez C, Campos ML, Bayfield MA, Eberlin MN, Ifa DR. Imprint desorption electrospray ionization mass spectrometry imaging for monitoring secondary metabolites production during antagonistic interaction of fungi. Anal Chem. 2015;87(24):12298–305.

48. Lanekoff I, Geydebrekht O, Pinchuk GE, Konopka AE, Laskin J. Spatially resolved analysis of glycolipids and metabolites in living Synechococcus sp. PCC 7002 using nanospray desorption electrospray ionization. Analyst. 2013;138(7):1971–8.

49. Jackson AU, Werner SR, Talaty N, Song Y, Campbell K, Cooks RG, et al. Targeted metabolomic analysis of Escherichia coli by desorption electrospray ionization and extractive electrospray ionization mass spectrometry. Anal Biochem. 2008;375(2):272–81.

50. Meetani MA, Shin Y, Zhang S, Mayer R, Basile F. Desorption electrospray ionization mass spectrometry of intact bacteria. J mass Spectrom. 2007;42(9):1186–93.

51. Chen H, Talaty NN, Takáts Z, Cooks RG. Desorption electrospray ionization mass spectrometry for high-throughput analysis of pharmaceutical samples in the ambient environment. Anal Chem. 2005;77(21):6915–27.

52. Williams JP, Scrivens JH. Rapid accurate mass desorption electrospray ionisation tandem mass spectrometry of pharmaceutical samples. Rapid Commun Mass Spectrom An Int J Devoted to Rapid Dissem Up-to-the-Minute Res Mass Spectrom. 2005;19(24):3643–50.

53. Cotte-Rodríguez I, Takáts Z, Talaty N, Chen H, Cooks RG. Desorption electrospray ionization of explosives on surfaces: sensitivity and selectivity enhancement by reactive desorption electrospray ionization. Anal Chem. 2005;77(21):6755–64.

54. Cotte-Rodríguez I, Chen H, Cooks RG. Rapid trace detection of triacetone triperoxide

(TATP) by complexation reactions during desorption electrospray ionization. Chem Commun. 2006;(9):953–5.

55. Cotte-Rodríguez I, Cooks RG. Non-proximate detection of explosives and chemical warfare agent simulants by desorption electrospray ionization mass spectrometry. Chem Commun. 2006;(28):2968–70.

56. Cotte-Rodriguez I, Hernandez-Soto H, Chen H, Cooks RG. In situ trace detection of peroxide explosives by desorption electrospray ionization and desorption atmospheric pressure chemical ionization. Anal Chem. 2008;80(5):1512–9.

57. Justes DR, Talaty N, Cotte-Rodriguez I, Cooks RG. Detection of explosives on skin using ambient ionization mass spectrometry. Chem Commun. 2007;(21):2142–4.

58. Eberlin LS, Haddad R, Neto RCS, Cosso RG, Maia DRJ, Maldaner AO, et al. Instantaneous chemical profiles of banknotes by ambient mass spectrometry. Analyst. 2010;135(10):2533–9.

59. Ifa DR, Gumaelius LM, Eberlin LS, Manicke NE, Cooks RG. Forensic analysis of inks by imaging desorption electrospray ionization (DESI) mass spectrometry. Analyst. 2007;132(5):461–7.

60. Khatami A, Prova SS, Bagga AK, Yan Chi Ting M, Brar G, Ifa DR. Detection and imaging of thermochromic ink compounds in erasable pens using desorption electrospray ionization mass spectrometry. Rapid Commun Mass Spectrom. 2017;31(12):983–90.

61. Jackson AT, Williams JP, Scrivens JH. Desorption electrospray ionisation mass spectrometry and tandem mass spectrometry of low molecular weight synthetic polymers. Rapid Commun Mass Spectrom An Int J Devoted to Rapid Dissem Up-to-the-Minute Res Mass Spectrom. 2006;20(18):2717–27.

62. Bereman MS, Nyadong L, Fernandez FM, Muddiman DC. Direct high-resolution peptide and protein analysis by desorption electrospray ionization Fourier transform ion cyclotron resonance mass spectrometry. Rapid Commun mass Spectrom. 2006;20(22):3409–11.

63. Shin Y-S, Drolet B, Mayer R, Dolence K, Basile F. Desorption electrospray ionization-mass spectrometry of proteins. Anal Chem. 2007;79(9):3514–8.

64. Keating JE, Minges JT, Randell SH, Glish GL. Paper spray mass spectrometry for high-throughput quantification of nicotine and cotinine. Anal Methods. 2018;10(1):46–50.

65. Wang H, Liu J, Cooks RG, Ouyang Z. Paper spray for direct analysis of complex mixtures

using mass spectrometry. Angew Chemie Int Ed. 2010;49(5):877–80.

66.   Wang H, Manicke NE, Yang Q, Zheng L, Shi R, Cooks RG, et al. Direct analysis of biological tissue by paper spray mass spectrometry. Anal Chem. 2011;83(4):1197–201.

67.   Sun W, Wu R, Last JA. Effects of exposure to environmental tobacco smoke on a human tracheobronchial epithelial cell line. Toxicology. 1995;100(1–3):163–74.

68.   Vallano PT, Shugarts SB, Woolf EJ, Matuszewski BK. Elimination of autosampler carryover in a bioanalytical HPLC-MS/MS method: a case study. J Pharm Biomed Anal. 2005;36(5):1073–8.

69.   Bakhtiar R, Majumdar TK. Tracking problems and possible solutions in the quantitative determination of small molecule drugs and metabolites in biological fluids using liquid chromatography–mass spectrometry. J Pharmacol Toxicol Methods. 2007;55(3):227–43.

70.   Schwartz JC, Senko MW, Syka JEP. A two-dimensional quadrupole ion trap mass spectrometer. J Am Soc Mass Spectrom. 2002;

71.   Douglas DJ, Frank AJ, Mao D. Linear ion traps in mass spectrometry. Mass Spectrom Rev. 2005;24(1):1–29.

72.   Eliuk S, Makarov A. Evolution of Orbitrap Mass Spectrometry Instrumentation. Annu Rev Anal Chem. 2015;

73.   Perry RH, Cooks RG, Noll RJ. Orbitrap mass spectrometry: Instrumentation, ion motion and applications. Mass Spectrom Rev. 2008;

74.   Scigelova M, Makarov A. Orbitrap mass analyzer - Overview and applications in proteomics. In: Proteomics. 2006.

75.   Brunelle RL, Reed RW. Forensic examination of ink and paper. CC Thomas; 1984.

76.   Throckmorton GJ. Erasable ink: its ease of erasability and its permanence. J Forensic Sci. 1985;30(2):526–30.

77.   Zimmerman J, Doherty P, Mooney D. Erasable felt tip writing instrument detection. J Forensic Sci. 1988;33(3):709–17.

78.   Welch J. Erasable ink; something old, something new. Sci Justice. 2008;48(4):187–91.

79.   AsiaOne. Incidents of Erasable Pen Misuse Increase in Japan [Internet]. 2014 [cited 2016 Nov 8]. Available from: http://www.asiaone.com/asia/incidents-erasable-pen-misuse-increase-japan

80.   Kaye BH. Science and the detective: selected reading in forensic science. John Wiley &

Sons; 2008.

81. Eldebss TMA, El-Zawawy WK, Gazy MB, Helal MR, Rashed KE, Egypt J. Using an erasable ink to forge documents, medico-legal study on evaluating them in detection and prevention the forgery. J Am Sci. 2015;11(11).

82. Lalli PM, Sanvido GB, Garcia JS, Haddad R, Cosso RG, Maia DRJ, et al. Fingerprinting and aging of ink by easy ambient sonic-spray ionization mass spectrometry. Analyst. 2010;135(4):745–50.

83. Jurisch M, Augusti R. Detection of signature forgery with erasable pens using paper spray mass spectrometry (PS-MS). Anal Methods. 2016;8(23):4543–6.

84. Seeboth A, Lötzsch D, Ruhmann R, Muehling O. Thermochromic Polymers□ Function by Design. Chem Rev. 2014;114(5):3037–68.

85. Kamitani T, Okuyama H. Thermosensitive decolorable ink composition [Internet]. United States: Mitsubishi Pencil Company, Ltd; United States Patent 8616797, 2012. Available from: http://www.freepatentsonline.com/8616797.pdf

86. Kao Y, Cheng S, Cheng C, Shiea J, Ho H. Detection of trace ink compounds in erased handwritings using electrospray-assisted laser desorption ionization mass spectrometry. J Mass Spectrom. 2014;49(6):445–51.

87. Fujita K. Reversible thermal discoloration aqueous ink composition and writing implement using the same and writing implement set. Google Patents; 2013.

88. Campbell DJ, Bosma WB, Bannon SJ, Gunter MM, Hammar MK. Demonstration of thermodynamics and kinetics using FriXion erasable pens. J Chem Educ. 2012;89(4):526–8.

89. Weyermann C, Kirsch D, Costa-Vera C, Spengler B. Photofading of ballpoint dyes studied on paper by LDI and MALDI MS. J Am Soc mass Spectrom. 2006;17(3):297–306.

90. Miyajima T, Tanaka N, Saito N. Erasable Ball-Point Pen Ink. United States; 1983.

91. Chu P-C, Cai BY, Tsoi YK, Yuen R, Leung KSY, Cheung N-H. Forensic analysis of laser printed ink by X-ray fluorescence and laser-excited plume fluorescence. Anal Chem. 2013;85(9):4311–5.

92. Chen H-S, Meng H-H, Cheng K-C. A survey of methods used for the identification and characterization of inks. Forensic Sci J. 2002;1(1):1–14.

93. Williams MR, Moody C, Arceneaux L-A, Rinke C, White K, Sigman ME. Analysis of black writing ink by electrospray ionization mass spectrometry. Forensic Sci Int. 2009;191(1–3):97–103.

94. Carlysle F. TLC the Forensic Way [Internet]. 2011. Available from: https://the-gist.org/2011/07/tlc-the-forensic-way/

95. Fabianska E, Trzcinska BM. Differentiation of ballpoint and liquid inks-a comparison of methods in use. Probl Forensic Sci. 2001;46:383–400.

96. Wiseman JM, Ifa DR, Zhu Y, Kissinger CB, Manicke NE, Kissinger PT, et al. Desorption electrospray ionization mass spectrometry: Imaging drugs and metabolites in tissues. Proc Natl Acad Sci. 2008;105(47):18120–5.

97. Girod M, Shi Y, Cheng J-X, Cooks RG. Mapping lipid alterations in traumatically injured rat spinal cord by desorption electrospray ionization imaging mass spectrometry. Anal Chem. 2010;83(1):207–15.

98. Mulligan CC. Field-portable mass spectrometers for onsite analytics: What's next? INFORM. 2009;20:625.

99. Snyder DT, Pulliam CJ, Ouyang Z, Cooks RG. Miniature and fieldable mass spectrometers: recent advances. Anal Chem. 2015;88(1):2–29.

100. Lawton ZE, Traub A, Fatigante WL, Mancias J, O'Leary AE, Hall SE, et al. Analytical validation of a portable mass spectrometer featuring interchangeable, ambient ionization sources for high throughput forensic evidence screening. J Am Soc Mass Spectrom. 2017;28(6):1048–59.

101. Haaf F, Sanner A, Straub F. Polymers of N-vinylpyrrolidone: synthesis, characterization and uses. Polym J. 1985;17(1):143.

102. da Silva Ferreira P, e Silva DF de A, Augusti R, Piccin E. Forensic analysis of ballpoint pen inks using paper spray mass spectrometry. Analyst. 2015;140(3):811–9.

103. Bull AT, Goodfellow M, Slater JH. Biodiversity as a source of innovation in biotechnology. Annu Rev Microbiol. 1992;46(1):219–46.

104. Colwell RR. Microbial diversity: the importance of exploration and conservation. J Ind Microbiol Biotechnol. 1997;18(5):302–7.

105. Weber T, Charusanti P, Musiol-Kroll EM, Jiang X, Tong Y, Kim HU, et al. Metabolic engineering of antibiotic factories: new tools for antibiotic production in actinomycetes.

Trends Biotechnol. 2015;33(1):15–26.

106. Leal IR, Silva JMC da, Tabarelli M, Lacher Jr TE. Mudando o curso da conservação da biodiversidade na Caatinga do Nordeste do Brasil. Megadiversidade. 2005;1(1):139–46.

107. Pacchioni RG, Carvalho FM, Thompson CE, Faustino ALF, Nicolini F, Pereira TS, et al. Taxonomic and functional profiles of soil samples from Atlantic forest and Caatinga biomes in northeastern Brazil. Microbiologyopen. 2014;3(3):299–315.

108. de Oliveira G, Araújo MB, Rangel TF, Alagador D, Diniz-Filho JAF. Conserving the Brazilian semiarid (Caatinga) biome under climate change. Biodivers Conserv. 2012;21(11):2913–26.

109. IBGE F. Manual Técnico da Vegetação Brazileira (Manuais Técnicos de Geociências no 01). Rio Janeiro, Brazil. 1992;

110. Leal IR, Tabarelli M, Da Silva JMC. Ecologia e conservação da Caatinga. Editora Universitária UFPE; 2003.

111. Waksman SA. The Actinomycetes-their nature, occurrence, activities, and importance. Actinomycetes-their nature, Occur Act importance. 1950;

112. Berdy J. Are actinomycetes exhausted as a source of secondary metabolites? Biotechnologija. 1995;

113. Flärdh K, Buttner MJ. Streptomyces morphogenetics: dissecting differentiation in a filamentous bacterium. Nat Rev Microbiol. 2009;7(1):36.

114. Basilio A, Gonzalez I, Vicente MF, Gorrochategui J, Cabello A, Gonzalez A, et al. Patterns of antimicrobial activities from soil actinomycetes isolated under different conditions of pH and salinity. J Appl Microbiol. 2003;95(4):814–23.

115. Lechevalier MP. Identification of aerobic actinomycetes of clinical importance. J Lab Clin Med. 1968;71(6):934–44.

116. Vasconcellos RLF de, Silva MCP da, Ribeiro CM, Cardoso EJBN. Isolation and screening for plant growth-promoting (PGP) actinobacteria from Araucaria angustifolia rhizosphere soil. Sci Agric. 2010;67(6):743–6.

117. Freitas SS, SILVEIRA APD. Microbiota do solo e qualidade ambiental. Campinas Inst Agronômico Campinas-IAC. 2007;

118. Yang Y-L, Xu Y, Straight P, Dorrestein PC. Translating metabolic exchange with imaging mass spectrometry. Nat Chem Biol. 2009;5(12):nchembio-252.

119. Liu W-T, Yang Y-L, Xu Y, Lamsa A, Haste NM, Yang JY, et al. Imaging mass spectrometry of intraspecies metabolic exchange revealed the cannibalistic factors of Bacillus subtilis. Proc Natl Acad Sci. 2010;107(37):16286–90.

120. Campbell IS, Ton AT, Mulligan CC. Direct detection of pharmaceuticals and personal care products from aqueous samples with thermally-assisted desorption electrospray ionization mass spectrometry. J Am Soc Mass Spectrom. 2011;22(7):1285.

121. Watrous JD, Dorrestein PC. Imaging mass spectrometry in microbiology. Nat Rev Microbiol. 2011;9(9):683.

122. Sica VP, Raja HA, El-Elimat T, Oberlies NH. Mass spectrometry imaging of secondary metabolites directly on fungal cultures. Rsc Adv. 2014;4(108):63221–7.

123. Angolini CFF, Vendramini PH, Araújo FDS, Araújo WL, Augusti R, Eberlin MN, et al. Direct protocol for ambient mass spectrometry imaging on agar culture. Anal Chem. 2015;87(13):6925–30.

124. Peti APF. Identificação de agentes antimicrobianos produzidos por actinobactérias de solo com potencial aplicação no controle da mastite bovina. Universidade de São Paulo;

125. Pawlak J, Zielinski J, Golik J, Gumieniak J, Borowski E. The Structure of Lienomycin, a Pentaene Macrolide Antitumor Antibiotic. J Antibiot (Tokyo). 1980;33(9):989–97.

126. Drautz H, Keller-Schierlein W, Zähner H. Metabolic products of microorganisms, 149. Lysolipin I, a new antibiotic from Streptomyces violaceoniger (author's transl). Arch Microbiol. 1975;106(3):175–90.

127. Lopez P, Hornung A, Welzel K, Unsin C, Wohlleben W, Weber T, et al. Isolation of the lysolipin gene cluster of Streptomyces tendae Tü 4042. Gene. 2010;461(1):5–14.

128. Dobler M, Keller-Schierlein W. Metabolites of microorganisms. 162nd communication. The crystal and molecular structure of lysolipin I. Helv Chim Acta. 1977;60(1):178–85.

129. Aparicio JF, Mendes M V, Antón N, Recio E, Martín JF. Polyene macrolide antibiotic biosynthesis. Curr Med Chem. 2004;11(12):1643–56.

130. Martin J-F. Biosynthesis of polyene macrolide antibiotics. Annu Rev Microbiol. 1977;31(1):13–36.

131. Bolard J. How do the polyene macrolide antibiotics affect the cellular membrane properties? Biochim Biophys Acta (BBA)-Reviews Biomembr. 1986;864(3–4):257–304.

132. Hartsel S, Bolard J. Amphotericin B: new life for an old drug. Trends Pharmacol Sci.

1996;17(12):445–9.

133. Milhaud J, Ponsinet V, Takashi M, Michels B. Interactions of the drug amphotericin B with phospholipid membranes containing or not ergosterol: new insight into the role of ergosterol. Biochim Biophys Acta (BBA)-Biomembranes. 2002;1558(2):95–108.

134. Weakliem CL, Fujii G, Chang J-E, Ben-Shaul A, Gelbart WM. Effect of tension on pore formation in drug-containing vesicles. J Phys Chem. 1995;99(19):7694–7.

135. Fujii G, Chang J-E, Coley T, Steere B. The formation of amphotericin B ion channels in lipid bilayers. Biochemistry. 1997;36(16):4959–68.

136. Liu H, Thorson JS. Pathways and mechanisms in the biogenesis of novel deoxysugars by bacteria. Annu Rev Microbiol. 1994;48(1):223–56.

137. Ulrych A, Derrick PJ, Adamek F, Novák P, Lemr K, Havlicek V. Dissociation of nystatin and amphotericin analogues: characterisation of minor anti-fungal macrolides. Eur J Mass Spectrom. 2010;16(1):73–80.

138. Omura S. Macrolide antibiotics: chemistry, biology, and practice. Elsevier; 2002.

139. NAKAGOMI K, TAKEUCHI M, TANAKA H, TOMIZUKA N, NAKAJIMA T. Studies on inhibitors of rat mast cell degranulation produced by microorganisms. J Antibiot (Tokyo). 1990;43(5):462–9.

140. Ujikawa K. Antifungal antibiotics produced by Brazilian actinomycetes and its preliminary determination in experimental media. Rev Bras Ciências Farm. 2003;39(2):149–58.

141. Girotto E, Mesas AE, de Andrade SM, Birolim MM. Psychoactive substance use by truck drivers: a systematic review. Occup Environ Med. 2013;oemed-2013.

142. Arria AM, Caldeira KM, Bugbee BA, Vincent KB, O'Grady KE. Trajectories of energy drink consumption and subsequent drug use during young adulthood. Drug Alcohol Depend. 2017;179:424–32.

143. 5-hour ENERGY® Shot Ingredients [Internet]. Livinng Essentials Marketing, LLC. 2017. Available from: https://5hourenergy.com/facts/ingredients/

144. Kowalska T, Sajewicz M, Sherma J. Planar chromatography-mass spectrometry. CRC Press; 2015.

145. Van Berkel GJ, Ford MJ, Deibel MA. Thin-layer chromatography and mass spectrometry coupled using desorption electrospray ionization. Anal Chem. 2005;77(5):1207–15.

146. Ifa DR, Wiseman JM, Song Q, Cooks RG. Development of capabilities for imaging mass spectrometry under ambient conditions with desorption electrospray ionization (DESI). Int J Mass Spectrom. 2007;259(1–3):8–15.

147. Ford MJ, Deibel MA, Tomkins BA, Van Berkel GJ. Quantitative thin-layer chromatography/mass spectrometry analysis of caffeine using a surface sampling probe electrospray ionization tandem mass spectrometry system. Anal Chem. 2005;77(14):4385–9.

148. Seng JA, Ellis SR, Hughes JR, Maccarone AT, Truscott RJW, Blanksby SJ, et al. Characterisation of sphingolipids in the human lens by thin layer chromatography–desorption electrospray ionisation mass spectrometry. Biochim Biophys Acta (BBA)-Molecular Cell Biol Lipids. 2014;1841(9):1285–91.

149. Paglia G, Ifa DR, Wu C, Corso G, Cooks RG. Desorption electrospray ionization mass spectrometry analysis of lipids after two-dimensional high-performance thin-layer chromatography partial separation. Anal Chem. 2010;82(5):1744–50.

150. Han Y, Levkin P, Abarientos I, Liu H, Svec F, Fréchet JMJ. Monolithic superhydrophobic polymer layer with photopatterned virtual channel for the separation of peptides using two-dimensional thin layer chromatography-desorption electrospray ionization mass spectrometry. Anal Chem. 2010;82(6):2520–8.

151. Kauppila TJ, Talaty N, Salo PK, Kotiaho T, Kostiainen R, Cooks RG. New surfaces for desorption electrospray ionization mass spectrometry: porous silicon and ultra-thin layer chromatography plates. Rapid Commun mass Spectrom. 2006;20(14):2143–50.

152. Ifa DR, Manicke NE, Rusine AL, Cooks RG. Quantitative analysis of small molecules by desorption electrospray ionization mass spectrometry from polytetrafluoroethylene surfaces. Rapid Commun Mass Spectrom. 2008;22(4):503–10.

153. Torres y Torres JL, Hiley SL, Lorimor SP, Rhoad JS, Caldwell BD, Zweerink GL, et al. Separation of Caffeine from beverages and analysis using thin-layer chromatography and gas chromatography–mass spectrometry. J Chem Educ. 2015;92(5):900–2.

154. Bagatela BS, Lopes AP, Cabral EC, Perazzo FF, Ifa DR. High-performance thin-layer chromatography/desorption electrospray ionization mass spectrometry imaging of the crude extract from the peels of Citrus aurantium L.(Rutaceae). Rapid Commun Mass Spectrom. 2015;29(16):1530–4.

155. Sneha M, Dulay MT, Zare RN. Introducing mass spectrometry to first-year undergraduates: Analysis of caffeine and other components in energy drinks using paper-spray mass spectrometry. Int J Mass Spectrom. 2017;418:156–61.

156. Van Berkel GJ, Kertesz V. Automated sampling and imaging of analytes separated on thin-layer chromatography plates using desorption electrospray ionization mass spectrometry. Anal Chem. 2006;78(14):4938–44.

157. Harry EL, Reynolds JC, Bristow AWT, Wilson ID, Creaser CS. Direct analysis of pharmaceutical formulations from non-bonded reversed-phase thin-layer chromatography plates by desorption electrospray ionisation ion mobility mass spectrometry. Rapid Commun Mass Spectrom. 2009;23(17):2597–604.

158. Kennedy JH, Wiseman JM. Direct analysis of Salvia divinorum leaves for salvinorin A by thin layer chromatography and desorption electrospray ionization multi-stage tandem mass spectrometry. Rapid Commun Mass Spectrom. 2010;24(9):1305–11.

159. Lin S-Y, Huang M-Z, Chang H-C, Shiea J. Using electrospray-assisted laser desorption/ionization mass spectrometry to characterize organic compounds separated on thin-layer chromatography plates. Anal Chem. 2007;79(22):8789–95.

160. Van Berkel GJ, Tomkins BA, Kertesz V. Thin-layer chromatography/desorption electrospray ionization mass spectrometry: investigation of goldenseal alkaloids. Anal Chem. 2007;79(7):2778–89.

161. Pavlik JW. Tlc detection of caffeine in commercial products. J Chem Educ. 1973;50(2):134.

162. Willard MAB, McGuffin VL, Smith RW. Statistical comparison of mass spectra for identification of amphetamine-type stimulants. Forensic Sci Int. 2017;270:111–20.

163. Bianco G, Abate S, Labella C, Cataldi TRI. Identification and fragmentation pathways of caffeine metabolites in urine samples via liquid chromatography with positive electrospray ionization coupled to a hybrid quadrupole linear ion trap (LTQ) and Fourier transform ion cyclotron resonance mass spec. Rapid Commun Mass Spectrom. 2009;23(7):1065–74.

164. Ndolo VU, Fulcher RG, Beta T. Application of LC–MS–MS to identify niacin in aleurone layers of yellow corn, barley and wheat kernels. J Cereal Sci. 2015;65:88–95.

165. Byrd N. Rapid, Sensitive and Cost-effective Detection of B Vitamins in Food by UPLC/MS/MS [Internet]. 2012. Available from:

https://www.agilent.com/cs/library/applications/5991-0647EN.pdf

166. Lioe H, Richard AJ. Neighbouring group processes in the deamination of protonated phenylalanine derivatives. Org Biomol Chem. 2005;3(20):3618–28.

167. Kubica P, Kot-Wasik A, Wasik A, Namieśnik J. "Dilute & shoot" approach for rapid determination of trace amounts of nicotine in zero-level e-liquids by reversed phase liquid chromatography and hydrophilic interactions liquid chromatography coupled with tandem mass spectrometry-electrospray ionization. J Chromatogr A. 2013;1289:13–8.

168. O'Brien BA, Bonicamp JM, Jones DW. Differentiation of amphetamine and its major hallucinogenic derivatives using thin-layer chromatography. J Anal Toxicol. 1982;6(3):143–7.

169. Sadek P. Solvent Miscibility and Viscosity Chart. The HPLC Solvent Guide. Wiley-Interscience; 2002.

170. Castillo M. FDA investigating 13 deaths tied to 5-hour Energy [Internet]. CBS Interactive Inc.; 2013. Available from: https://www.cbsnews.com/news/fda-investigating-13-deaths-tied-to-5-hour-energy/

171. Thomas L. Energy drink caffeine amounts often missing or mislabeleditle [Internet]. 2012. Available from: http://mynorthwest.com/5781/energy-drink-caffeine-amounts-often-missing-or-mislabeled/

172. Pat Crawford and Wendi Gosliner. Energy drinks are killing young people. It's time to stop that. [Internet]. 2017. Available from: https://www.washingtonpost.com/opinions/energy-drinks-are-killing-young-people-its-time-to-stop-that/2017/05/25/6343be9c-3ff8-11e7-9869-bac8b446820a_story.html?noredirect=on&utm_term=.5826f22a4219

173. Baber N. International conference on harmonisation of technical requirements for registration of pharmaceuticals for human use (ICH). Br J Clin Pharmacol. 1994;37(5):401–4.

174. Leader IP, Halket J, Finch P. Synthesis and identification of two potential oxidation degradants of oxymetazoline. Rapid Commun mass Spectrom. 2004;18(14):1645–54.

175. Takeoka GR, Dao LT, Wong RY, Harden LA. Identification of benzalkonium chloride in commercial grapefruit seed extracts. J Agric Food Chem. 2005;53(19):7630–6.

176. Dahlström M, Lindgren F, Berntsson K, Sjögren M, Mårtensson LGE, Jonsson PR, et al.

Evidence for different pharmacological targets for imidazoline compounds inhibiting settlement of the barnacle Balanus improvisus. J Exp Zool Part A Ecol Integr Physiol. 2005;303(7):551–62.

177. Ali MS, Ghori M, Saeed A. Simultaneous determination of ofloxacin, tetrahydrozoline hydrochloride, and prednisolone acetate by high-performance liquid chromatography. J Chromatogr Sci. 2002;40(8):429–33.

178. Garrett R, Rezende CM, Ifa DR. Revealing the spatial distribution of chlorogenic acids and sucrose across coffee bean endosperm by desorption electrospray ionization-mass spectrometry imaging. LWT-Food Sci Technol. 2016;65:711–7.

179. Badu-Tawiah A, Bland C, Campbell DI, Cooks RG. Non-aqueous spray solvents and solubility effects in desorption electrospray ionization. J Am Soc Mass Spectrom. 2010;21(4):572–9.

180. Touchstone JC. Practice of thin layer chromatography. John Wiley & Sons; 1992.

181. Sábio S, Franciscone PA, Mondelli J. Effect of conventional and experimental gingival retraction solutions on the tensile strength and inhibition of polymerization of four types of impression materials. J Appl Oral Sci. 2008;16(4):280–5.

182. Sherma J, Fried B. Handbook of thin-layer chromatography. Vol. 89. CRC press; 2003.

183. Peng J-B, Jia H-M, Liu Y-T, Zhang H-W, Dong S, Zou Z-M. Qualitative and quantitative characterization of chemical constituents in Xin-Ke-Shu preparations by liquid chromatography coupled with a LTQ Orbitrap mass spectrometer. J Pharm Biomed Anal. 2011;55(5):984–95.

184. Manicke NE, Dill AL, Ifa DR, Cooks RG. High-resolution tissue imaging on an orbitrap mass spectrometer by desorption electrospray ionization mass spectrometry. J mass Spectrom. 2010;45(2):223–6.

185. Da Costa C, Reynolds JC, Whitmarsh S, Lynch T, Creaser CS. The quantitative surface analysis of an antioxidant additive in a lubricant oil matrix by desorption electrospray ionization mass spectrometry. Rapid Commun Mass Spectrom. 2013;27(21):2420–4.

186. Rossi A, Castrati L, Colombo P, Flammini L, Barocelli E, Bettini R, et al. Development and validation of a DESI-HRMS/MS method for the fast profiling of esomeprazole and its metabolites in rat plasma: a pharmacokinetic study. Drug Test Anal. 2016;8(2):208–13.

187. Wiley WC, McLaren IH. Time-of-flight mass spectrometer with improved resolution. Rev

Sci Instrum. 1955;26(12):1150–7.

188. Freeman JB, Serfass EJ. Analytical Mass Spectrometry Utillizing Relative Abundance Ratios. Anal Chem. 1954;26(9):1403–5.

189. Londry FA, March RE. Systematic factors affecting high mass-resolution and accurate mass assignment in a quadrupole ion trap. Int J Mass Spectrom Ion Process. 1995;144(1–2):87–103.

190. Ikonomou MG, Blades AT, Kebarle P. Electrospray-ion spray: a comparison of mechanisms and performance. Anal Chem. 1991;63(18):1989–98.

191. Green FM, Salter TL, Gilmore IS, Stokes P, O'Connor G. The effect of electrospray solvent composition on desorption electrospray ionisation (DESI) efficiency and spatial resolution. Analyst. 2010;135(4):731–7.

192. Schwab N V, Ore MO, Eberlin MN, Morin S, Ifa DR. Functionalized porous silicon surfaces as DESI-MS substrates for small molecules analysis. Anal Chem. 2014;86(23):11722–6.

193. Matheis K, Fuchs B, Lemmnitzer K, Süss R, Griesinger H, Minarik S, et al. Combining TLC separation with MS detection-a revival of TLC. J Glycomics Lipidomics. 2015;5(1):1.

194. Klein NP, Bartlett J, Rowhani-Rahbar A, Fireman B, Baxter R. Waning protection after fifth dose of acellular pertussis vaccine in children. N Engl J Med. 2012;367(11):1012–9.

195. Dillon TM, Bondarenko P V, Rehder DS, Pipes GD, Kleemann GR, Ricci MS. Optimization of a reversed-phase high-performance liquid chromatography/mass spectrometry method for characterizing recombinant antibody heterogeneity and stability. J Chromatogr A. 2006;1120(1–2):112–20.

196. Staub A, Guillarme D, Schappler J, Veuthey J-L, Rudaz S. Intact protein analysis in the biopharmaceutical field. J Pharm Biomed Anal. 2011;55(4):810–22.

197. Vydac G. The handbook of analysis and purification of peptides and proteins by reversed-phase HPLC. Hesperia, CA, USA Grace Vydac. 2002;

198. Iavarone AT, Jurchen JC, Williams ER. Effects of solvent on the maximum charge state and charge state distribution of protein ions produced by electrospray ionization. J Am Soc Mass Spectrom. 2000;11(11):976–85.

Appendix A: Supplementary Information for Chapter 2
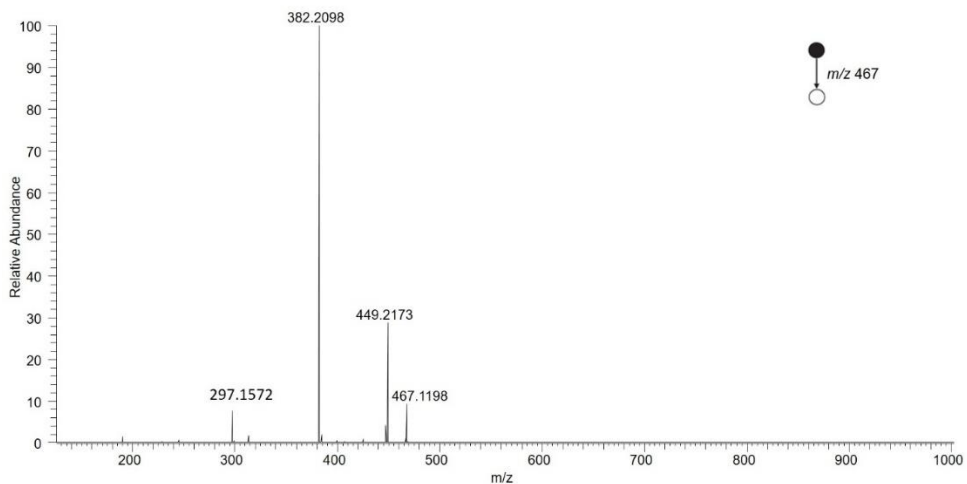
Figure A1: Tandem mass spectrometry (MS/MS) of thermochromic ink trace of *m/z* 467.1198 using an Orbitrap mass spectrometer.
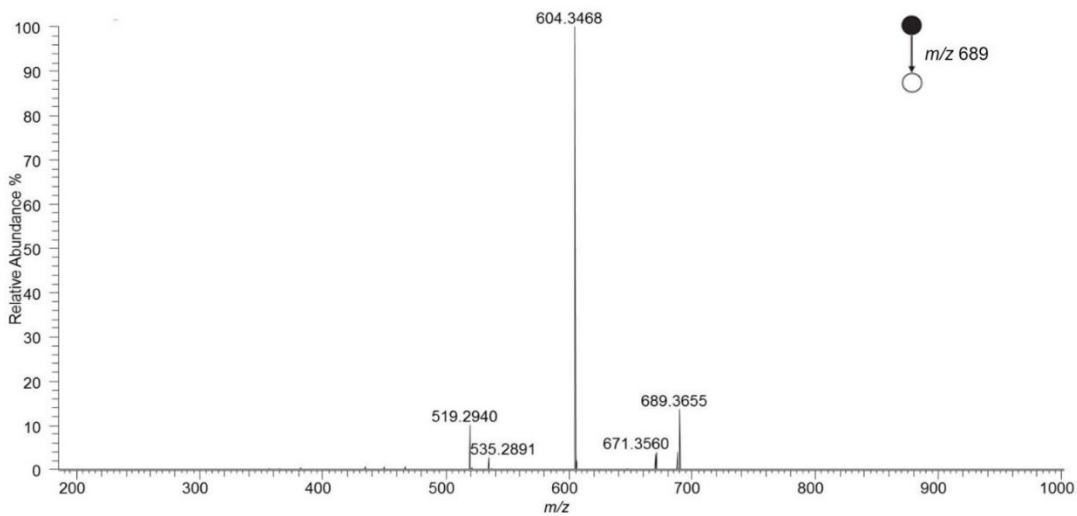
Figure A2: Tandem mass spectrometry (MS/MS) of thermochromic ink trace of *m/z* 689.3655 using an Orbitrap mass spectrometer.
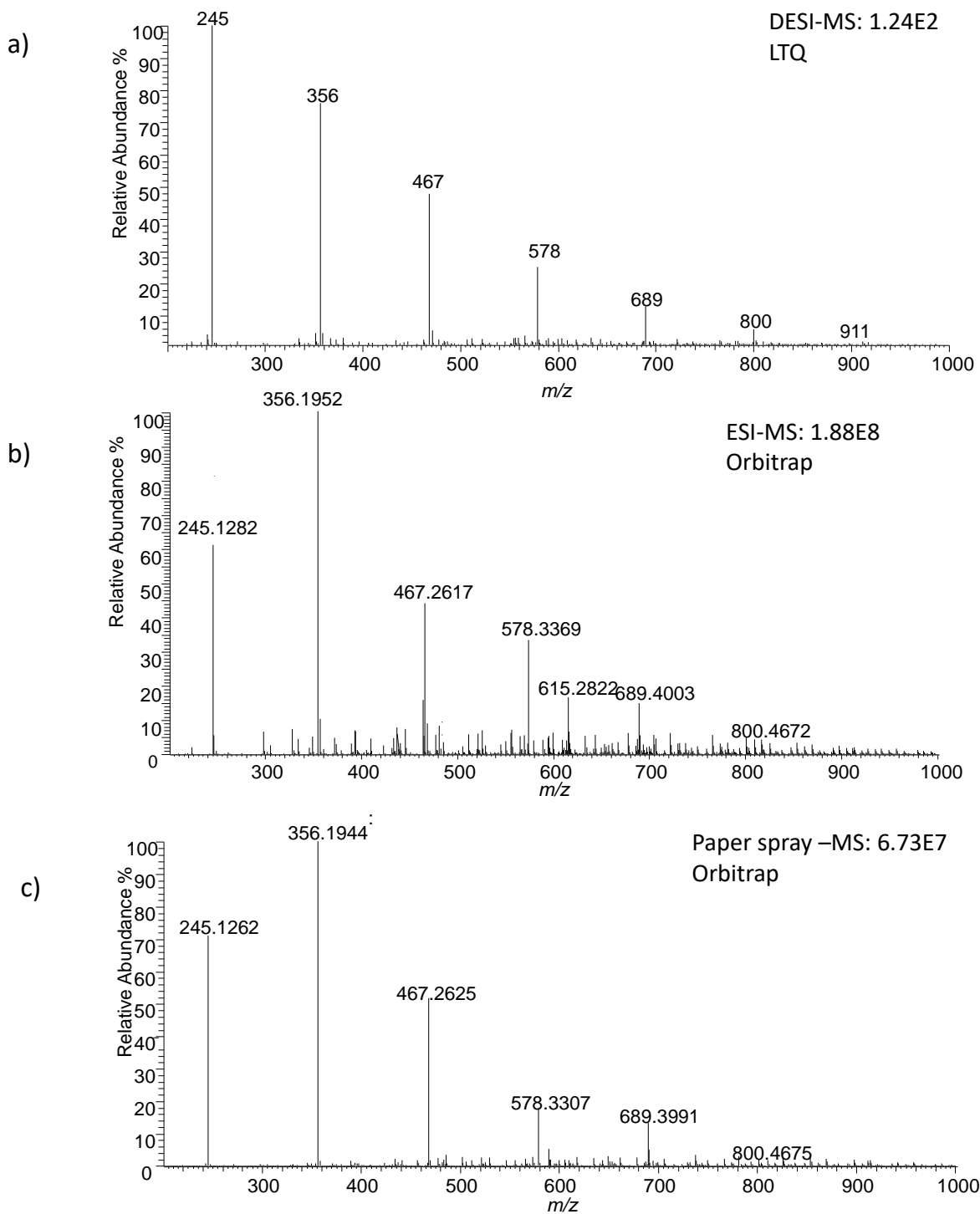
Figure A3: a. DESI (+) LTQ mass spectrum of an ink spot on paper. b. ESI (+) Orbitrap mass spectrum of a solution of ink in CH₃OH. c. Paper Spray (+) Orbitrap mass spectrum of an ink spot on paper. Intensities are higher for the Orbitrap compared to the LTQ.
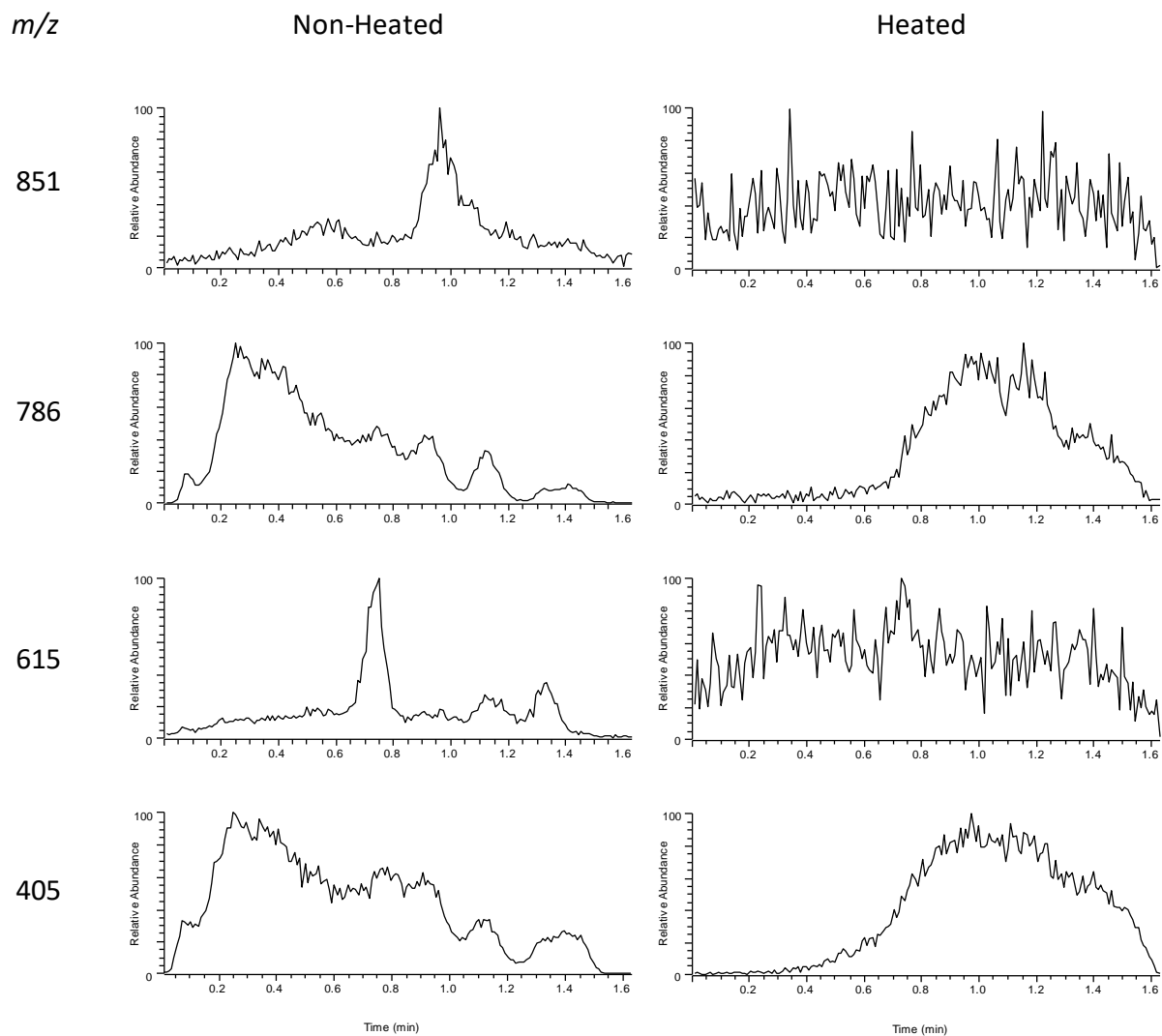
Figure A4: (+) DESI-MS selected ion monitoring (SIM) mass spectra of the ions *m/z* 405, 615, 786 and 851 separated on TLC plate acquired on a LTQ mass spectrometer. These data were obtained by running the DESI-spray across the eluted spots in the TLC plate as indicated in Figure A8.
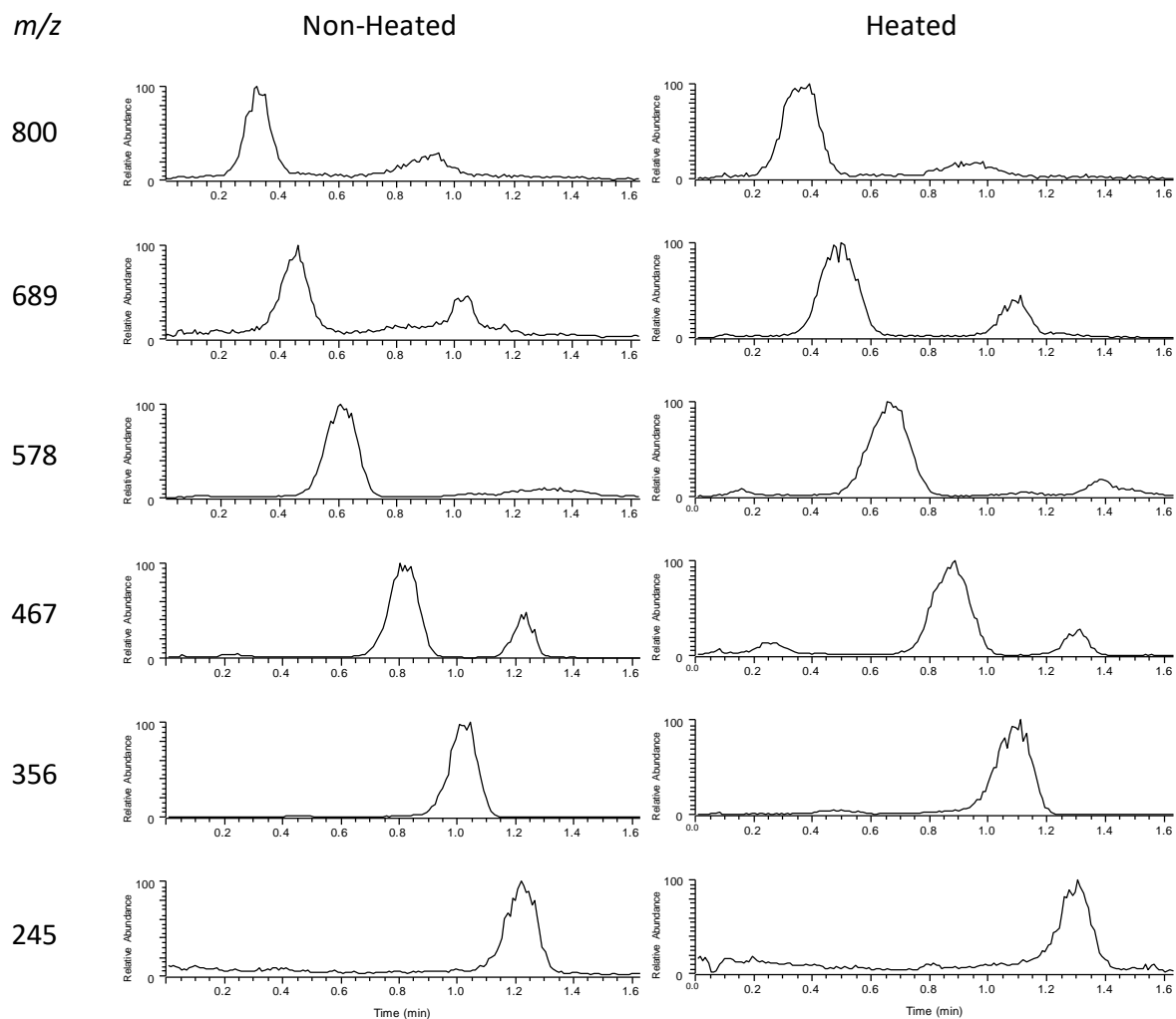
Figure A5: (+) DESI-MS selected ion monitoring (SIM) mass spectra of polymers separated on a TLC plate acquired on a LTQ mass spectrometer. These data were obtained by running the DESI-spray across the eluted spots in the TLC plate as indicated in Figure A8.
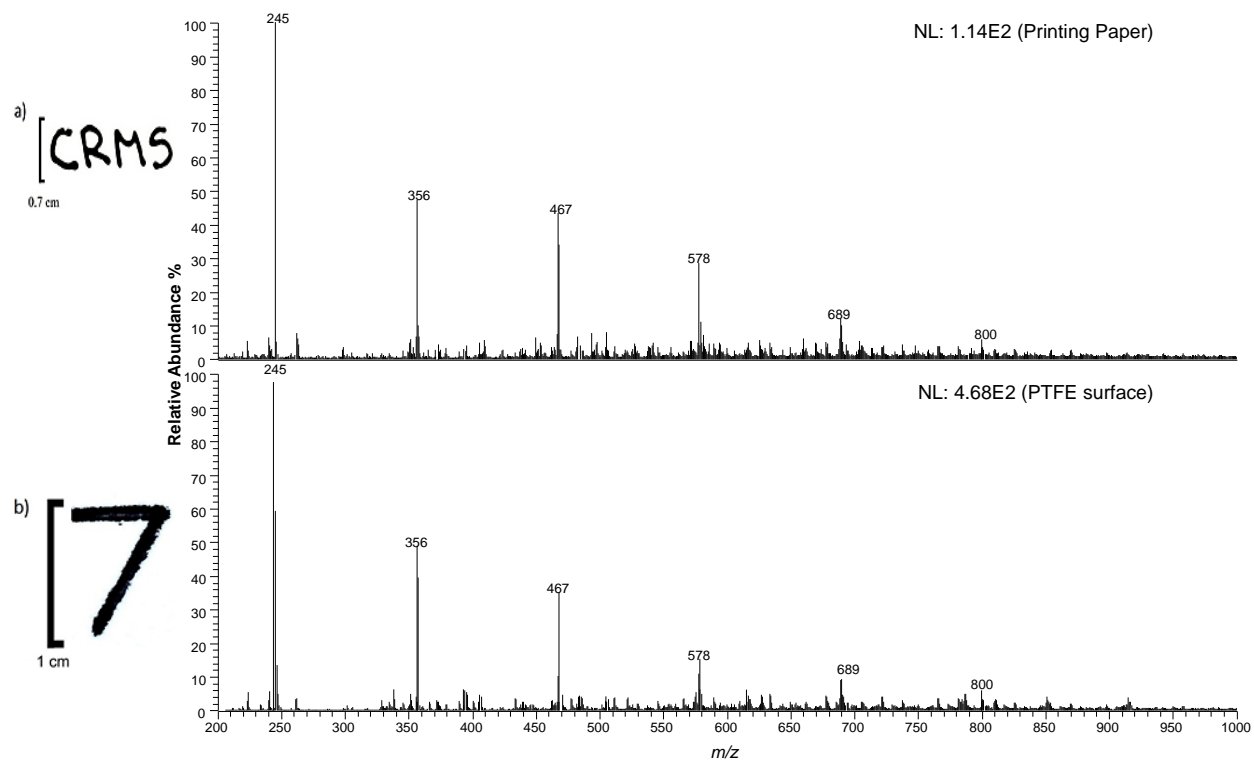
Figure A6: Signal intensity comparison of full scan spectra while imaging 'CRMS' on printing

paper surface and '7' on PTFE surface using a LTQ mass spectrometer.
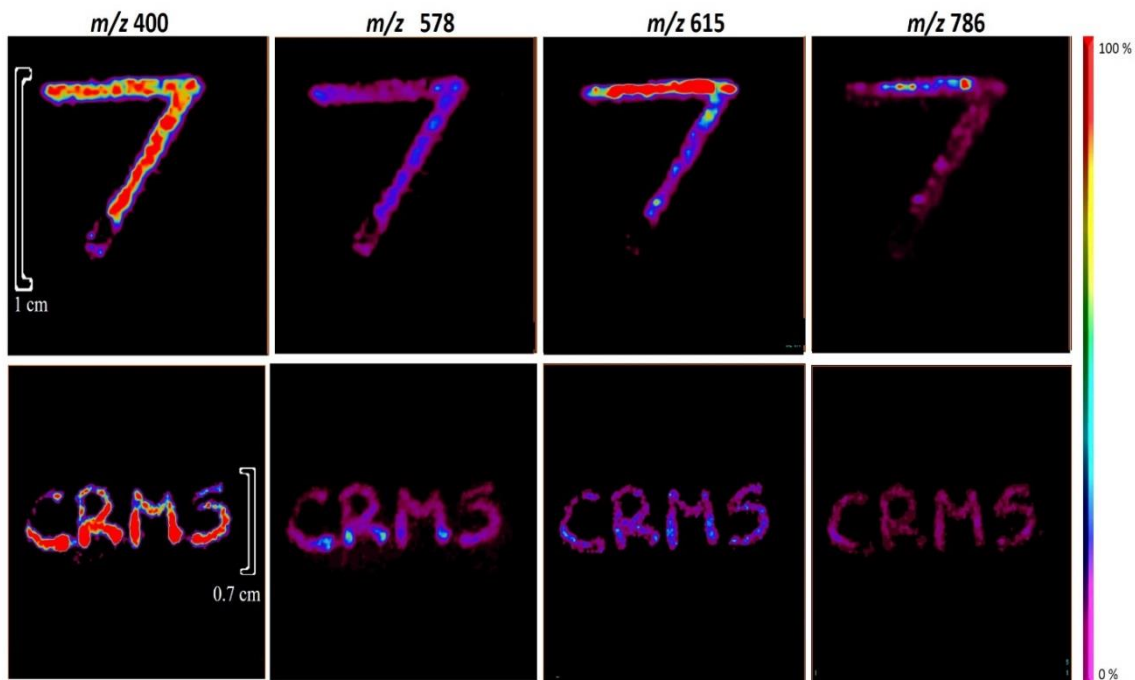
Figure A7: DESI ion images of heated chemical markers at *m/z* 400, 578, 615 and 786 from a forged '7' and 'CRMS' using a LTQ mass spectrometer.
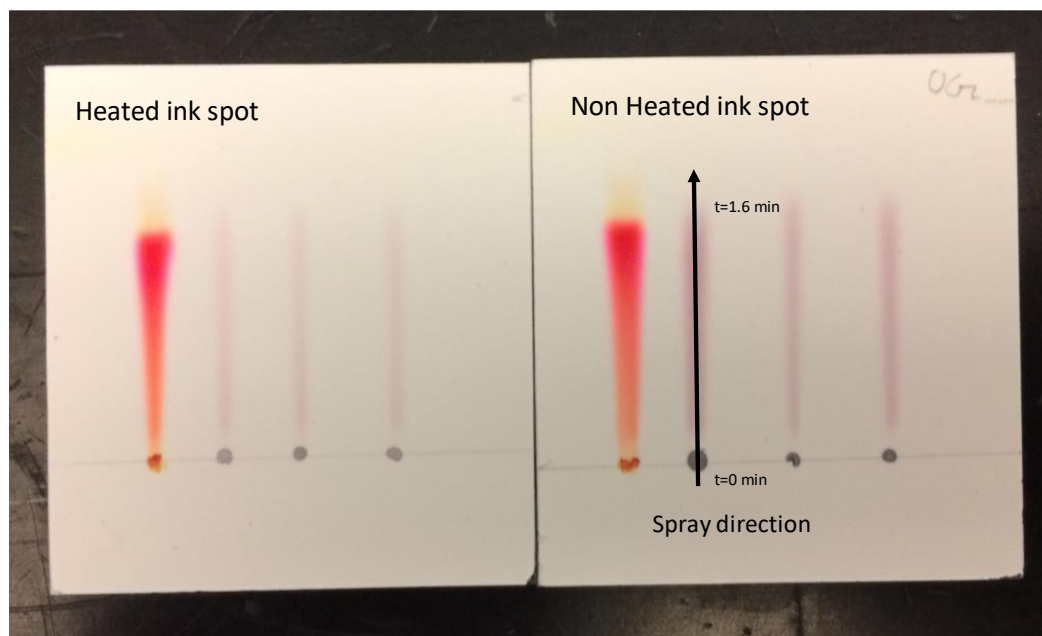
Figure A8: TLC plate optical images upon running heated (left) and non-heated ink (right). An ink spot was made for reference using a Sharpie red pen.
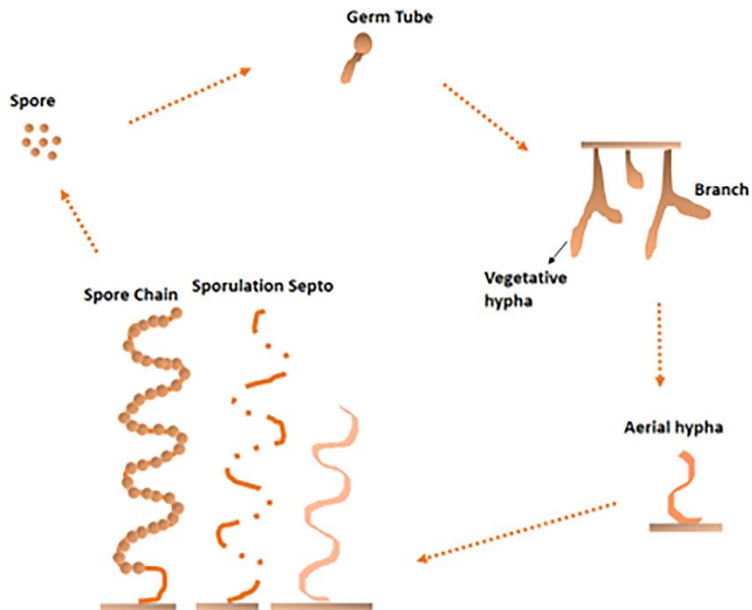
Figure B1: Morphological differentiation stages of *Streptomyces* spp.
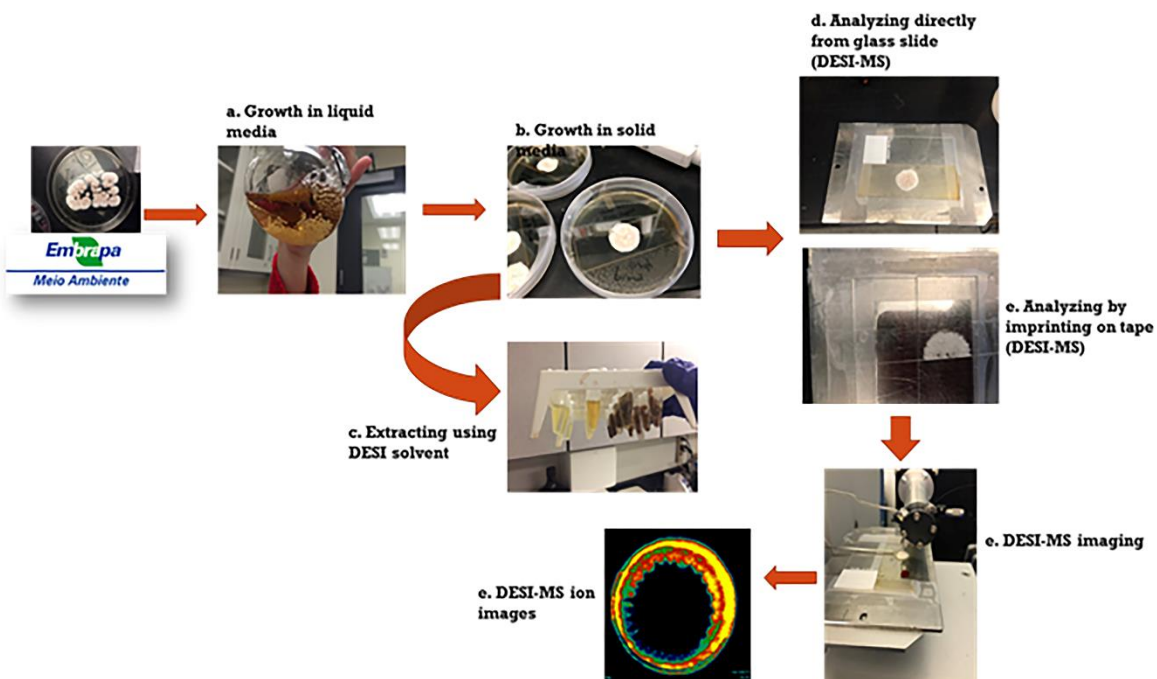
Figure B2: Workflow depicting the processes underwent while analyzing secondary metabolites from CAAT 1-54 by DESI-MS/MSI and Orbitrap.
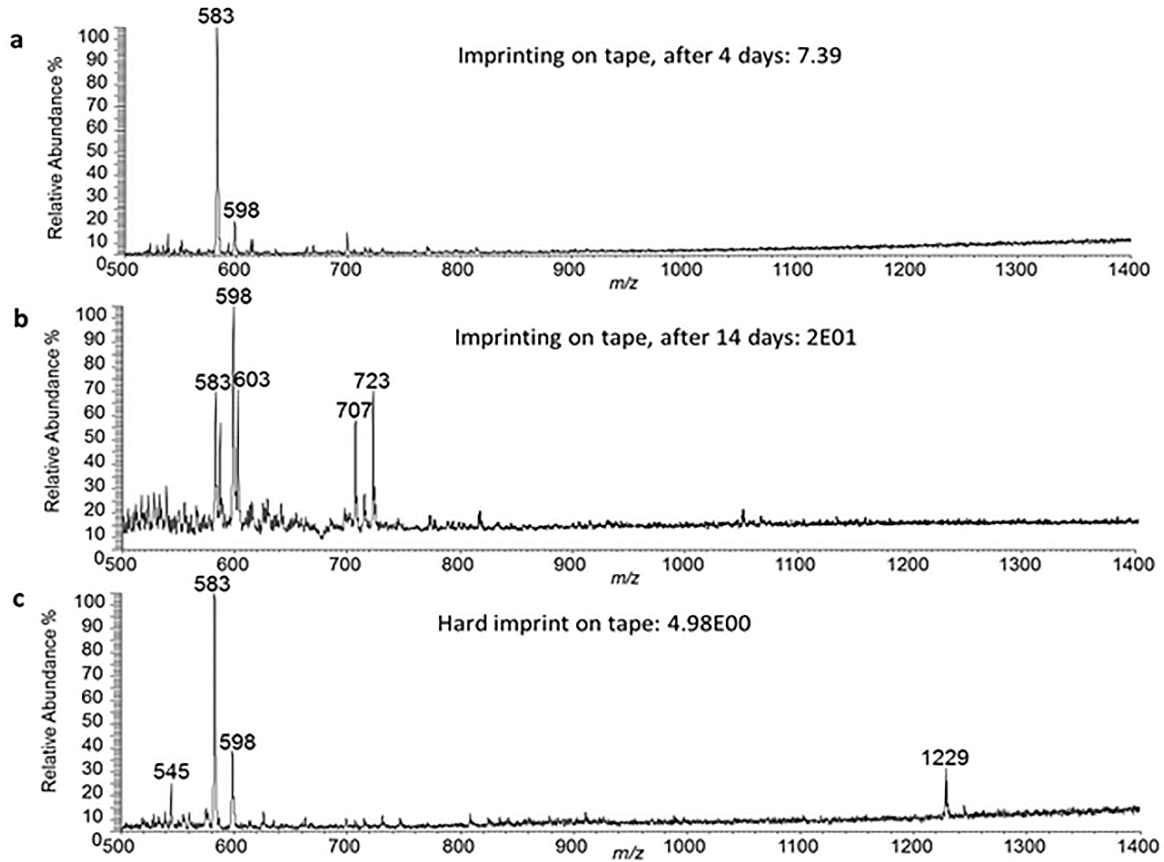
Figure B3: DESI-MS scan of colony after imprinting on double sided tape. a) DESI-MS scan of an imprint from the colony after 4 days of incubation at 37°C on potato agar plate for 4 days. 7.39E00 represents the intensity of the most abundant ion. b) DESI-MS scan of an imprint from the colony after 14 days of incubation at 37°C on potato agar plate for 14 days. 2E01 represents the intensity of the most abundant ion. c) DESI-MS scan of a hard imprint (pressing harder and longer) from the colony after 14 days of incubation at 37°C on potato agar plate for 14 days. 4.98E00 represents the intensity of the most abundant ion.
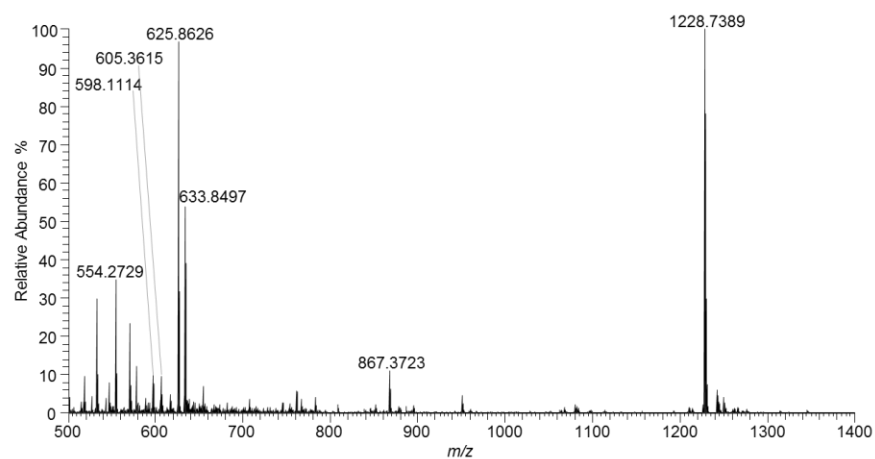
Figure B4: HRMS spectrum of crude extract.
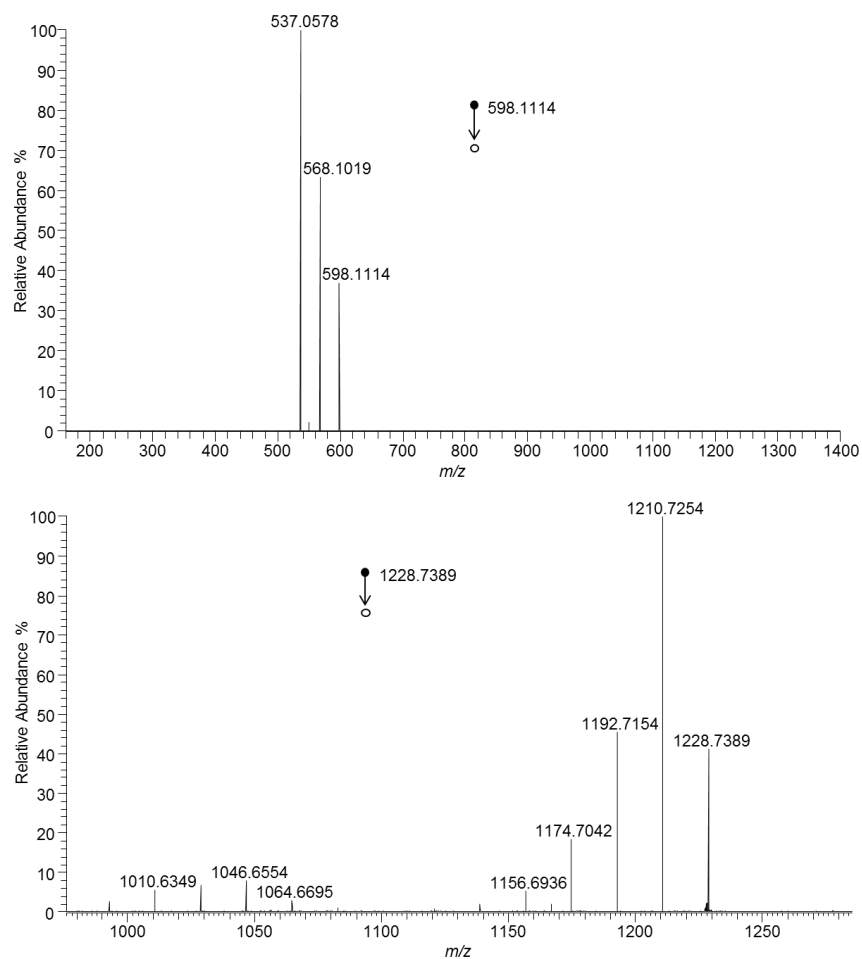
Figure B5: Tandem mass spectrometry a) *m/z* 598.1099 showing two fragment ions at *m/z* 568 and *m/z* 537. b) *m/z* 1229.7389 showing several fragment ions.
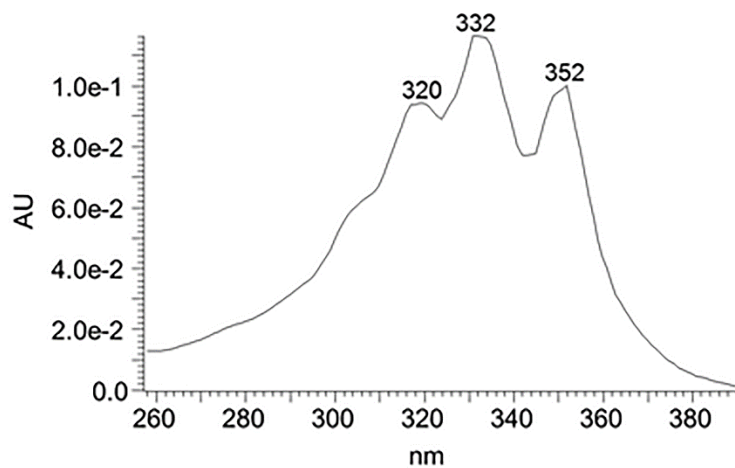
Figure B6: UV absorption profile of the ion at *m/z* 1229.

Chemical Formulae: $C_6H_{12}O_5$
Exact mass: 164.0685

Chemical Formulae: $C_6H_{13}NO_4$
Exact mass: 163.0845
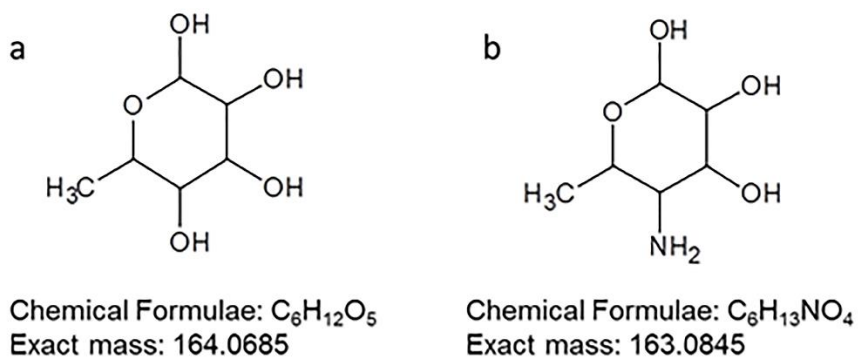
Figure B7: Structures of sugars: a) Rhamnose and b) Mycosamine
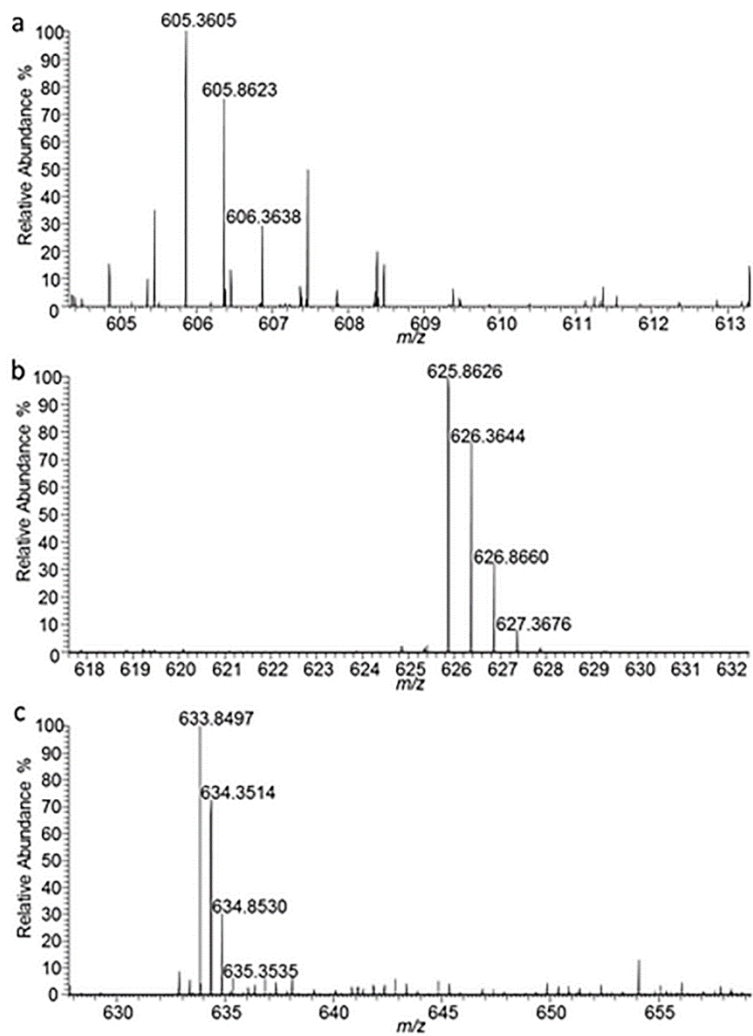
Figure B8. Double charged ion profile of: a) *m/z* 605.3605, b) *m/z* 625.8626, c)*m/z* 633.8497
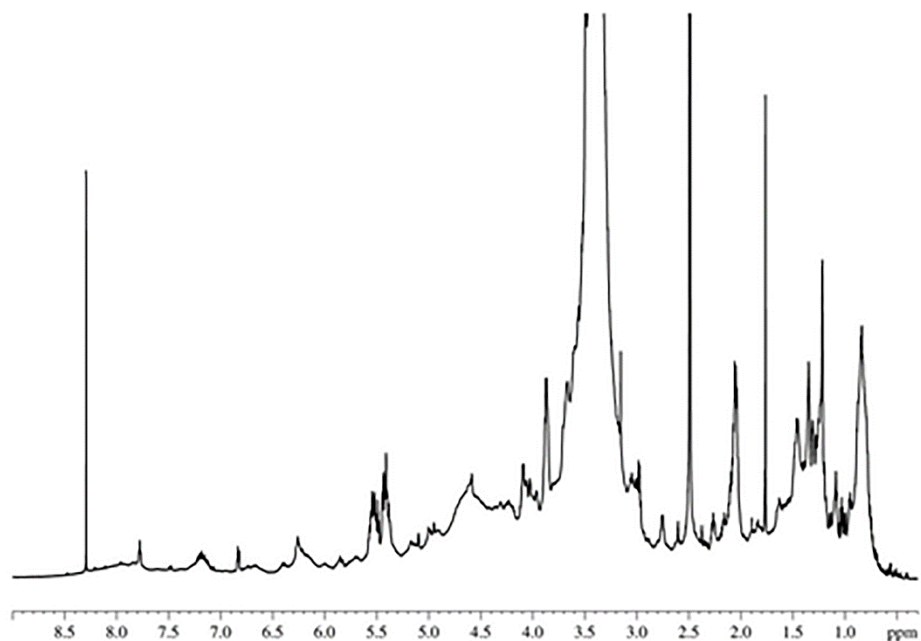
Figure B9: A 600 MHz ^{1}H NMR spectrum of the compound of *m/z* 1228 in DMSO-d$_6$.
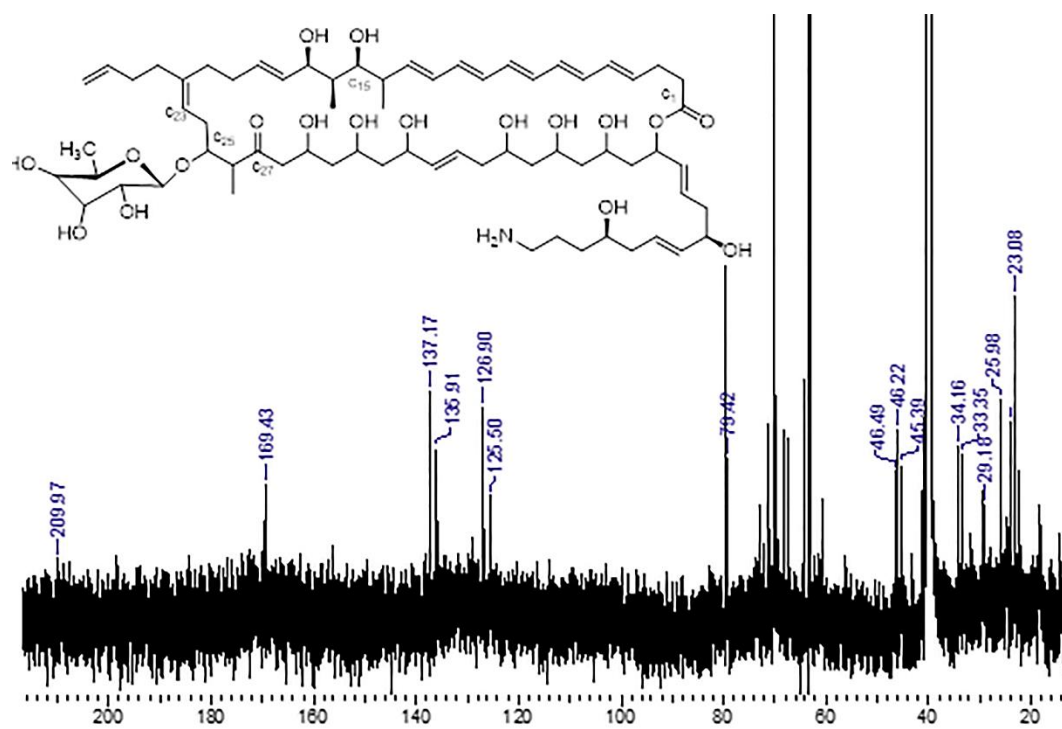
Figure B10: A 150 MHz ^{13}C NMR spectrum of the compound of *m/z* 1228 in DMSO-d$_6$.
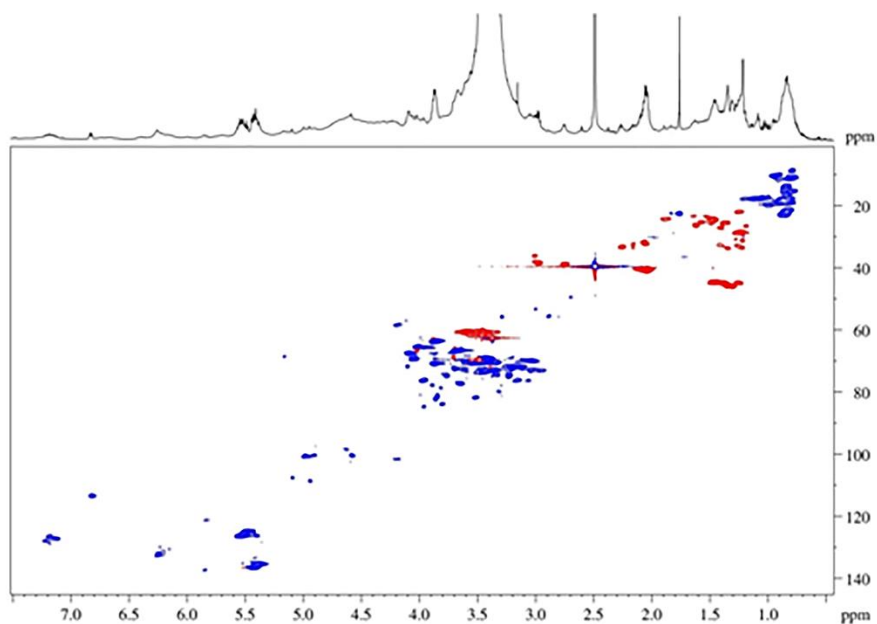
Figure B11: 2D ^1H-^{13}C HSQC-DEPT spectrum of the sample in DMSO-d6. Contours indicating CH and CH$_3$ correlations (positive) are shown in blue while CH$_2$ (negative) are shown in red.
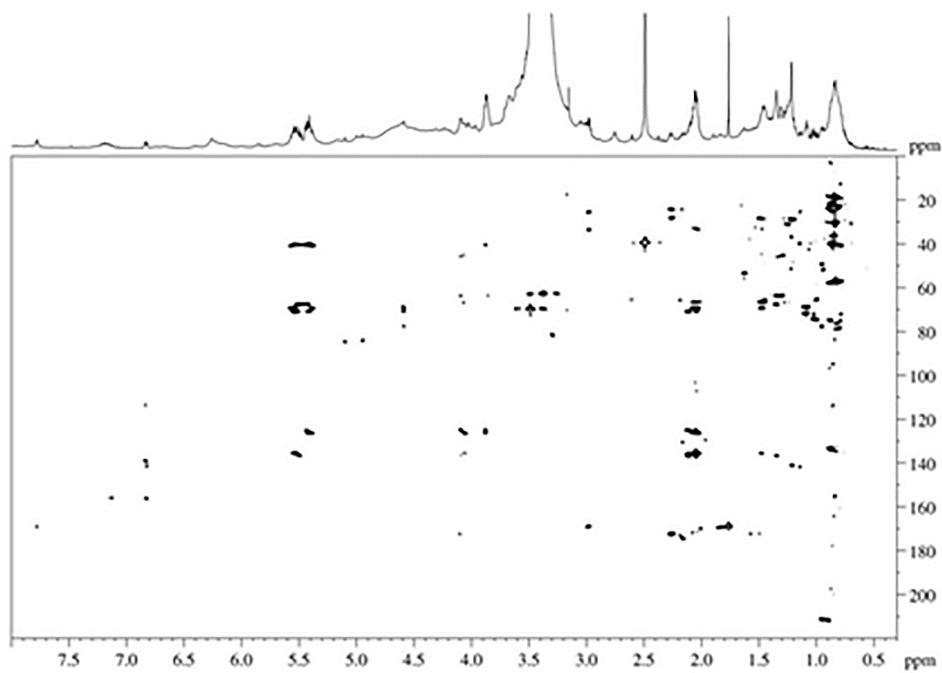
Figure B12: 2D ^1H-^{13}C HMBC spectrum of the sample in DMSO-d$_6$.
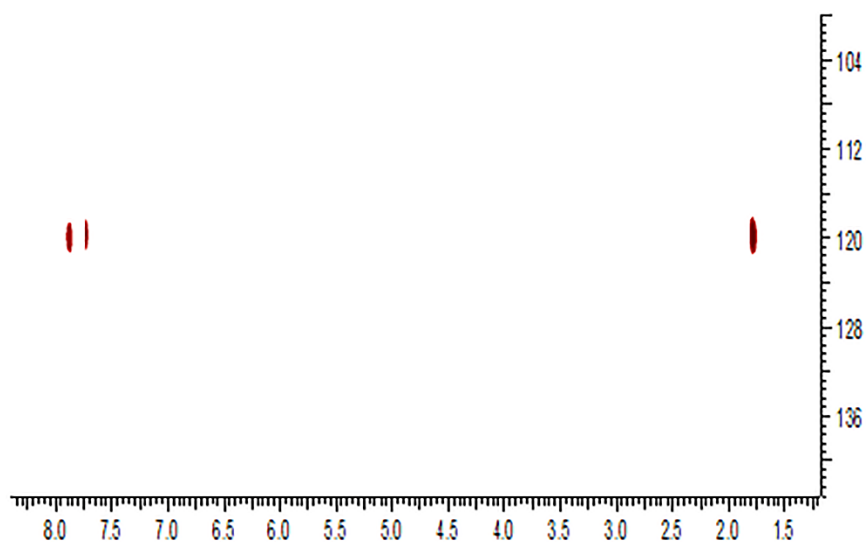
Figure B13. ^{15}N-NMR spectrum of sample in DMSO-d$_6$.
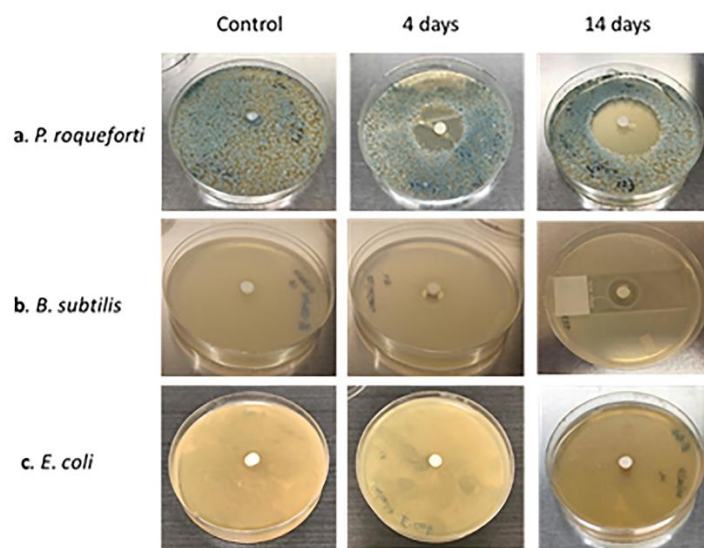
Figure B14. Optical images of disc diffusion assay performed with a) *P. roqueforti*, b) *B. subtilis*, and c) *E. coli*. The first column is the negative control plates where the discs are impregnated with fresh autoclaved ISP 2 media. The second column shows the plates where the discs are impregnated with the media obtained after incubating CAAT 1-54 for 4 days at 37°C. The third column are of the plates where the discs are impregnated with the media obtained after incubating CAAT 1-54 for 14 days at 37°C.

Appendix C: Supplementary Information of Chapter 4

Determination of solvent spray

Table C1: Signal Intensity for Berry flavor energy drink and standard amphetamine.

Compound	CH₃OH	CH₃CN	CH₃CN / CH₃OH (70:30, v/v)	CH₃CN /H₂O (70:30, v/v)
m/z **136**	2.78E3	4.89E3	1.50E2	5.52E2
m/z **195**	3.30E2	1.31E3	5.77E1	7.49E2
m/z **123**	4.82E2	7.92E2	3.38E1	4.21E2
m/z **166**	1.50E3	2.67E2	1.31E1	6.24E2
m/z **170**	6.35E2	No signal	1.31E2	2.02E3

50 mL of methanol with 1.5% NH_4OH contains 28% NH_3 is used as TLC solvent. 0.1 µL of standard amphetamine, 0.3 µL of Berry flavor energy drink are spotted on the TLC plate.

Determination of mobile phase

Table C2: Relative retention factor for standard amphetamine and energy drink components at different mobile phase condition.

Mobile Phase Combinations	Relative Retention Factor (RF)				
	m/z **136**	*m/z* **195**	*m/z* **123**	*m/z* **166**	*m/z* **170**
CH₃OH + 1.5% NH₄OH	0.33	0.70	0.72	0.64	0.74
CH₃OH /Ethyl Acetate (1:1	0.04	0.79	0.64	0.23	N/A
CH₃OH /Ethyl Acetate (1: + 1.5% NH₄OH	0.13	0.71	0.69	0.18	0.66
CH₃OH /Ethyl Acetate (2: + 1.0% NH₄OH	0.16	0.84	0.81	0.15	0.76
CH₃OH /CHCl₃ (2:3)	0.03	*0.98	0.72	0.23	0.78
CH₃OH / CHCl₃ (1:1)	0.03	*0.85	0.78	0.38	0.65

*mean of RF value from standard caffeine, berry and extra-strength samples.
0.1µL of stock amphetamine and 0.1µL of both samples were spotted for TLC separation and analyzed by DESI-MS. RF values for *m/z* 195, *m/z* 123, *m/z* 166 and *m/z* 170 are averaged from the results of both berry and extra-strength sample.

Concentration of caffeine in 5-hour Energy drink- Berry flavor

190mg caffeine in 57 mL: $\frac{190\ mg}{57\ mL} = 3.33mg/mL$

Concentration of caffeine in 5-hour Energy drink- Extra strength

200mg caffeine in 57 mL: $\frac{200\ mg}{57\ mL} = 3.51mg/mL$

Table C3: Caffeine standard calibration curve Caffeine concentration versus ion intensity.

Conc./ mg/mL	Trail 1	Trial 2	Trial 3	Average	RSD %
2	2.28E+02	1.78E+02	8.77E+01	1.65E+02	43.2
3	3.64E+02	2.78E+02	1.29E+02	2.57E+02	46.3
4	4.78E+02	3.29E+02	1.94E+02	3.34E+02	42.6
5	5.68E+02	4.34E+02	2.67 E+02	4.23E+02	35.7
Berry	504	368	210	361	40.80
Extra	572	411	239	407	40.88

Table C4: Data for internal standard calibration curve.

Caffeine standard (mg/mL)	Ion ratio between *m/z* 195 and *m/z* 204			Average ratio	RSD
	Trial 1	Trial 2	Trial 3		
2	0.582	0.562	0.578	0.574	0.018437
3	0.994	0.987	0.989	0.990	0.003642
4	1.234	1.281	1.243	1.253	0.01991
5	1.517	1.563	1.548	1.543	0.015204
6	1.872	1.849	1.867	1.863	0.006493

Table C5: Spot analysis of *new batch* of 5 hour Energy drink sample on TLC plate using 3mg/mL of caffeine-d$_9$.

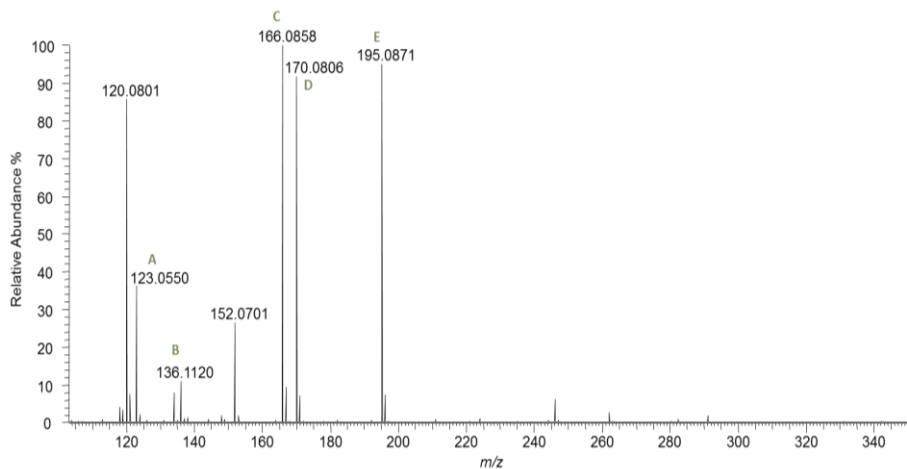|	*m/z* 195	*m/z* 204	Ratio Intensity	Spot Concentration (mg/mL)	Concentration (mg/mL)
Berry	2.71E+02	4.48E+02	0.60	1.80	4.50
Extra strength	2.55E+02	4.13E+02	0.62	1.85	4.63

Figure C1: Full scan spectrum obtained using orbitrap mass spectrometer. Components from the 50X extra strength energy drink were detected are: niacinamide (A), phenylalanine (C), pyridoxine (D) and caffeine (E). Amphetamine (2µg/mL) was spiked and is labeled as B.
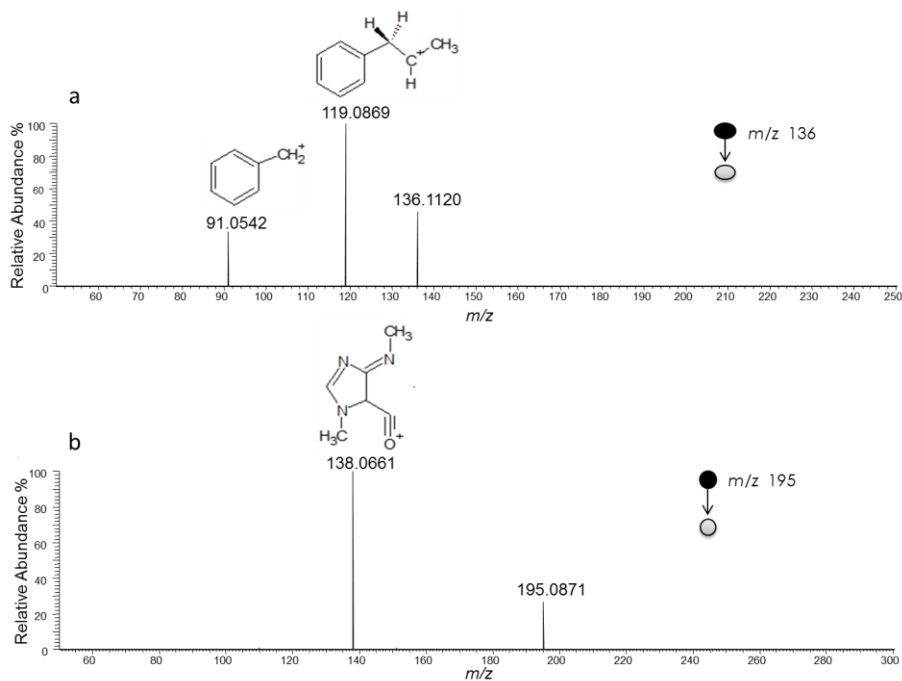

Figure C2: MS^2 ion spectra of the protonated caffeine molecule at *m/z* 195 and amphetamine *m/z* 136 using orbitrap mass spectrometer: (a) MS^2 spectrum of *m/z* 136 using 22% collision energy; (b) MS^2 spectrum of *m/z* 195 using 30% collision energy.
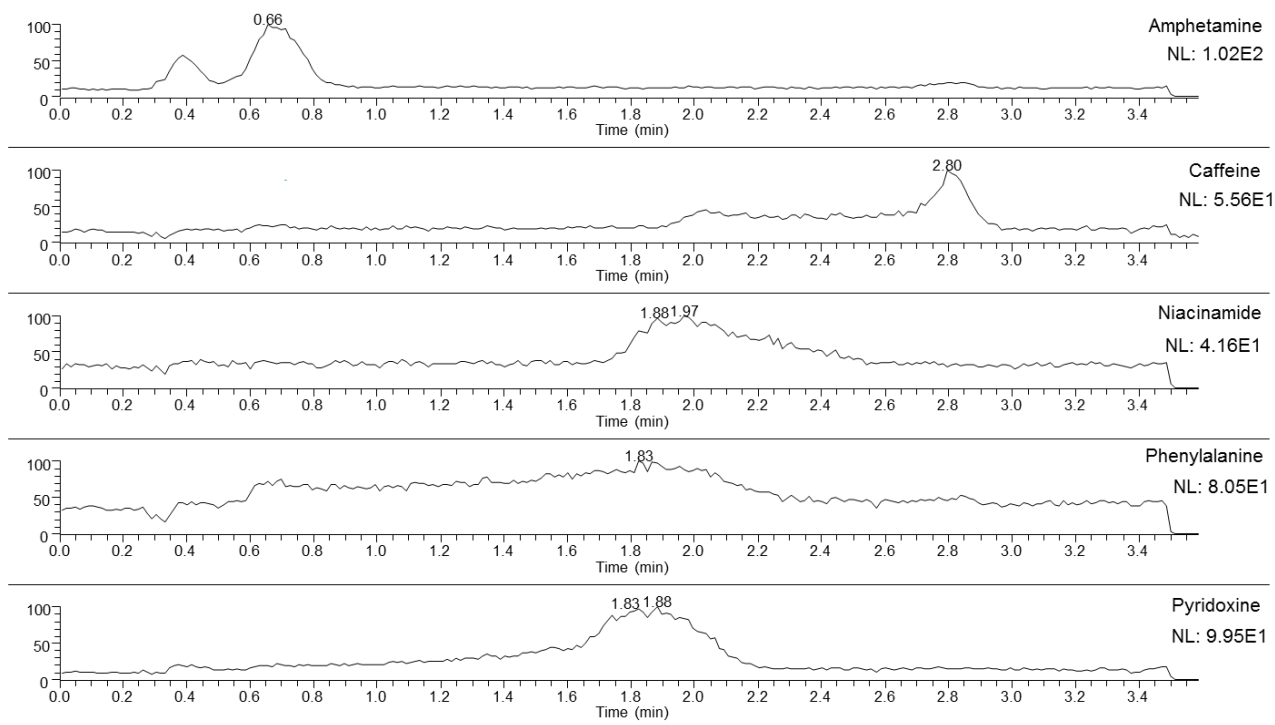
Figure C3: Ion chronogram mapping 5-hour energy drink components and standard amphetamine from a TLC plate developed with chloroform and methanol (1:1) prior to analysis by DESI-MS with acetonitrile/ water(7: 3) as the spray solvent.
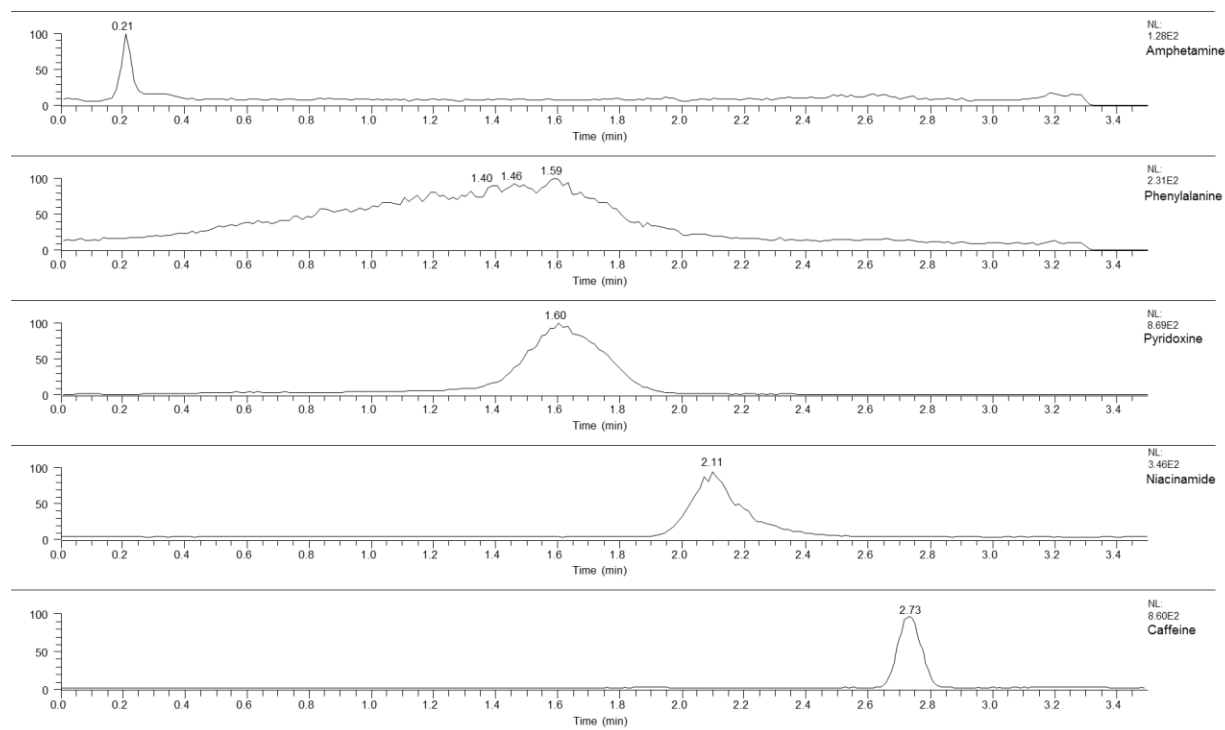
Figure C4: Ion chronogram of a mixture having energy drink spiked with amphetamine standard. 0.1µL amphetamine (1 mg/mL) and 0.1µL extra strength sample were mixed followed by ammonium hydroxide treatment(10% final concentration). TLC plate developed using Chloroform/methanol (1:1) as the mobile phase and analysed by DESI-MS with CH$_3$CN /H$_2$O (7:3) as spray solvent to map ions: Amphetamine (*m/z* 136), caffeine (*m/z* 195), niacinamide (*m/z* 123), pyridoxine (*m/z* 170) and phenylalanine (*m/z* 166).
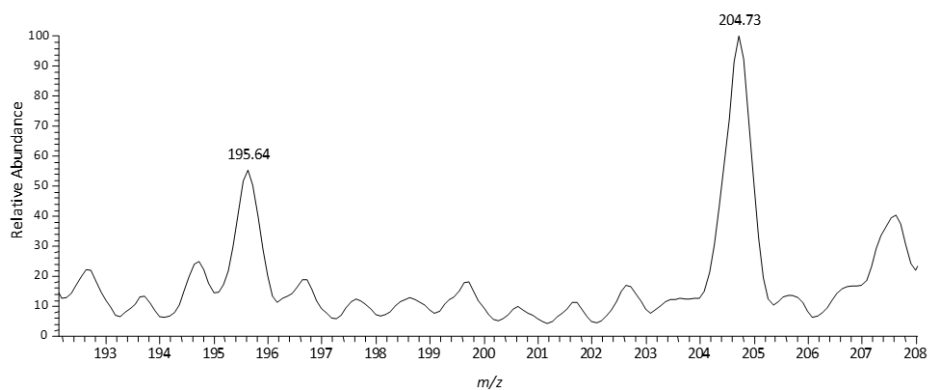
Figure C5: Zoomed spectrum from DESI-MS analysis of a spot having 2.5X diluted berry sample and 3 mg/mL deuterated caffeine standard.
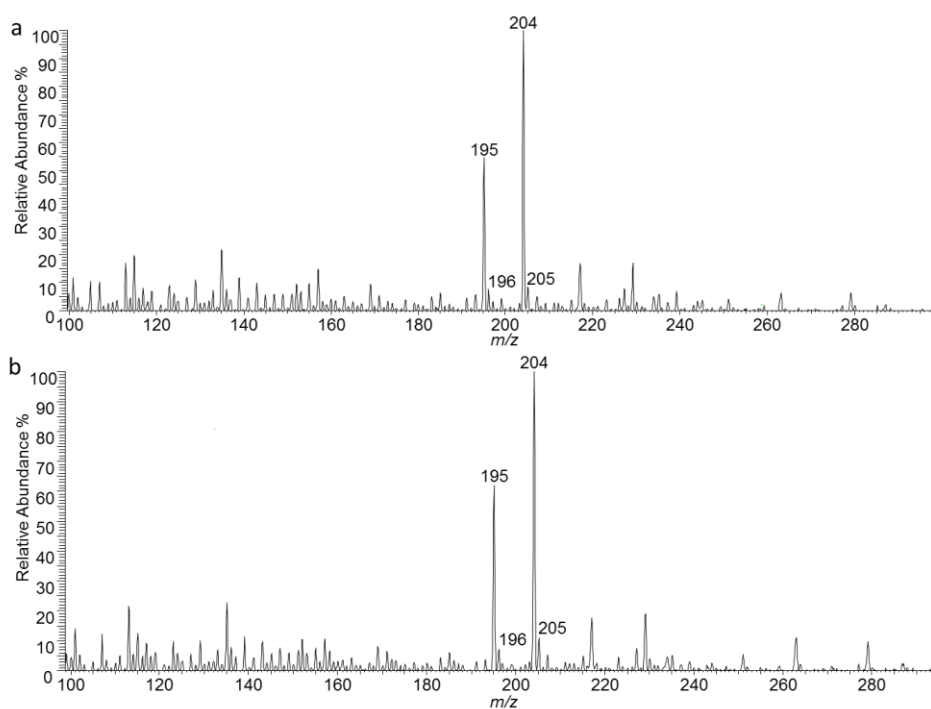

Figure C6: Spectra obtained upon performing paper spray with mixture of energy drink spiked with deuterated caffeine. Top panel is 2.5X diluted berry flavored drink with deuterated caffeine spiked to make a final concentration of 3mg/mL. The bottom panel is 2.5X diluted extra strength energy drink with deuterated caffeine spiked to make a final concentration of 3mg/mL

Appendix D: Supplementary Information of Chapter 5

Table D1: Data used to plot standard curve of ion intensity of tetrahydrozoline at different standard concentrations.

Conc. (µg/mL)	Total Ion Intensity for *m/z* 201			Average ion intensity	Standard deviation
	Series 1	Series 2	Series 3		
200	21800	11700	10930	14810	6065.75
100	10780	5390	7340	7836.67	2729.11
50	7060	3630	5050	5246.67	1723.44
30	4070	2250	4720	3680	1280.35
20	3670	1890	3780	3113.33	1060.86
10	2690	1280	3280	2416.67	1027.63
5	1206	497	3009	1570.67	1295.10
12.X	5370	2800	4710	4293.33	1334.70
30X	3010	1510	3790	2770	1158.79
R^2	0.9946	0.9914	0.9915	0.9965	----

Table D2: Area under the peak of tetrahydrozoline at different standard concentrations of tetrahydrazoline.

Conc. (µg/mL)	Area under the chronogram peak of *m/z* 201			Average	Std Dev.
	Series 1	Series 2	Series 3		
200	316419	205742	212080	244747	62150.62
100	179473	118569	117021	138354.33	35618.22
50	98248	69819	72037	80034.67	15812.15
30	53435	46098	40766	46766.33	6360.89
20	32984	27647	27912	29514.33	3007.74
10	19396	15947	16676	17339.67	1817.76
5	7149	4250	5190	5529.67	1479.05
R^2	0.9933	0.9883	0.9921	0.9923	
12.5X	72343	52629	51926	58966	11590.15
30X	33517	27740	26152	29136.33	3875.97

Table D3: Ion intensity peak of naphazoline at different standard concentrations.

Conc. (μL/mL)	Total Ion Intensity for *m/z* 211			Average	Std Dev
	Series 1	Series 2	Series 3		
100	2790	3670	1890	2783.33	890.0187 264
80	2080	2820	1540	2146.67	642.60
50	1480	1573	831	1294.67	404.23
30	786	1161	656	867.67	262.22
20	659	641	321	540.33	190.16
10	411	488	242	380.33	125.83
5	204	255	131	196.67	62.32
R^2	0.9931	0.9909	0.9898	0.9964	
3X	1160	1470	786	1138.67	342.50
10X	423	482	265	390	112.20

Table D4: Area under the elution peak of naphazoline at different standard concentrations.

Conc. (μg/mL)	Area under the chronogram peak of *m/z* 211			Average area	Standard Deviation
	Series 1	Series 2	Series 3		
100	45554	23372	34925	34617	11094.21
80	40248	17369	25904	27840.33	11561.76
50	22194	10976	15607	16259	5637.35
30	15491	7866	11410	11589	3815.65
20	10667	5715	7653	8011.67	2495.41
10	3914	2988	3077	3326.33	510.88
5	1774	1022	1323	1373	378.49
R^2	0.9915	0.9919	0.9925	0.9960	------
3X	19334	9863	14017	14404.67	4747.39
10X	5940	3745	4338	4674.33	1135.49

Table D5: Quantitation by calibration curve plotted using relative intensity ratio of mixture having standard and deuterated tetrahydrozoline. Three runs were performed in three separate plates. Their average ratio and standard deviation was plotted to obtain the calibration curve.

Sample (µg/mL)	m/z 201			m/z 205			ratio			Average Ratio	SD
	run 1	run 2	run 3	run 1	run 2	run 3	run 1	run 2	run 3		
5	73.7	77.6	75.65	277	300	294.5	0.266	0.259	0.257	0.261	0.005
10	4.41E+02	4.39E+02	4.40E+02	8.27E+02	8.29E+02	8.48E+02	0.533	0.530	0.519	0.527	0.007
20	4.98E+02	4.60E+02	4.75E+02	4.41E+02	4.19E+02	4.28E+02	1.129	1.098	1.110	1.112	0.016
30	6.94E+02	6.77E+02	6.71E+02	4.45E+02	4.36E+02	4.54E+02	1.560	1.553	1.477	1.530	0.046
50	6.92E+03	7.69E+03	7.13E+03	2.67E+03	3.11E+03	2.87E+03	2.592	2.473	2.484	2.516	0.066
12.5X	903	871	887	443	424	435.5	2.038	2.054	2.037	2.043	0.010

Table D6: Quantitation by calibration curve plotted utilizing relative intensity ratio of mixture having standard naphazoline and deuterated tetrahydrozoline. Three runs were performed in three separate plates. Their average ratio and standard deviation was plotted to obtain the calibration curve.

| Sample (µg/mL)	m/z 205			m/z 211			ratio			Average Ratio	SD
	run 1	run 2	run 3	run 1	run 2	run 3	run 1	run 2	run 3		
5	3600	3810	3830	959	969	947	0.266	0.254	0.24	0.256	0.010
10	2750	3520	2710	1576	2030	1560	0.573	0.577	0.576	0.575	0.002
20	1360	2460	1980	1430	2820	2210	1.05	1.15	1.12	1.105	0.048
30	1590	1820	1670	2440	2770	2800	1.53	1.52	1.68	1.578	0.086
50	652	1330	1130	1640	3290	2880	2.52	2.47	2.55	2.513	0.038
3X	643	848	469	1290	1730	954	2.01	2.04	2.03	2.027	0.015
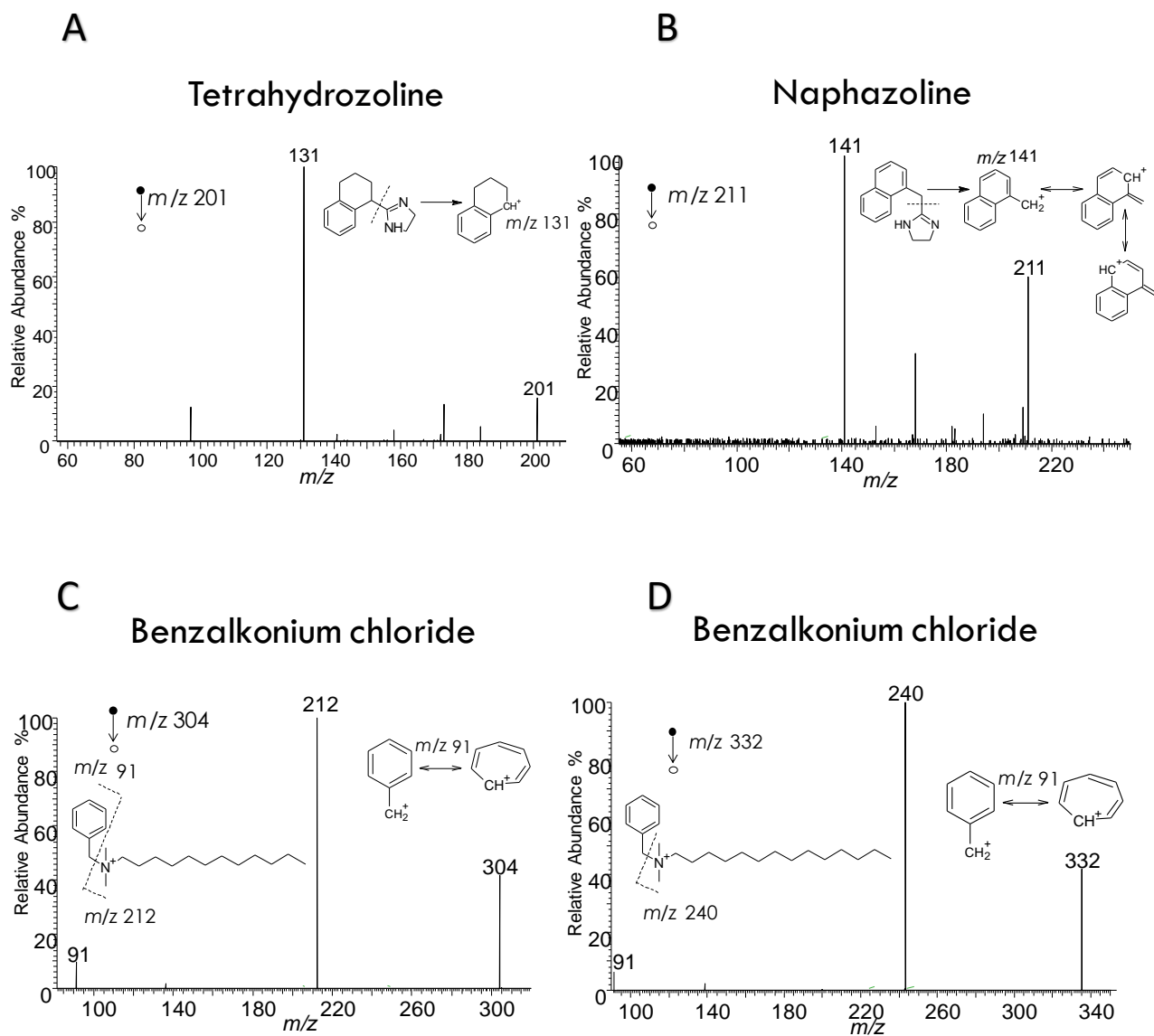
Figure D1: MS/MS spectra of active and additive components using LTQ Orbitrap Elite Mass Spectrometer. A: Fragmentation of tetrahydrozoline (*m/z* 201). B: Naphazoline fragmentation (*m/z* 211). C: Fragmentation of benzalkonium chloride of C_{12} alkyl side chain (*m/z* 304). D: Benzalkonium chloride of C_{14} alkyl side chain (*m/z* 332).
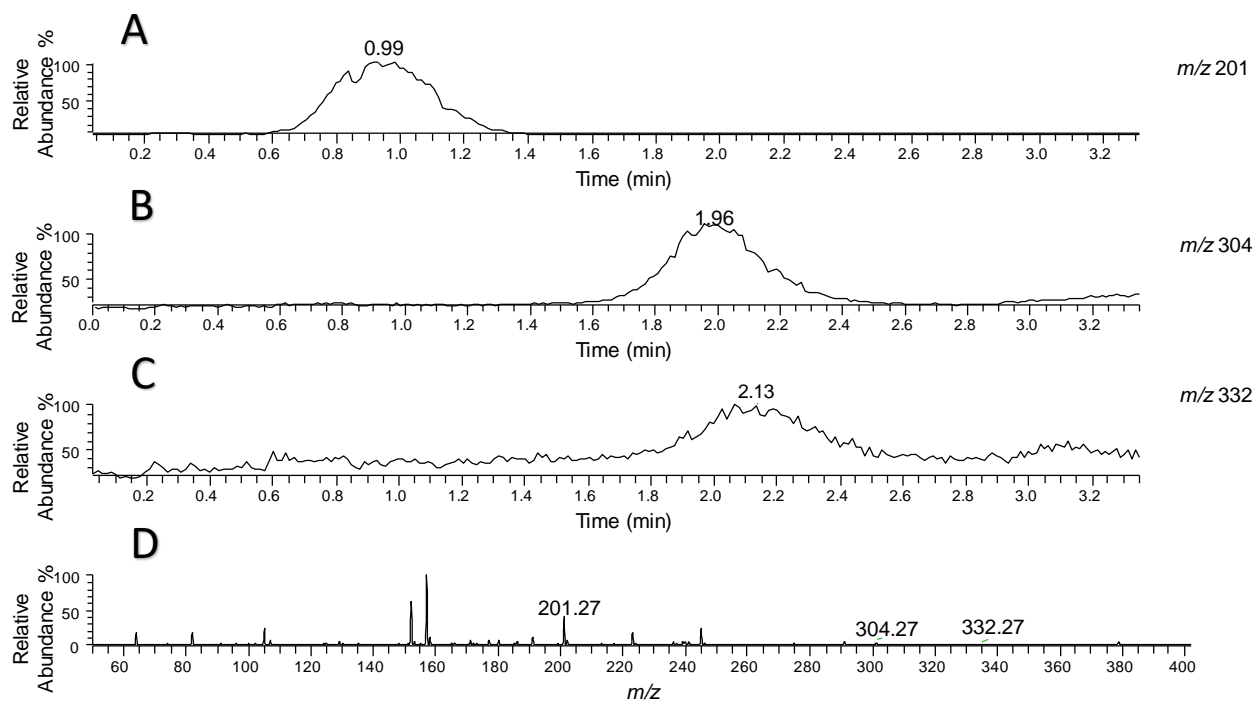
Figure D2: Chronograms and full spectrum of Visine for red eye original sample showing the separation of the active component from the preservative by DESI-MS. Chloroform: methanol (1:1) was the TLC mobile phase used. Acquisition time per line was 3.30 min. A: Tetrahydrozoline chronogram (*m/z* 201; RF: 0.30). B: Chronogram of benzalkonium chloride C_{12} alkyl side chain (*m/z* 304; RF: 0.59). C: Benzalkonium chloride C_{14} alkyl side chain chronogram (*m/z* 332; RF: 0.64). D: Full spectrum of the sample showing *m/z* 201, 304 and 332 peaks.
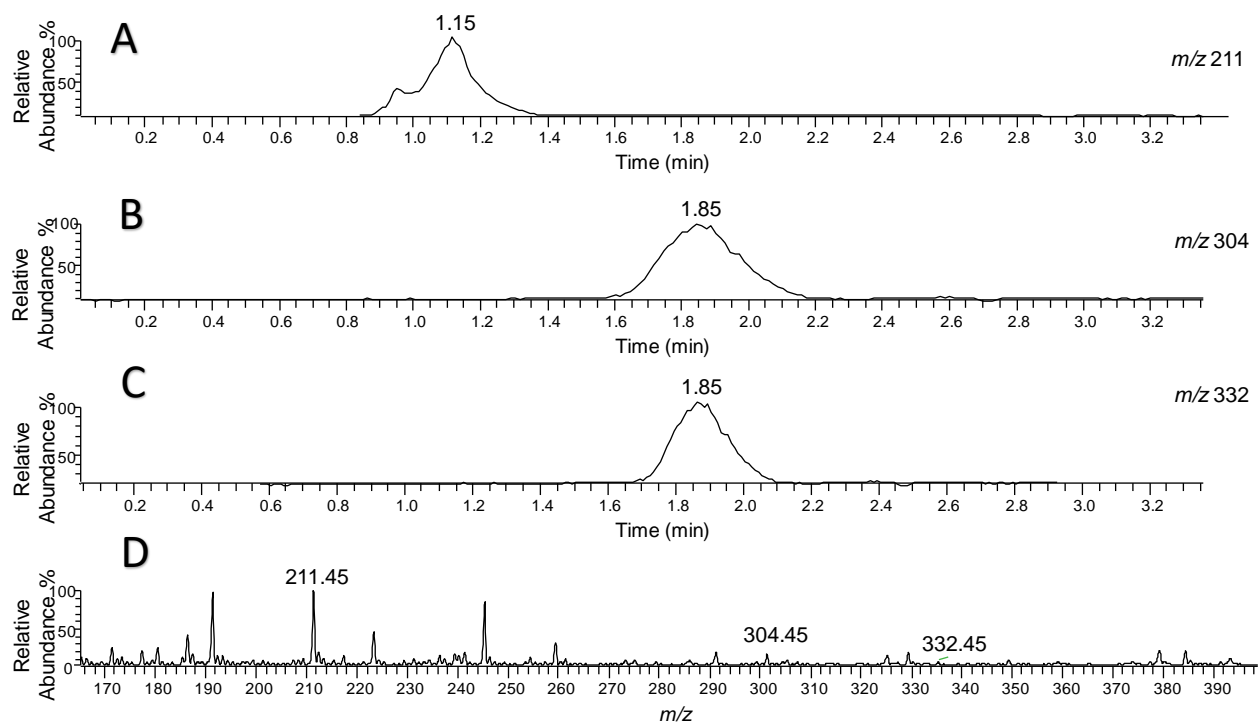
Figure D3: Chronograms and full spectrum of Clear Eyes Allergy sample showing the separation of the active component from the preservative by DESI-MS. Chloroform: methanol (1:1) was the TLC mobile phase used. Acquisition time per line was 3.38 min. A: Naphazoline chronogram (*m/z* 211, RF: 0.34). B: Chronogram of benzalkonium chloride C_{12} alkyl side chain (*m/z* 304; RF: 0.55). C: Benzalkonium chloride C_{14} alkyl side chain chronogram (*m/z* 332; RF: 0.55). D: Full spectrum of the sample showing *m/z* 211, 304 and 332 peaks.
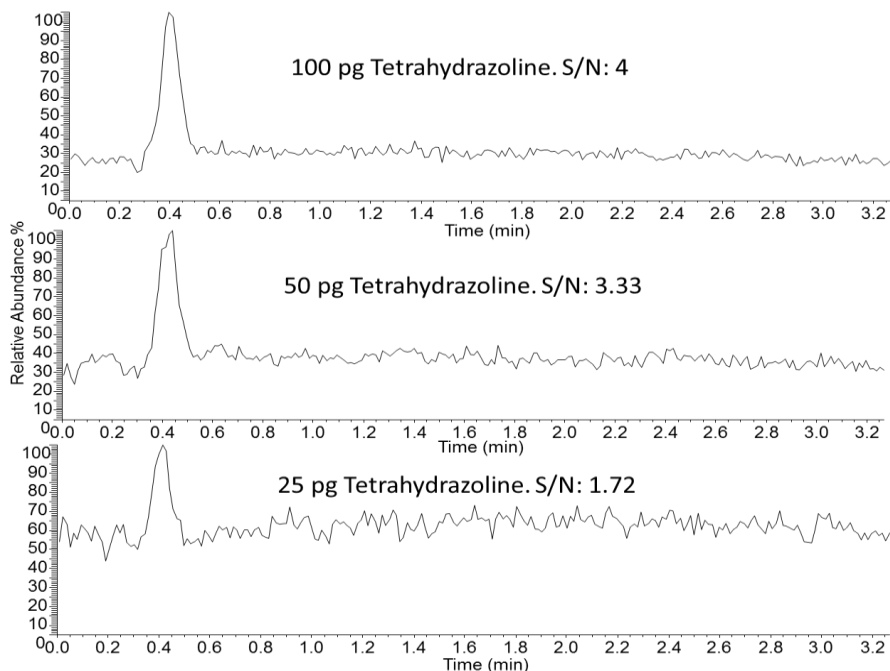
Figure D4: Signal to noise (S/N) variation upon changes on the spot amount of tetrahydrozoline. LOD of tetrahydrozoline was determined to the 50 pg giving a S/N ratio of 3.33.
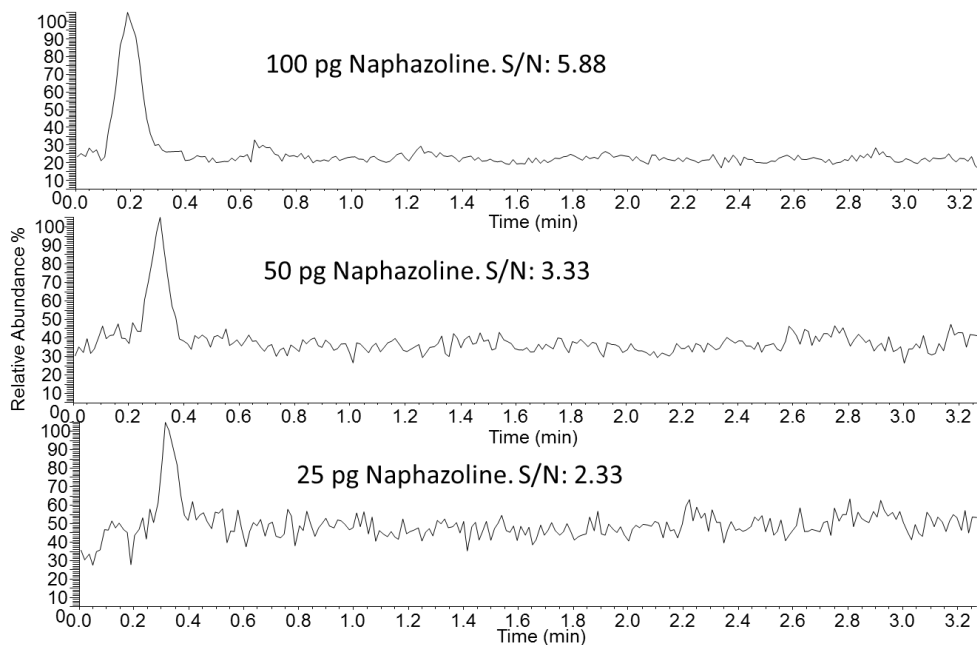

Figure D5: Signal to noise (S/N) variation upon changes on the spot amount of naphazoline. LOD of Naphazoline was determined to the 50 pg having a S/N ratio of 3.33.
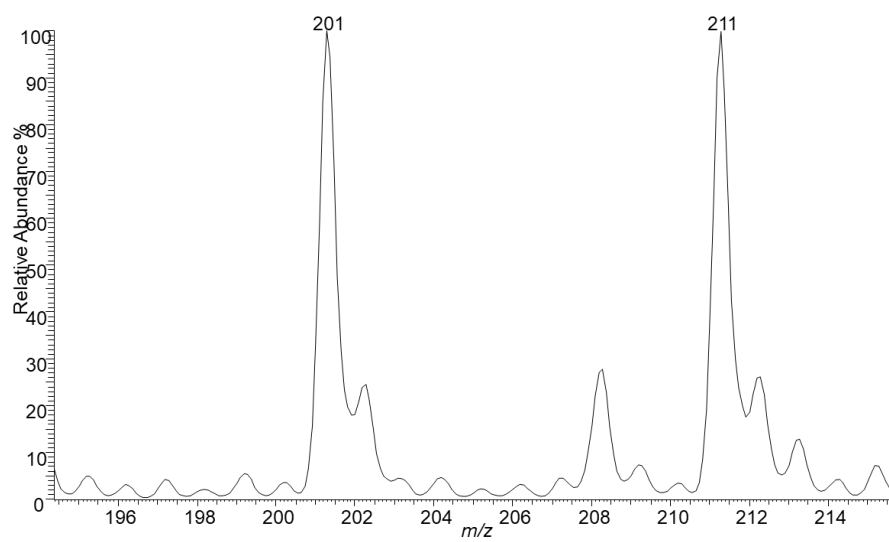
Figure D6. Zoomed spectrum showing relative abundance of both Tetrahydrozoline (*m/z* 201) and Naphazoline (*m/z* 211) by DESI-MS upon spotting a mixture having equimolar concentration (20 µg/mL each) of both on a TLC plate.